AN ECOLOGICAL AND BIOGEOCHEMICAL CHARACTERIZATION OF A SUBTERRANEAN ESTUARY IN THE YUCATAN PENINSULA, MEXICO

A Thesis

by

SEPP LEIF HAUKEBO

Submitted to the Office of Graduate and Professional Studies of
Texas A&M University
in partial fulfillment of the requirements for the degree of

MASTER OF SCIENCE

Chair of Committee,	Thomas Iliffe
Committee Members,	Rainer Amon
	Jay Rooker
Head of Department,	Michael Masser

May 2014

Major Subject: Wildlife and Fisheries Sciences

ABSTRACT

Subterranean estuaries are biogeochemical reactors within the coastal aquifer and represent a processing zone of dissolved chemical constituents prior to submarine groundwater discharge (SGD). Highly stratified hydrologic layers and sharp physicochemical boundaries characterize anchialine caves, a subset of subterranean estuaries. This study serves as a biogeochemical and ecological characterization of Sistema Crustacea, an anchialine cave in the Yucatan Peninsula with dense populations of cave-adapted invertebrates.

Investigations of the physicochemical parameters found dissolved oxygen (DO) minimums and concurrent pH maximums as good indicators of localized microbial respiration within the shallow and deep haloclines. Beneath the deep halocline, a local DO and temperature maximum serve as evidence of counter current, tidal pumping of open seawater. Such evidence indicates that conventional circulation may not dominate groundwater flow along the Caribbean coast of Yucatan as some studies suggest.

Spatial variability of chromophoric dissolved organic matter (CDOM) was investigated using fluorescence spectroscopy and parallel factor analysis (PARAFAC). A terrestrial source dominated the CDOM signal within the freshwater layers. However, there was a clear shift in the brackish and marine layers to CDOM derived from microbial activity. The greatest concentration of DOC occurred in the freshwater pool with decreasing values in the deeper hydrologic layers. Evidence for non-conservative removal of dissolved organic carbon (DOC) and total nitrogen (TN) suggests that

Sistema Crustacea acts as a sink for terrestrially derived organic matter destined to reach the coast. The anomalies detected in the physicochemical profiles suggest microbial respiration is partly responsible for this carbon and nitrogen removal as well as the shift in CDOM sources.

Swimming diver transects were used to characterize the invertebrate community throughout Sistema Crustacea and confirmed early observations that there are two ecologically distinct sections of the cave. The Eastern Section is characterized by high density of cave shrimp (*Typhlatya pearsei)*, distributed in the brackish and marine layer, and remipedes (*Xibalbanus tulumensis*), observed solely in the marine layer. The Western Section shares the same entrance, but transects found a different species of remipede (*Xibalbanus fuchscocksburni*) and no *T. pearsei*.

DEDICATION

This thesis is dedicated to my parents: for teaching me not what to think about the natural world but how. I would also like to dedicate this to my wife, for her endearing support throughout this pursuit of knowledge.

ACKNOWLEDGEMENTS

It takes the help of many to educate an individual and to each that played a role, I am forever grateful. I would like to thank my committee chair, Dr. Iliffe for introducing me to the world of caves. To explore those spaces visited by few is an adventurous endeavor and I am thankful for that. I must also thank Gregg Stanton for teaching me the art of cave diving, an education that has taken me to the unimaginable reaches of the earth.

I would also like to thank Dr. Rooker for his mentoring. Throughout my undergraduate and graduate studies he has changed the way I think about life in the marine sciences. He has taught me much about how to think strategically in the scientific world. I am also thankful to his grad students for involving me in their research and exposing me to a broad range of ecological studies, experiences that have helped to get me where I am today.

Great thanks are due to Dr. Amon for lending his time, lab space, and expertise in all things biogeochemical. I have always enjoyed our conversations and as a result I now believe that talking through a scientific concept can be as important as thinking though one. Equal thanks are in order to Dr. Walker for her patience and mentoring in the sample processing, data processing, and writing portions of my research. It takes a great deal of effort to teach someone *how* to investigate organic carbon sources but it takes a great deal more to *inspire* someone to investigate organic carbon sources, for that I am equally grateful.

Thanks also to my friends, colleagues, faculty, and staff at Texas A&M University at Galveston. It takes a community to educate an individual and TAMUG is a community that invests much in each of its students. A special thanks to my friends and dive partners: Brett Gonzalez, Julie Neisch, Joe Bosquez, Joey Pakes, and David Brankovits. Our adventures both below ground and above will not go untold.

Finally, thanks to my wife for her unwavering support and understanding. I've learned much from you throughout my education, lessons that cannot be translated into text or classrooms.

TABLE OF CONTENTS

LIST OF FIGURES

Page

Page

LIST OF TABLES

Page

CHAPTER I

GENERAL INTRODUCTION

Introduction

The Yucatan Peninsula is a limestone platform, the northern portion of which is devoid of any surface rivers. With minimal time for interstitial filtration or biodegradation, the aquifer is highly susceptible to organic matter loading from both natural and anthropogenic sources. In addition, wastewater treatment only began 15 years ago and septic systems subject to leakage are still used in the majority of the region (Aranda-Cirerol et al. 2006). The aquifer serves as the primary source of freshwater to the human population and numerous groundwater dependent ecosystems (GDEs) along the Caribbean coastline including sea grass beds and mangroves. The Caribbean coast of the Yucatan also hosts the second longest barrier reef system in the world, the Mesoamerican Barrier Reef. Over the last 20 years however, this reef system has undergone more than 50% loss of coral cover. This coral loss is primarily attributed to disease outbreaks associated with increased coastal eutrophication derived from increased nutrient loading within local submarine groundwater discharge (SGD) (Metcalfe et al. 2011). In the face of a rapidly developing tourism industry, groundwater and coral resource management could greatly benefit from an increased understanding of the biogeochemical processes within the coastal aquifer.

Prior to the resulting SGD along the coastline, water and nutrients flow through the coastal aquifer, an intense biogeochemical reaction zone. Moore (1999) first referred

to this region as a subterranean estuary. Stratified hydrologic layers characterize subterranean estuaries and their subcategory of anchialine caves. Based on the Ghyben-Herzberg model, the hydrologic layering in anchialine caves, or any other coastal aquifer, is driven by differences in density, with a freshwater lens overlying a fully marine layer separated by a well-defined halocline (Vacher 1988). The freshwater layer is described as a lens due to the thinning of the layer at the outer, coastal boundaries. Some systems may also contain a middle, brackish layer referred to as the mixing zone or zone of diffusion, with a shallow halocline above and deep halocline below. The presence of these distinct hydrologic layers allows for a variety of habitats and the presence of sharp boundaries between physicochemical parameters including temperature, salinity, dissolved oxygen (DO), pH, and redox potential (Pohlman 2011). Such variety in physicochemical conditions leads to increased potential for numerous geochemical processes, which can in turn influence the conditions within each hydrologic layer and the properties of SGD along the coast. The density boundaries associated with each water layer are also believed to prevent the movement of contaminants from the marine layer into the freshwater lens. Therefore, deep well injection of wastewater into the underlying marine groundwater is a common method of disposal (Beddows et al. 2007). While deep well injection is legal in Mexico, future ramifications of nutrient contamination could be environmentally detrimental.

Physicochemical Parameters and Ecological Implications

Much like their surface counterparts, subterranean estuaries contain distinct hydrologic layers and a mixing zone. Due to the lack of sunlight however, DOM processing within subterranean estuaries depends greatly upon the redox potential of the surrounding environment and microbially mediated redox reactions (Santos et al. 2008). Examples of such reactions in anchialine caves include nitrification, methanogenesis, methanotrophy, sulfate reduction, and sulfur species oxidation. Microhabitats within the water column determine which of these biogeochemical reactions are thermodynamically favored (Pohlman 2011). For example, in the presence of oxygen, oxic respiration of organic matter yields the greatest free energy. Once the oxygen becomes depleted, other reactions become more thermodynamically favorable (Fig. 1.1). The terminology described by Sket (1996) suggests that waters in anchialine caves can range from normoxic (10.6 – 2.7 mg/L) to hypoxic (2.7 – 0.0 mg/L) to anoxic (0.0 mg/L). Sket (1996) goes on to further define the hypoxic range as: moderate (2.7 – 1.33 mg/L), severe (1.33 – 0.7 mg/L), extreme (0.7 – 0.27 mg/L), and suboxic (0.27 – 0.0 mg/L).

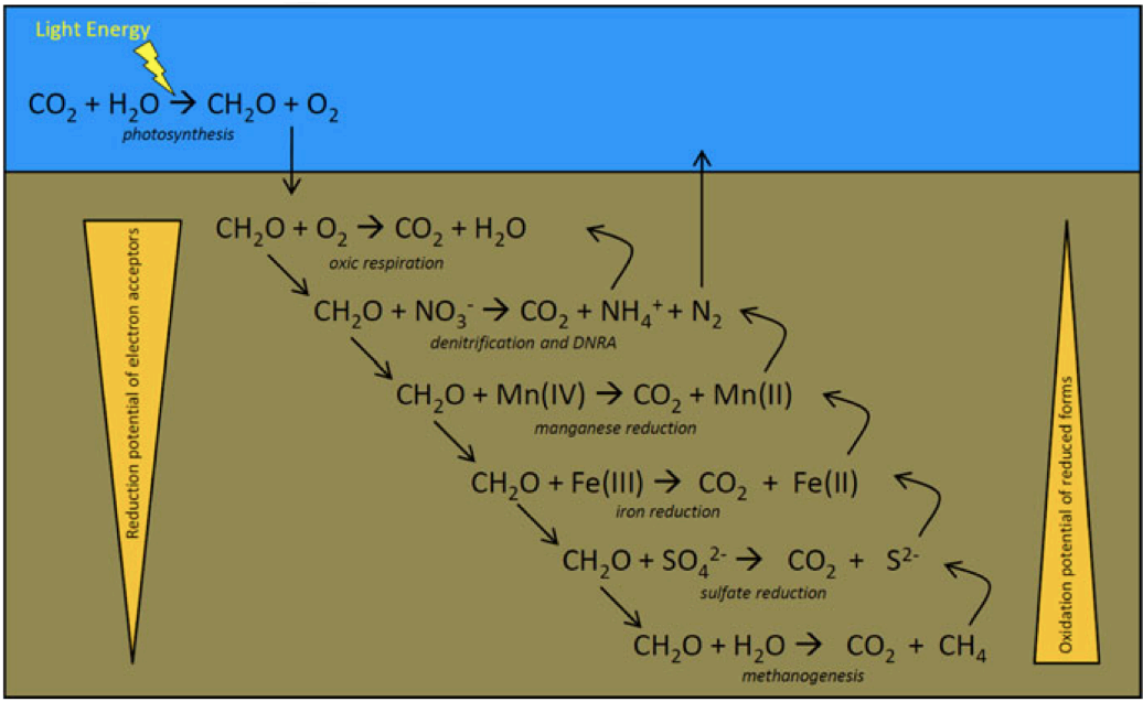

Fig. 1.1. Order of redox reactions based on reduction potential of electron acceptors (left arrow) and oxidation potential of reduced forms (right arrow). Source: (Pohlman 2011)

Within anchialine caves, the sharp transition of habitats with differing oxic states allows microbes to couple certain energy yielding reactions. Most anchialine caves exhibit normoxic waters in the shallow, freshwater lens. Within the upper oxidizing layer, organic matter (OM) is oxidized, while sulfate (derived from marine waters) becomes reduced, thus producing hydrogen sulfide (H_2S) (Eq. 1.1).

$$2CH_2O + SO_4^{2-} => 2HCO_3^- + H_2S \quad (1.1)$$

The sharp density boundary associated with the halocline creates a trap for particulate organic matter (POM) that in turn becomes an energy source to microbes and filter feeding invertebrates; it is unclear if the pycnocline also traps dissolved organic matter (DOM). Therefore, OM that is not oxidized in the upper layers can accrue within

the halocline, pass through to the lower layers, or accumulate within sediment on the cave floor (Pohlman 2011). Any H_2S that migrates into normoxic waters becomes oxidized yielding an acidic solution as indicated in Eq. 1.2 (Socki et al. 2002).

$$H_2S + 2O_2 => SO_4^{2-} + 2H^+ \quad (1.2)$$

A portion of the energy yielded from this reaction is utilized to convert inorganic carbon (CO_2) into microbial biomass during the chemoautotrophic process of sulfide oxidation (Pohlman 2011), thereby introducing a new source of organic carbon to a carbon-limited environment. In addition to altering biological processes within the water column, this reaction affects the geochemical formation of the cave system. The acidic solution produced from sulfide oxidation (Eq. 1.2) within the halocline, is responsible for the dissolution of carbonates and is one of the major methods of anchialine cave expansion (Socki et al. 2002). This acidic solution has been known to discharge along the coast as acidic SGD. Known locally as "ojos" (Spanish for eyes), SGD along the Caribbean coast of the Yucatan may provide important insight into the long-term responses of coral reefs exposed to ocean acidification (Crook et al. 2012).

Based on the production of bicarbonate (HCO_3^-) alkalinity during sulfate reduction and hydrogen ions during sulfide oxidation, pH can be a good indicator of redox potential and microbial activity in the water column of anchialine caves (Socki et al. 2002). Sharp declines in DO can also be a key indicator of microbial respiration. Therefore the presence of microbial hot spots, these areas of intense biogeochemical processes (Mcclain et al. 2003), can be detected by investigating the physicochemical parameters throughout the water column.

Investigation of an anchialine remipede habitat in Bundera Sinkhole, Western Australia revealed physicochemical anomalies in DO, dissolved inorganic nitrogen (DIN), and sulfur species throughout the water column (Seymour et al. 2007). Strong H_2S smell and white, milky clouds were observed in the upper portion of the water column. Analysis of bacteria distribution via flow cytometric analysis (FCM) detected elevated populations at the same depth as the H_2S maximum and DO minimum. Researchers concluded that white chemolithotrophic sulfur oxidizing bacteria were responsible for the spike in H_2S and the sharp decline in DO. High concentrations of ammonium (NH_4) were also found within the anoxic sulfide layer. In the absence of oxygen, nitrate (NO_3^-) becomes the preferred electron acceptor allowing dentrification to proceed (Eq. 1.3).

$$5CH_2O + 4NO_3^- + 4H^+ \Rightarrow 5CO_2 + 7H_2O + 2N_2 \quad (1.3)$$

The source of nitrate could be meteorological runoff or nitrification in which ammonium (NH_4^-) is oxidized to an intermediate nitrite (NO_2^-) (Eq. 1.4a), which is further oxidized to nitrate (Eq. 1.4b).

$$2NH_4^+ + 3O_2 \Rightarrow 4H^+ + 4H_2O + NO_2^- \quad (1.4a)$$

$$2NO_2^- + O_2 \Rightarrow 2NO_3^- \quad (1.4b)$$

Within Bundera Sinkhole, ammonium levels were much lower in the marine layer where a sharp increase in nitrate and DO occurred. The inverse distribution of ammonium and nitrate within the DIN profiles provided strong evidence for nitrification (Seymour et al. 2007).

Evidence of microbial communities that perform oxic respiration (Eq. 1.5) coupled with nitrification has also been observed in an anchialine cave in the Yucatan (Pohlman et al. 1997).

$$CH_2O + O_2 \Rightarrow CO_2 + H_2O \quad (1.5)$$

In the presence of organic matter, oxygen is the preferred electron acceptor (Fig. 1.1). Excessive organic matter influx can therefore drive conditions within the water column to anoxia via oxic respiration (Pohlman 2011). Researchers investigating Cenote Mayan Blue, located along the Caribbean coast of the Yucatan Peninsula, found a spike in nitrate and also detected a pH minimum within the halocline. However, unlike Bundera Sinkhole, the peak was accompanied by a DO minimum. While nitrification is thermodynamically favorable in aphotic, hypoxic conditions, the presence of oxygen is required for it to proceed (Pohlman 2011). Therefore, the hypoxic environment of the halocline favored nitrification, while the oxygen for the nitrification process presumably came from the normoxic marine layer beneath the halocline. Similar to sulfide oxidation, a portion of the energy yielded from the oxidation of organic matter (CH_2O) is assimilated into microbial biomass (Pohlman 2011). Unlike sulfide oxidation, there is no creation of new organic carbon, and only recycled carbon from POM and DOM enters the microbial food web. While the energy yield from nitrification is capable of sustaining the microbial community, the carbon assimilation efficiency is considered too low to support higher trophic levels such as those observed in Cenote Mayan Blue (Pohlman et al. 1997). For unknown reasons, Pohlman et al. did not suggest sulfide

oxidation coupled with sulfate reduction as an additional energy source to the trophic web, but instead hypothesized methanogenesis.

In a freshwater cave in the Upper Floridian Aquifer (UFA), evidence exists for microbially mediated methanogenesis (Eq. 1.6), the heterotrophic consumption of organic matter that generates methane (CH_4), coupled with methanotrophy, the aerobic oxidation of methane (Opsahl and Chanton 2006) (Eq. 1.7).

$$6CH_2O \Rightarrow 3CO_2 + 3CH_4 \quad (1.6)$$

$$CH_4 + 2O_2 \Rightarrow CO_2 + 2H_2O \quad (1.7)$$

Within the waters of this cave of the UFA, extremely hypoxic waters, ranging from 0.3 - 0.7 mg/L, and elevated methane levels (300-458 nM) both suggest that methanogenesis is the dominant microbial process. Organic matter for this heterotrophic process was derived from allochthonous sources including the soils and wetlands overlying the cave system. Methane produced within the hypoxic waters presumably migrated into normoxic waters (4.6 ± 1.3 mg/L) where the methane became oxidized and incorporated into the trophic web (Opsahl and Chanton 2006). Methane levels within Cenote Angelita (ca. 500 nM), near Cenote Mayan Blue, were similar to the methane levels found in the UFA. Such elevated levels in Cenote Angelita indicate that methanogenesis may be an additional source of chemosynthetic energy in nearby Cenote Mayan Blue (Pohlman 2011).

In each of the examples mentioned above, stable isotope values for $\delta^{13}C$ from stygobitic species were very negative, indicating microbial communities made up a significant base to the trophic web (Humphreys 1999; Opsahl and Chanton 2006;

Pohlman et al. 1997). Among the microbial processes that have been found to support higher trophic levels in anchialine caves, the most thermodynamically favored electron acceptor (and energy yielding reaction) is oxygen (via oxic respiration), followed by nitrogen (via denitrification), and sulfate (via sulfate reduction) (Pohlman 2011). Several other microbial processes have been observed in anchialine caves including oxidation of ferrous and manganese (II) carbonates by heterotrophic bacteria (Pohlman 2011 and sources therein). However, evidence has not been presented indicating these processes provide a trophic base to sufficiently support the higher trophic levels (Pohlman 2011).

It is apparent that anchialine caves host a great diversity of microbial processes. Based on a review of geological studies in anchialine caves, Mylroie and Mylroie (2011) suggested that anchialine caves with increased habitat complexity also exhibit increased biodiversity. Their review refers to primarily vertical and horizontal passage complexity which provides stygobitic communities refuge from sea level low stands. Evidence suggests that refugia provided during low stands can sustain existing stygobitic communities and simultaneously allow for colonization from marine lineages. I agree with this premise and propose expanding it to include the variability of microhabitats. The great variety of microbial processes that have been found to support higher trophic levels in anchialine caves depend on a range of oxic boundaries and hydrological conditions (Pohlman 2011). A significant shift in the oxic status from either a resource pulse or significant climate event (i.e., increased tidal surge during a hurricane) can provide positive or negative feedback within the microbial loop. Significant events can therefore dictate the specific composition and vitality of the microbial base to the trophic

web, subjecting the higher trophic levels to variability of food source. In theory, systems that host a series of redox states also have a much broader trophic base of microbial communities and can adapt to significant events of adversity.

Based on previous research, physicochemical anomalies within the water column can be utilized to understand the ecological and geochemical role of microbial communities within anchialine caves (Opsahl and Chanton 2006; Pohlman et al. 1997; Seymour et al. 2007). In a branch of ecology where the investigation of a new cave system often leads to the discovery of a new species (T. Iliffe pers. comm.), it is essential to understand the spatial variability of the physicochemical parameters and the diversity of microhabitats.

Structure of Thesis

Chapter I is an introduction to the Yucatan Peninsula and the anchialine cave environment. An overview of the study site, Sistema Crustacea, is provided, followed by an outline of the thesis research, specific objectives, working hypothesis, and rational for the investigation. Chapter II is an overview of the study in which the spatial physicochemical parameters were investigated throughout Sistema Crustacea. Temporal variations of the parameters over four years were also compared. Additionally, stable isotope analysis of oxygen ($\delta^{18}O$) and hydrogen ($\delta^{2}H$) were used to constrain sources of water within different hydrologic layers and sections of the cave. Chapter III is focused on how chromophoric dissolved organic matter (CDOM) was used to constrain the source of DOM in various sections of the cave. Dissolved organic carbon (DOC)

concentrations were used to determine the relative contribution of each of those sources. Chapter IV provides an overview of the visual censusing used to investigate the invertebrate population within various sections of Sistema Crustacea. Chapter V is a summary of the work and conclusions derived from all components of the study.

Study Site

Sistema Crustacea (previously referred to as Cenote Aayin Aak) is a solutional limestone cave located 0.5 km inland from the coast and several kilometers south of Puerto Morelos, Quintana Roo, Mexico (Fig. 1.2). The system was selected for this study because of its unusually high biomass of crustaceans, particularly cave adapted remipedes and shrimp. The lack of nearby development suggests little anthropogenic influence in the system. However, the cenote was previously (5 years ago) used as a latrine by a nearby camp of construction workers. I expect the effects of which have since been flushed by rainfall runoff and groundwater flow. Cenote Crustacea is both the largest and primary entrance for diving exploration in Sistema Crustacea (Fig. 1.2). A second, smaller entrance named Cenote Thermosbaenacea, was included in this investigation, but a third entrance to the system, Cenote Jigsaw, was not. A strong hydrogen sulfide odor has been reported emanating from Cenote Jigsaw and should be considered in future studies (Neiber et al. 2012).

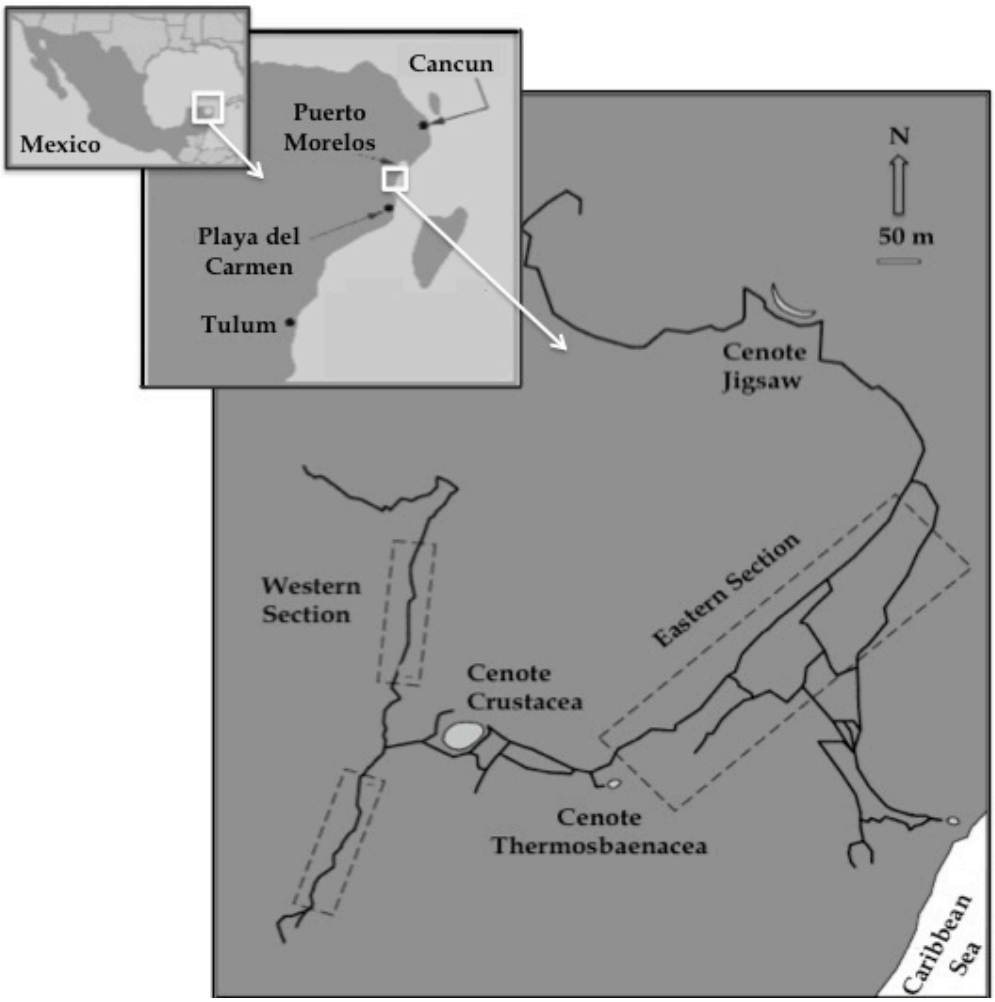

Fig. 1.2. Map of Mexico with an inset of the Yucatan Peninsula showing Puerto Morelos, Quintana Roo. The large inset shows the map view of the Eastern and Western Sections of Sistema Crustacea including Cenote Crustacea, Cenote Thermosbaenacea, and Cenote Jigsaw.

For consistency throughout this paper, the entire cave system will be referred to as Sistema Crustacea, whereas Cenote Crustacea only refers to the portion of the system from the Cenote Crustacea pool entrance to the beginning of Cenote Thermosbaenacea, in the Eastern Section. The water column of Sistema Crustacea is composed of an upper freshwater lens, overlying a middle brackish water layer, with a fully marine layer at the

deepest section of the cave. A shallow halocline (H1) serves as the fresh–brackish water interface, while a deep halocline (H2) separates the brackish from the marine water (Fig. 1.3).

Based on observations made by previous researchers, the system is composed of two distinct sections: an Eastern Section (Fig. 1.3) with unusually high abundance of *Xibalbanus tulumensis* and *Typhlatya pearsei*; and a Western Section with much lower abundance levels, more typical of other anchialine caves in the Yucatan (Neiber et al. 2012).

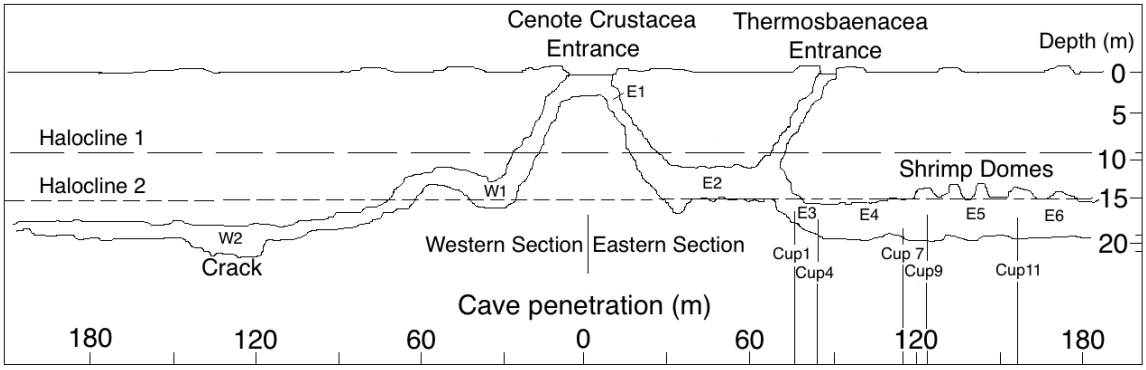

Fig. 1.3. Schematic diagram of Sistema Crustacea outlining proposed sampling zones within the Eastern and Western Sections. Halocline depths are based on measurements from March 2011.

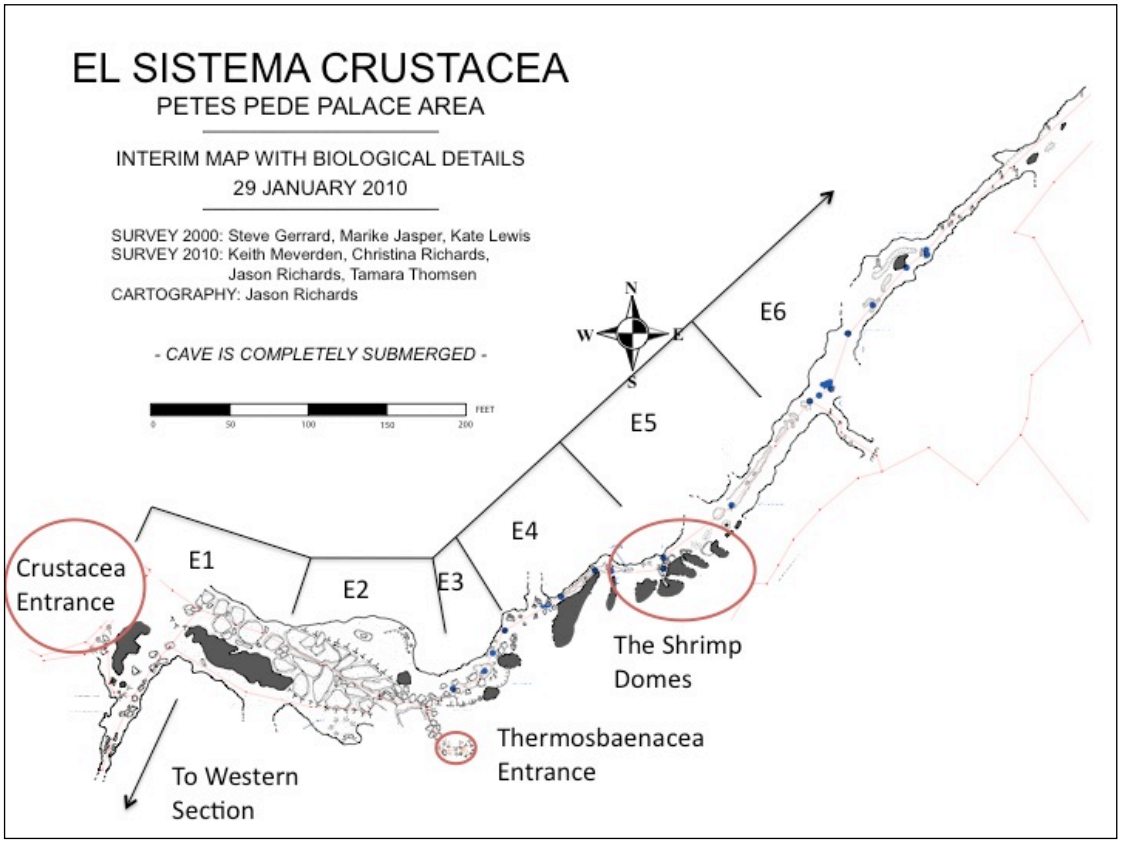

Fig. 1.4. Map view of the Eastern Section within Sistema Crustacea including zones E1, E2, E3, E4, E5, and E6.

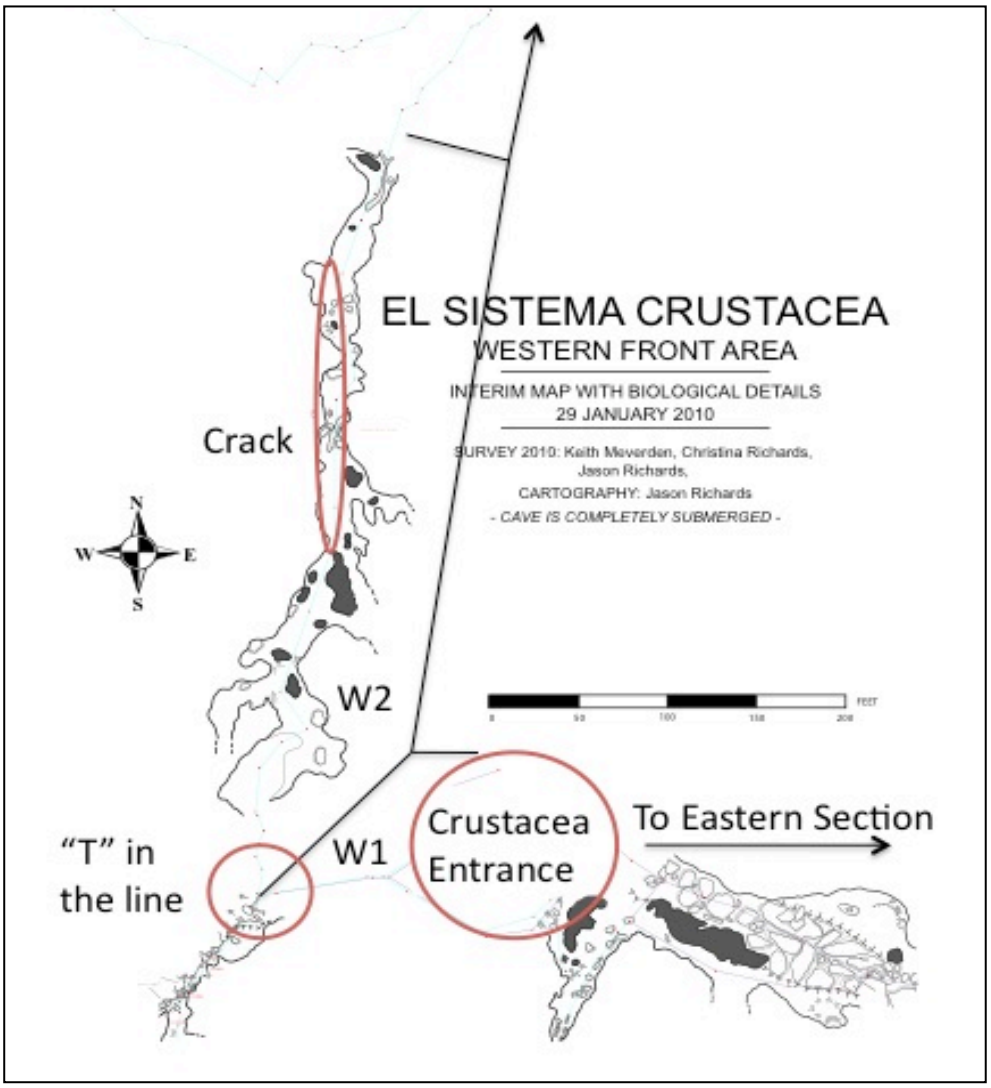

Fig. 1.5. Map view of the Western Section within Sistema Crustacea including the crack, the "T" in the main line, and zones W1 and W2.

The East Section is divided into sampling zones E1 – E6 (Figs. 1.3 and 1.4). E1 is in the entrance/cavern zone and extends to the edge of the photic zone. E2 begins in the aphotic zone. Zones E3, E4, E5, and E6 are designated by Styrofoam cups numbered 1 to 11. These cups are secured to the main cave line in the passage and were originally

used by Jill Yager to determine remipede distribution. Zone E3 ranges from Cup 1 to 4; E4 ranges from Cup 4 to 9; E5 ranges from Cup 9 to 11; and E6 ranges from Cup 11 onward.

The West Section is divided into zones W1 and W2 (Figs. 1.3 and 1.5). W1 ranges from the edge of the cavern zone to the "T" in the main guideline (ca. 33 m penetration). W2 extends from the "T" into the north section of the cave passage onward.

Thesis Research

The overall objective of this study is to characterize important biogeochemical properties and processes within the hydrological layers of Sistema Crustacea. In addition, I aim to investigate the spatial variability of DOM within various sections of the cave. In a region where SGD is the primary source of water and a significant source of nutrients to the coastal ecosystems, there is increasing need to understand the carbon and nitrogen cycling. This investigation provides insight into the processes that affect coastal carbon and nitrogen budgets. In addition, the ecological characterization of each section will help to determine the influence of physicochemical parameters and DOM variability on the invertebrate community within Sistema Crustacea. With a growing anthropogenic influence along this coast, it will become increasingly important to monitor ecosystem health within the coastal aquifer. This paper thereby presents a baseline study of the ecological health of a unique anchialine cave in a region greatly dependent upon groundwater resources.

Specific Objectives

1) Measure physicochemical water parameters including temperature, salinity, pH, and dissolved oxygen within the cave waters.
2) Constrain the sources of water in various layers of the cave using physicochemical characteristic as well as ^{18}O and ^{2}H isotopes.
3) Determine spatial variability of DOC and CDOM
    a. Constrain the sources of CDOM (using PARAFAC) from various locations of the cave and potential nearby endmembers including the entrance pool, an inland groundwater well, an inland karst window, a mangrove pool, and the open sea.
    b. Quantify DOC and TN within various locations of the cave and nearby end members.
4) Determine spatial variability of the invertebrate community
    a. Conduct visual censuses of the invertebrate community.
    b. Characterize ecological diversity in each layer and section of the cave.

Working Hypothesis

I propose a working hypothesis made up of these predictions:

1) DOC concentration and CDOM intensity will decrease with increasing distance, both linear penetration and depth, from the entrance of Cenote Crustacea.

2) CDOM sources within the hydrologic layers will follow the same trend as the water sources, shifting from terrestrial humics in the freshwater to marine humics in the deep layer, with the brackish layer made up of a mix of both.
3) Cave zones with increased DOC levels will exhibit increased species richness (S) and diversity (H').
4) The shallow and deep halocline will exhibit significantly greater DOC concentrations than the surrounding layers.
5) CDOM sources within the shallow and deep halocline will exhibit primarily microbial sources exhibited by protein peaks.
6) Biogeochemical processes within the water column are capable of qualitatively and quantitatively altering the DOM budget within this system.

CHAPTER II

HYDROLOGICAL PARAMETERS WITHIN SISTEMA CRUSTACEA

Introduction

Anchialine caves around the globe contain communities of stygobitic (marine and freshwater, cave adapted) invertebrates and fishes (Botosaneanu and Iliffe 2002; Humphreys and Danielopol 2005; Iliffe 1986). Extensive microbial communities have also been discovered in subterranean estuaries around the world. In several cases, the microbial communities are the primary autochthonous source of energy and represent the base level of trophic webs in these lightless environments (Gonzalez et al. 2011; Opsahl and Chanton 2006; Pohlman et al. 1997; Sarbu et al. 1996). Anchialine caves are hydrologically comprised of a freshwater layer overlaying a marine layer of water separated by a distinct halocline. The halocline is characterized by a sharp transition in salinity, temperature, density, pH, dissolved oxygen (DO), and redox potential. OM from varying sources has also been found to collect in the pycnocline (Pohlman 2011). The accumulation of OM, when coupled with a sharp change in redox potential, allows for a variety of life supporting, microbially based redox reactions to take place. In order to conserve these underground ecosystems and the GDEs they support, it is important to first characterize and assess the relationship between the physicochemical environment and the respective water sources throughout the system.

In conventional saline circulation models, freshwater flows toward the coast, driven by a hydrostatic head within the freshwater lens. This flow entrains the marine

layer below the halocline resulting in a net coastal movement of both layers (Cooper 1959). The shallow marine layer is subsequently replaced by seawater that has infiltrated the limestone platform at depth (Fig. 2.1). Recent evidence however, indicates a decoupling of the fresh and saline layers leading to an opposite direction of flow in the marine layer. Based on instrumental monitoring and dye tracing, recharge of recent saline water proceeds into the platform, even when freshwater flow continued coastward (Beddows et al. 2007). In this "counter current" model, warmer oxygenated Caribbean Sea water enters the aquifer beneath the mixing zone and flows inland, preferentially along a conduit system. Based on the differences in flow direction and the use of wastewater injection in the Yucatan, it is important to understand groundwater circulation throughout the region.

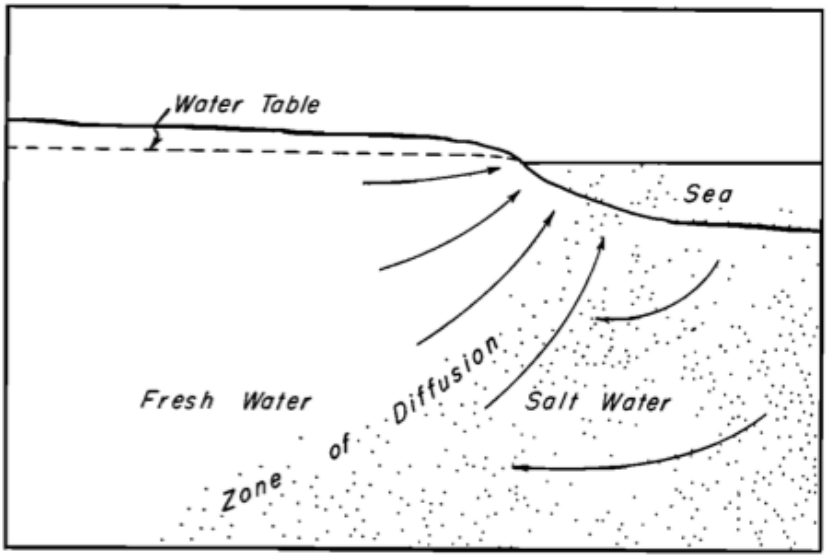

Fig. 2.1. Direction of flow in the conventional entrainment and convection driven circulation models within a coastal carbonate platform. Source: (Cooper 1959)

In the current chapter, I characterize physicochemical conditions and the hydrologic framework within different sections of an anchialine cave system. An improved understanding of these conditions will help to determine which biogeochemical processes may occur, affecting organic matter dynamics. In addition, I compare the physicochemical makeup to the isotopic signature of hydrologic layers and nearby endmembers in order to constrain the relative sources of water throughout the system. Increased understanding of the water sources can help to model circulation patterns in carbonate platforms, benefiting coastal groundwater management in the Yucatan and similar regions around the globe.

Natural water is made up of light and heavy isotopes of both hydrogen (^{1}H and ^{2}H a.k.a. deuterium) and oxygen (^{16}O and ^{18}O). For all isotopes, the chemical bond associated with lighter isotopes is weaker and easier to break. Therefore, when a compound undergoes a physical or chemical process, the lighter isotopes react before the heavier isotopes. As water evaporates, the lighter isotopes (both ^{1}H and ^{16}O) react first resulting in a water vapor that is lighter than the water left behind. The water vapor becomes more "depleted" in the heavy isotopes (^{2}H and ^{18}O) relative to the remaining water, whereas the remaining water becomes "enriched" in the heavy isotopes, relative to the water vapor (Gat 1996). Isotope concentrations are expressed in units of δ, which represents the deviation of the fraction of the heavy isotope (R_{sample}) to that of some standard ($R_{standard}$) (Fry 2006), typically the Vienna Standard Mean Ocean Water (VSMOW)

$$\boldsymbol{\delta}^{18}O \text{ or } \boldsymbol{\delta}^{2}H\ (‰) = [(R_{sample}/R_{standard}) - 1] \mathbf{x}\ 1000 \qquad (2.1)$$

Isotopic composition of groundwater is conserved throughout subsurface flow; therefore the source of the groundwater can be determined by comparing its isotopic composition to that of nearby endmembers (Gat 1971). The composition of the final mixture will therefore approach the intermediate between isotopically distinct endmembers, as shown by the equation:

$$Q_F = Q_1 + Q_2 \quad (2.2)$$

where Q_1 and Q_2 are the isotopic compositions of the two endmembers and Q_F is the composition of the final mixture. While salinity is used to differentiate the origin as marine or fresh, isotopic composition can be used to further constrain the source of freshwater (meteorological vs. groundwater) and salt water (recent marine influx vs. deep brine layers).

Processes that dictate isotopic fractionation are similar for hydrogen and oxygen; therefore they behave alike in the hydrologic cycle. The strong relationship between the hydrogen and oxygen isotopes in rainwater is reflected in a regression line known as the global meteoric water line (GMWL):

$$\delta D = 8*\delta^{18}O + d \quad (2.3)$$

where the slope of the line is 8 and the deuterium excess (d) is typically around 10 $^{o}/_{oo}$. The slope is indicative of the atmospheric humidity (Fig. 2.2) and the degree of evaporation. Water subject to evaporation will plot below the GMWL with a smaller slope between 4 and 7 (Ingraham 1998). The deuterium excess represents the atmospheric vapor source of local precipitation. A high d-excess in groundwater

represents recycled precipitation, whereas smaller or negative values represent raindrop evaporation (Peng et al. 2010).

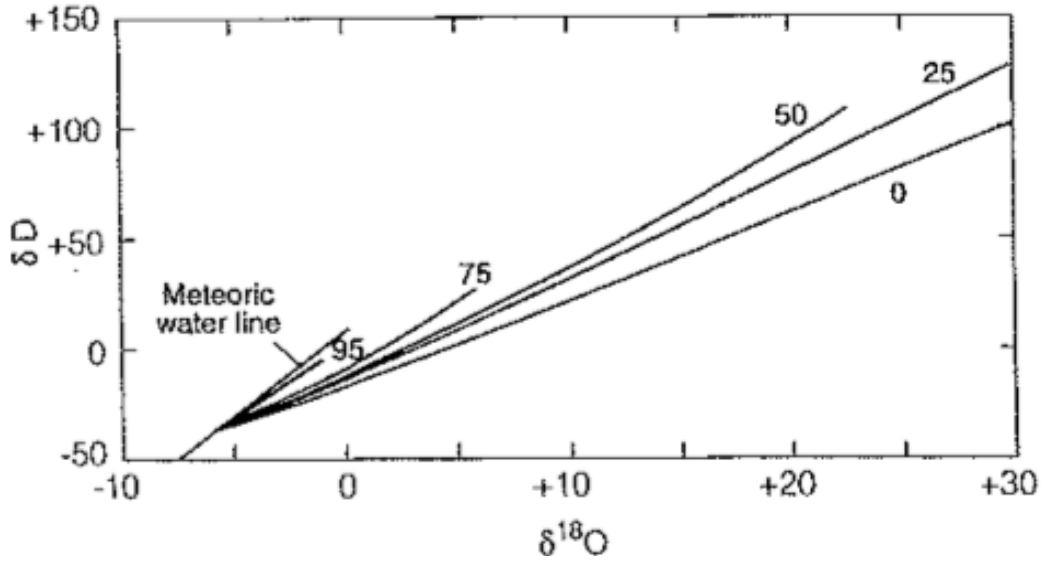

Fig. 2.2. Isotopic composition of meteoric water lines under differing ambient humidity. The numbers associated with each line represent the percent of remaining water. Source: (Ingraham 1998).

The GMWL is derived from rainfall samples all over the globe and used for comparisons on such a scale. Regional comparisons can be made using a local meteoric water line (LMWL): a regression line of oxygen and hydrogen isotopic values from local surface, groundwater, and precipitation samples. Two LMWLs, similar to each other, were reported from literature on hydrology in the Yucatan including Socki et al. (2002) (Eq. 2.4) and Hodell et al. (2012) (Eq. 2.5).

$$\delta D = 8.11 * \delta^{18}O + 10.4 \quad (2.4)$$

$$\delta D = 7.18 * \delta^{18}O + 8.1 \quad (2.5)$$

The LMWL from Socki et al. was measured from samples taken in the northern Yucatan Peninsula, near Merida, with nearby sea samples from the Gulf of Mexico. This LMWL closely resembles the GMWL, indicating the aquifer in this region is not subject to evaporative enrichment (Socki et al. 2002). The LMWL of Hodell et al. (2012) was collected from Lake Chichancanab, near the center of the Yucatan Peninsula. This LMWL exhibits a smaller slope (7.18) and d-excess (8.10) indicating some evaporation and a more depleted atmospheric vapor source. LMWLs and circulation models created from isotope data can be essential tools in understanding water budgets in groundwater dependent ecosystems. It is surprising the lack of isotope work that has been done on this part of the Yucatan, a region almost solely dependent on groundwater as a freshwater source.

Methods

During a week of scientific cave dives beginning on March 16th 2011 (the end of the Yucatan's rainy season), water samples, field observations, and *in situ* measurements of physicochemical water parameters were taken in Sistema Crustacea. Certified scientific cave divers using open circuit SCUBA and following the standards set by the National Speleological Society – Cave Diving Section (NSS-CDS) conducted all data collection inside the cave. A semidiurnal tide persists along the coast near Puerto Morelos with a mean tidal range of 17 cm and takes place ca. 50 minutes later each day (Coronado et al. 2007). In order to maintain tidal consistency between sampling and *in*

situ measurements, dives were conducted at 10 AM the first day and progressed 50 min. later throughout the next three days.

An YSI 600 XLM Multi-Parameter Datasonde was used to measure *in situ* salinity, temperature, dissolved oxygen (DO), pH, and depth throughout the water column. Measurements were taken every four seconds in order to create depth profiles of the environmental variables. The lead diver carried the datasonde with the probes in front to ensure an undisturbed water column. Sistema Crustacea is not a tourist destination as are many of the "show cenotes" in the area and is rarely dived. Previous observations in the system indicated that water stratification returns to normal conditions within 24 hours of the previous dive.

To compare the spatial variability of the physicochemical parameters across the entire system, three profiles were taken in the Eastern Section: the first profile of Cenote Crustacea began at the surface of the entrance pool and ended 2 m immediately beneath H2 (Fig. 2.3); the second profile began 2 m above H1 in Cenote Thermosbaenacea and ended 2 m beneath H2, at Cup 4; the third profile began 2 m above H2 in the Shrimp Domes and ended 2 m immediately beneath H2, at Cup 9. One profile was taken from the Western Section for further comparison: the fourth profile began at the surface of the Cenote Crustacea entrance pool and ended beneath H2, in the deepest section of the crack. In order to compare the temporal variability of the parameters, data was used from profiles taken in Cenote Crustacea during December 2003, June 2004, July 2006, and March 2011. Each of these profiles began in the Cenote Crustacea entrance and extended into the Eastern Section.

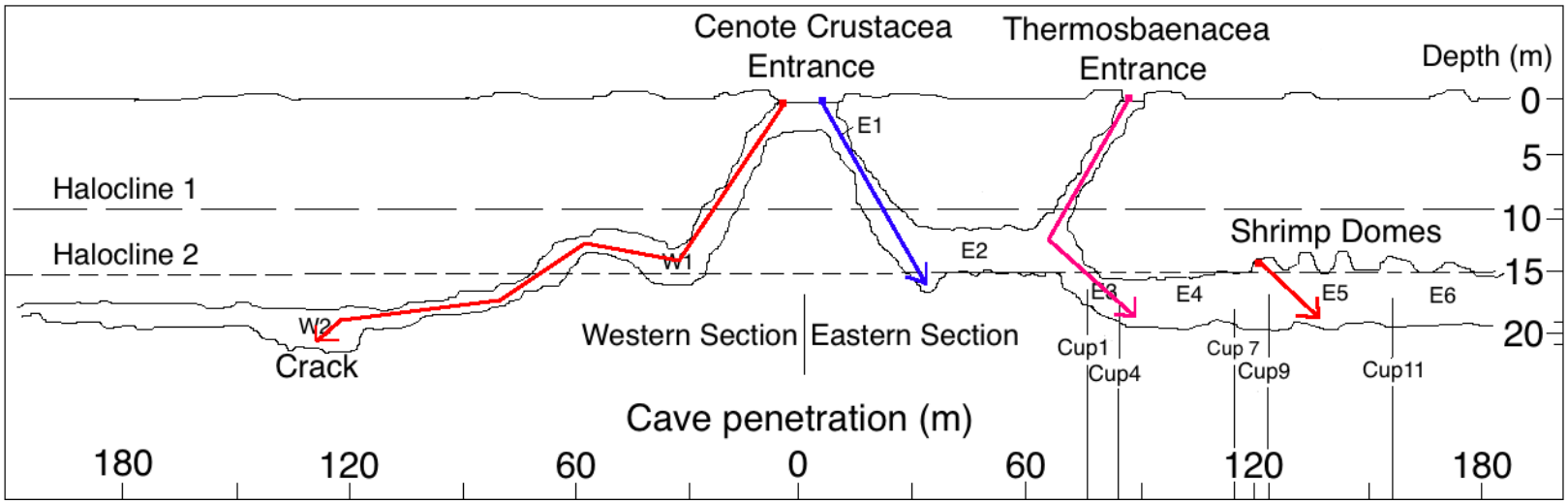

Fig. 2.3. Schematic diagram of Sistema Crustacea outlining physicochemical profiles within the Eastern and Western (long red line) Sections. Eastern Section profiles include Cenote Crustacea (blue line), Cenote Thermosbaenacea (pink line), and Cup 9 (short red line). Eastern (E1 – E6) and Western zones (W1-W2) are labeled here in the center of the passage. Cups 1-11 represent boundaries of sampling stations.

Collection of Water Samples for Isotope Analysis

Water samples were collected from specific locations within the cave and from nearby endmembers (Table 2.1). Endmember samples were collected from: the Cenote Crustacea pool, the open sea (20 m offshore), an inland groundwater well (2 km inland in Puerto Morelos), an inland karst window (10 km inland), a nearby mangrove swamp (0.5 km from the coast), and rain water. The rain endmember was collected during a short meteoric event (ca. 15 minutes). After collection, a portion of each sample to be used for isotope analysis was transferred into a 10 mL glass vial and sealed with a coned cap to eliminate headspace. All samples were transported on ice and kept refrigerated until laboratory analysis.

Cave water samples were collected at the same time as the *in situ* water parameter analysis. A second diver collected the samples outside of the lead diver's wake, in undisturbed water. Visual cues, such as halocline mixing or silt percolation from the roof of the cave, were used to indicate diver-disturbed water. Water samples were collected in acid washed 125 mL Nalgene Fluorinated Polyethylene (FLPE) bottles to prevent carbon contamination in the CDOM and DOC samples. In order to prevent implosion at depth, the FLPE bottles were prefilled with distilled water. At the designated depth for each sample, the diver inverted the bottle and filled it with air from the spare regulator. The diver then moved the bottle to undisturbed water and righted the bottle to allow sample water to trickle in as the air bubbles flowed out.

Table 2.1. Water sampling matrix for Sistema Crustacea, March 2011.

Sample	Location	Zone	Depth (m)	Linear penetration (m)
1	Pool	Pool	1.0	0
2	2-E1_fr_2011	E1	7.6	4
3	3-E1_H1_2011	E1	9.5	6
4	4-E2a_br_2011	E2	11.6	8
5	5-E2b_br_2011	E2	14.6	18
6	6-E2c_br_2011	E2	14.5	28
7	7-E2d_br_2011	E2	14.6	38
8	8-E3_br_2011	E3	12.7	76
9	9-E3_H2_2011	E3	14.8	78
10	10-E3_ma_2011	E3	16.8	80
11	11-E4_br_2011	E4	12.4	118
12	12-E4_H2_2011	E4	14.8	120
13	13-E4_ma_2011	E4	15.6	122
14	14-E5_br_2011	E5	12.2	130
15	15-E5_H2_2011	E5	14.3	132
16	16-E5_ma_2011	E5	16.1	134
17	17-E6_br_2011	E6	12.9	160
18	18-E6_H2_2011	E6	14.9	162
19	19-E6_ma_2011	E6	16.1	164
20	20-W1_ma_2011	W1	15.1	78
21	21-W2_ma_2011	W2	18.7	130
22	22-W2Cr_ma_2011	W2	21.4	132
27	27-Karst_2011	n/a	0.0	n/a
28	28-Rain_2011	n/a	0.0	n/a
29	29-Well_2011	n/a	0.3	n/a
31	31-Sea_ma_2011	n/a	0.3	n/a
32	32-Mangrove_2011	n/a	0.3	n/a

March 2011 cave samples were collected at varying depths to create a profile for hydrological parameters. Samples names were represented by the sample number, the zone where it was collected, and the layer collected. All freshwater layer samples were denoted by the ending "_fr" and were collected 2 m above H1. All brackish layer samples were denoted by the ending "_br" and were collected 2 m above H2. All marine layer samples in the cave were denoted by the ending "_ma" and were collected 2 m below H2. Samples were first collected in zone E1 within the freshwater layer (labeled as 2-E1_fr) and within H1 (3-E1_H1). Samples in zone E2 were collected immediately 2 m below H1 in the brackish layer (4-E2a_br) and subsequently from 10, 20, and 30 m increasing penetration into the cave (5-E2b_br, 6-E2c_br, and 7-E2d_br). These samples were collected to determine the relative water source with increasing distance from the Cenote Crustacea entrance. Zone E3 samples were collected at Cup 1 from the brackish layer (8-E3_br), within H2 (9-E3_H2), and the marine layer (10-E3_ma). Replications of these samples were taken in zones E4, E5, and E6.

Only one sample was collected from Zone W1 in the marine layer at the "T" in the cave line (20-W1_ma). W2 samples were collected above the crack in the marine layer (21-W2_ma) and within the crack (22-W2Cr_ma) of the Western Section. Due to the remote location of this investigation and the transportation distance to labs at Texas A&M University at Galveston, a small number of samples were collected with limited replication.

Oxygen and Hydrogen Isotope Analysis

Hydrogen and oxygen isotopes in water from Sistema Crustacea were analyzed simultaneously by a cavity ring down spectrometer using a Picarro L2120-i isotope analyzer. Eight injections were measured from each sample and the first three injections were omitted to reduce any memory effect of the previous sample. The mean of the remaining injections was used to represent each sample. Calibration of the spectrometer was performed using two standards from the International Atomic Energy Agency (IAEA): Vienna Standard Mean Ocean Water 2 (V-SMOW2) and Greenland Ice Sheet Precipitation (GISP). Sample results were calibrated to V-SMOW2 by measuring three internal lab standards at the beginning, middle, and end of the 27-sample set. Internal standards included an isotopically enriched water source (tap water), a median value source (alpine spring water), and a heavily depleted source (Arctic river mix). These standards were calibrated against V-SMOW2 and GISP. Results are presented in parts per thousand ($^{o}/_{oo}$) relative to V-SMOW2.

Results

Field Observations

At the bottom of the open water entrance pool of Cenote Crustacea, divers noticed a strong hydrogen sulfide (H_2S) odor. Large quantities of leaf litter in various stages of decomposition were also observed on the floor of the open water. In addition divers observed a white cloud floating in portions of the shallow and deep haloclines within Cenote Crustacea (Fig. 2.4).

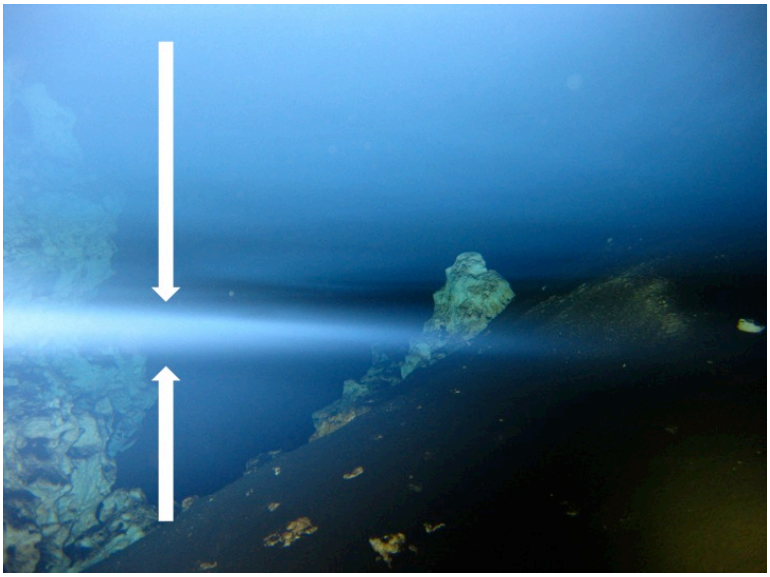

Fig. 2.4. Arrows point to the white cloud observed within shallow halocline of the Eastern Section, Cenote Crustacea at 9 m depth. Photo by Julie Niesch.

Physicochemical Water Parameters

Results from the physicochemical investigation are divided into three parts: (1) the detailed results of the physicochemical conditions in Cenote Crustacea (Fig. 2.5), (2) the spatial variability of the conditions throughout the entire Sistema Crustacea (Fig. 2.5 and 2.6), and (3) the temporal variability of Cenote Crustacea from four separate years (Fig. 2.7). Depth vs. time was plotted (data not shown) to ensure a consistent speed of decent throughout the profile.

Salinity and Temperature

The water in the open pool section of Cenote Crustacea was fresh (1.3‰) compared to deeper waters in the cave (Fig. 2.5A). At 9.7 m, the salinity sharply

increased to 12.9 ‰ marking the lower boundary of H1. Constant salinity in the brackish layer (13.5‰) extended from 10 to 14.4 m deep. At 14.8 m, the salinity sharply increased to 33.4‰ marking the lower boundary of H2. Salinity in the marine layer (35.7 ‰) was similar to the nearby seawater endmember (36.0 ‰).

Waters within the Cenote Crustacea entrance pool exhibited the highest temperatures (27.2 °C) in the system (Fig. 2.5B). Beneath the photic zone, the temperature gradually decreased with depth and linear penetration into the cave until reaching a local minimum (24.3 °C) at 7.6 m. Beneath this minimum, the temperature began to increase until 9.7 m marking the lower boundary of the shallow thermocline, the same depth as the shallow halocline. The temperature throughout the brackish layer (25.1 °C) was roughly equal to the median of the freshwater layer above and the marine layer below. A sharp increase in temperature at 14.8 m marked the lower boundary of the deep thermocline, the same depth as the deep halocline. A secondary temperature maximum (26.6 °C) existed at 17 m. in the marine layer, below which the temperature began to decrease.

Dissolved Oxygen and pH

The open pool was normoxic (4.2 mg/L) and exhibited the highest DO concentration within Cenote Crustacea (Fig. 2.5C). Concentrations decreased gradually with depth and linear penetration into the cave until reaching extreme hypoxia (0.4 mg/L) at the lower boundary of H1 (9.7 m). Within the brackish layer, the DO remained within the extreme hypoxia range (0.6 – 0.7 mg/L). At approximately 17 m, two meters

below H2, there was a local DO maximum (1.8 mg/L). Below this maximum, DO began to decrease again within the marine layer, the same depth at which the temperature began to decrease.

The pH of the Cenote Crustacea pool was basic (8.14) and decreased with depth (Fig. 2.5D). A local minimum in the pH (6.92) was observed at the lower boundary of H1 (9.7 m) and waters remained acidic throughout the entire brackish layer. A system minimum (6.90) occurred within H2. In the marine layer however, the pH increased with depth to a local maximum (7.24) at 17 m, the same depth at which a local DO maximum was observed. The pH in the marine layer was still lower than the literature values for pH in the Caribbean Sea along the Yucatan coast of, between 7.90 and 8.10 (Mutchler et al. 2007).

Spatial Variability of Physicochemical Parameters

Three separate profiles were taken for comparison within the Eastern Section: Cenote Crustacea, Cenote Thermosbaenacea, and Cup 9 (Fig. 2.5). A single profile was also taken in the Western Section; the Cenote Crustacea profile was used as the representative for the Eastern Section (Fig. 2.6).

Salinity profiles in Cenote Thermosbaenacea and Cup 9 were similar to the Cenote Crustacea profile (Fig. 2.5A). However, the depth of H2 became progressively shallower with proximity to the coast. H2 was a full 1 m shallower in the Cup 9 profile than the Cenote Crustacea profile. Little difference was found between the salinity profiles of the Western and Eastern Sections (Fig. 2.6A).

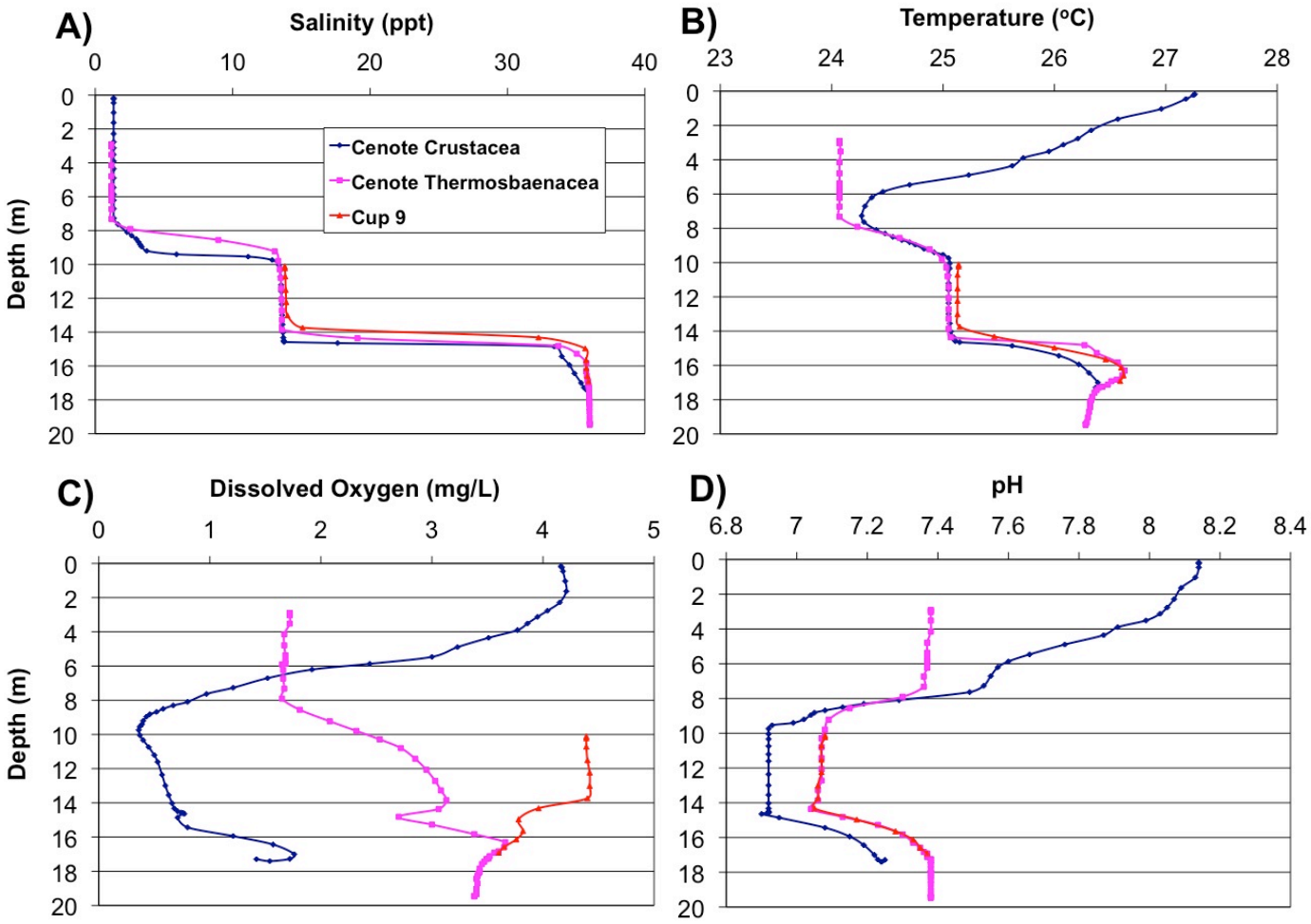

Fig. 2.5. Physicochemical profiles of (A) salinity, (B) temperature, (C) dissolved oxygen, and (D) pH in the Eastern Section of Sistema Crustacea, March 2011. Three separate profiles began at the Cenote Crustacea entrance (blue line), Cenote Thermosbaenacea entrance (pink line), and Cup 9 (red line).

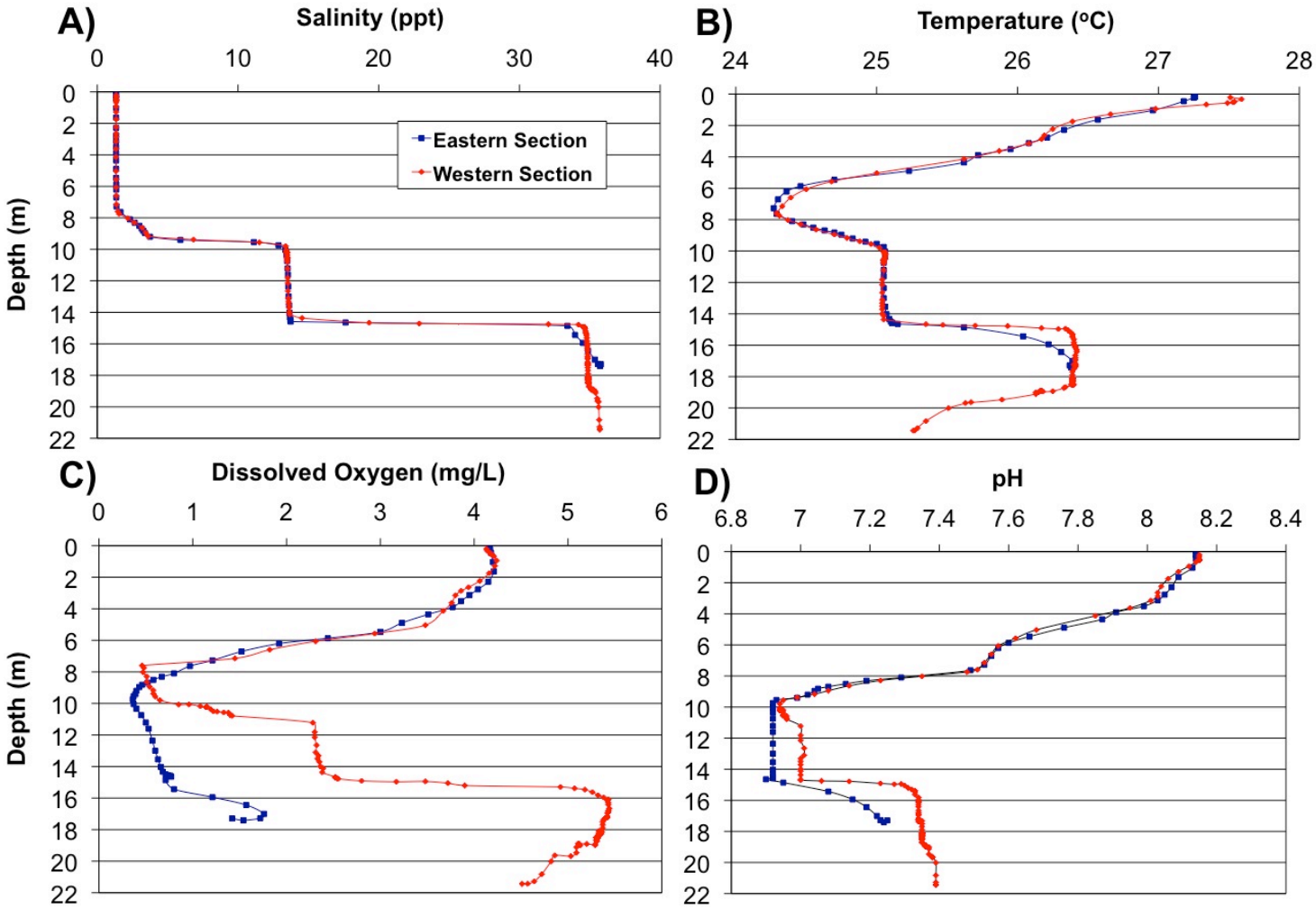

Fig. 2.6. Physicochemical profiles of (A) salinity, (B) temperature, (C) dissolved oxygen, and (D) pH in the Eastern (blue line) and Western Sections (red line) of Sistema Crustacea, March 2011. Both profiles began in the Cenote Crustacea entrance.

The temperatures of the brackish and marine layers in the three Eastern profiles were quite similar (Fig. 2.5B). However, temperatures in the freshwater layer were higher in Cenote Crustacea than Cenote Thermosbaenacea, most likely due to the larger, un-shaded opening in the Crustacea pool. There was little difference between the temperature profiles for the fresh and brackish layers in the Eastern and Western Sections (Fig. 2.6B). Within the marine layer of the Western Section, the temperature remained constant until the thermocline at 18 m, beneath which the temperature decreased significantly with depth. The crack in the Western Section exhibited the lowest temperature of the marine waters.

The shallow, aphotic zone of the freshwater was moderately hypoxic in Cenote Thermosbaenacea (1.7 mg/L) compared to the same layer in Cenote Crustacea (4.04 mg/L)(Fig. 2.5C). In the brackish layer however, DO was lowest in Cenote Crustacea (0.37 mg/L) and increased with each profile further into the cave. The highest DO concentration occurred in the brackish layer of the Cup 9 profile (4.4 mg/L), even greater than the open water pool of Cenote Crustacea (4.2 mg/L). Within H2 of Cenote Thermosbaenacea and Cup 9, local DO minima occurred. However, within the same halocline of Cenote Crustacea, a local maximum occurred.

DO levels were similar in the freshwater layer of the Eastern and Western Sections (Fig. 2.6C). However, the DO profiles varied greatly in the deeper layers of these sections. In the Western Section, DO maxima were higher in the brackish (2.3 mg/L) and marine layers (5.4 mg/L) compared to Cenote Crustacea (0.7 and 1.8 mg/L, respectively). The Western Section also contained a sharp increase from 1 to 2.3 mg/L at

11 m, marking the lower boundary of an oxycline that was not present in Cenote Crustacea. Beneath the thermocline at 18 m and passing into the cold-water crack, the DO levels began to decrease with depth, from 5.3 mg/L to 4.5 mg/L.

Overall, the pH in the aphotic zone of the freshwater layer was more basic in Cenote Crustacea (8) than Cenote Thermosbaenacea (7.4) (Fig. 2.7D). Within the brackish layer, however, the pH was slightly acidic (6.9) in the Cenote Crustacea profile and slightly basic (7.1) in the other two profiles. The pH profiles in the freshwater layer of the Western and Eastern Sections closely resembled each other (Fig. 2.6D). Within the Western Section however, there was a small increase from 6.9 to 7.1 at 11 m, the same depth as the unusual oxycline. Beneath this chemocline, the brackish layer was neutral (7.0) and inherently more similar to the Thermosbaenacea and Cup 9 profiles than to Cenote Crustacea.

Temporal Variability of Physicochemical Parameters

Physicochemical parameters were compared from datasonde profiles taken in the Eastern Section of Sistema Crustacea, starting in the Cenote Crustacea pool, during December 2003, June 2004, July 2006, and March 2011 (Fig. 2.7A-D). Although these datasets do not strictly compare conditions over the years, the physicochemical parameters are representative of different seasons and inherently different climate, rainfall, and oceanic conditions. It is important however to note the increased variability of each parameter over time.

The salinity of the brackish layer and the depth of H1 varied throughout the years (Fig. 2.7A). Water temperature was the most variable within with upper layers, whereas the deeper layers exhibited less than 1^{o}C difference between the years (Fig. 2.7B). Similarly, DO also varied over the years with the most variability found in the upper layers (Fig. 2.7C). The DO profile from 2003 included measurements below 0.0, suggesting the oxygen sensor malfunctioned during the dive; this profile was therefore omitted from the dataset. The pH profiles also varied throughout the years (Fig. 2.7D).

Water Isotopes

Annual climate throughout the Yucatan is divided into a dry season (March-May), a rainy season (June-October), and a "nortes" season (November-February). Nortes are frontal passages carrying rainfall (20-50 mm) and strong (50-90 km/hr) northerly winds (Alvarez-Gongora and Herrera-Silveira 2006). During the month of February and the first 15 days of March, 2011, the mean air temperature was 22.8^{o}C with a mean humidity of 77.4%. During this time, the total precipitation was 47.86 mm with the majority of the rain (46.16 mm) falling on February 11th and 12th, nearly one month before the 2011 fieldwork, based on reports from the nearest weather station at Cancun International Airport (www.wunderground.com/history). Winds during these two days were out of the north indicating the system was likely a norte.

A LMWL (Fig. 2.8) was created using linear regression of the isotopic composition of water collected from rain, surface features, and groundwater:

$$\delta D = 4.7*\delta^{18}O - 4.8 \quad (2.6)$$

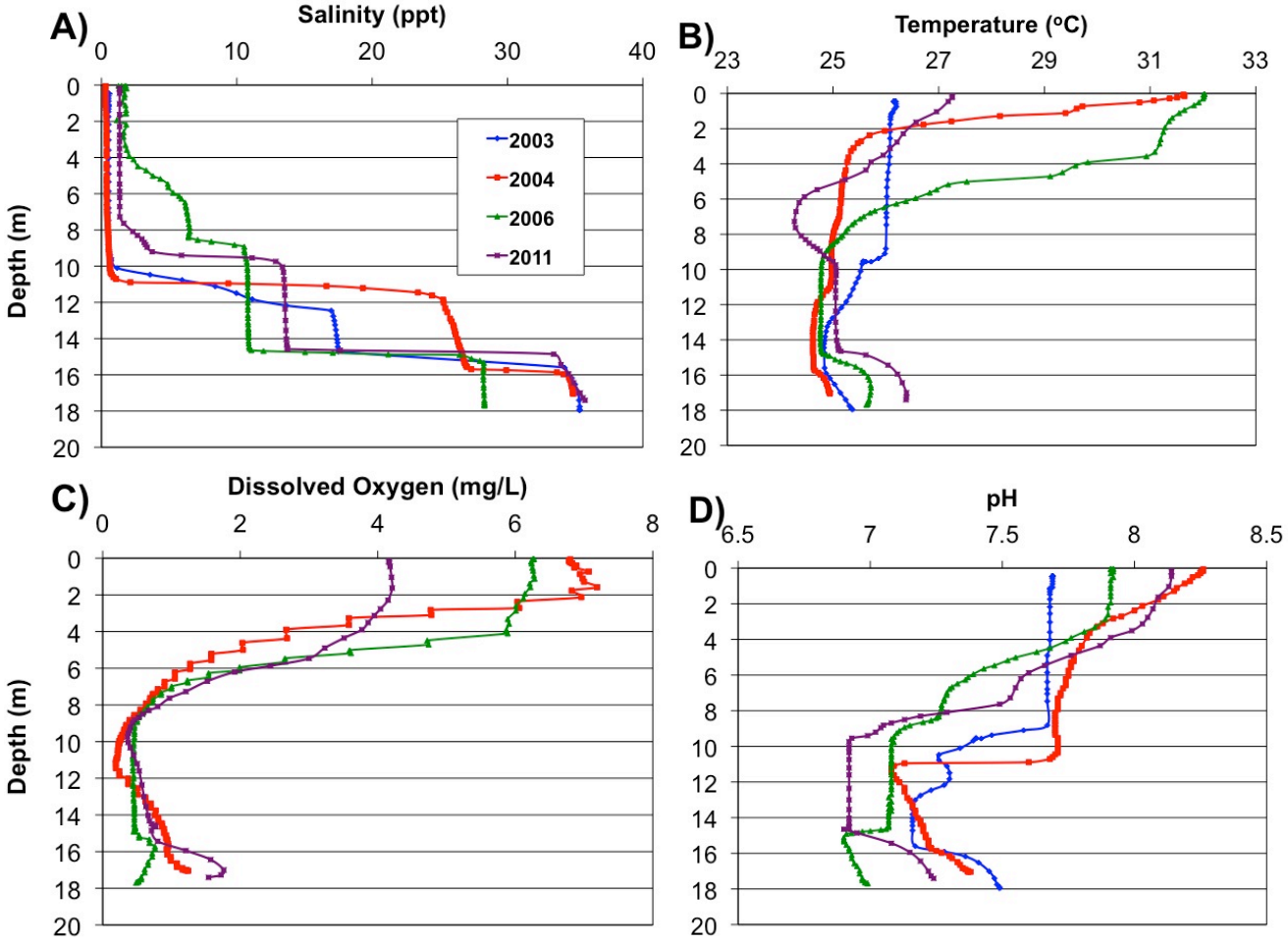

Fig. 2.7. Physicochemical profiles of (A) salinity, (B) temperature, (C) dissolved oxygen, and (D) pH in Eastern Section of Sistema Crustacea for December 2003 (blue line), June 2004 (red), July 2006 (green), and March 2011 (purple). Each profile began in the Cenote Crustacea entrance. Dissolved oxygen was inaccurately measured in 2003 and omitted from the profile.

The LMWL reported from Socki et al. (2002)($\delta D = 8.1*\delta^{18}O + 10.4$) and Hodell et al. (2012)($\delta D = 7.2*\delta^{18}O + 8.1$) were more similar to each other than the measured LMWL, which had a smaller slope (m = 7.2) and d-excess (-4.8). The LMWLs from literature were more similar to the GMWL ($\delta D = 8*\delta^{18}O + 10$) than the measured LMWL. Isotope investigations of surface samples collected from the Péten Lakes in Guatemala (Lachniet and Patterson 2009) found a LMWL (Eq. 2.7) much closer to our LMWL.

$$\delta D = 3.8*\delta^{18}O - 3.8 \quad (2.7)$$

Our measured LMWL and the GMWL shared a common data point at the intersection near the well sample (Fig. 2.8). This sample exhibited the most depleted isotope values ($\delta^{18}O = -4.7^{0}/_{00}$, $\delta D = -28.7^{0}/_{00}$) and was the farthest inland groundwater sample. The next most depleted values (Table 2.2) were in the rain sample ($\delta^{18}O = -2.7^{0}/_{00}$, $\delta D = -17.5^{0}/_{00}$). The mangrove sample was the most enriched ($\delta^{18}O = 6.1^{0}/_{00}$, $\delta D = 29.2^{0}/_{00}$), followed by the karst window ($\delta^{18}O = 4^{0}/_{00}$, $\delta D = 17.6^{0}/_{00}$), and the Cenote Crustacea pool ($\delta^{18}O = 3.0^{0}/_{00}$, $\delta D = 2.9^{0}/_{00}$). These three samples were the only surface samples collected from inland locations. The open sea sample ($\delta^{18}O = -0.3^{0}/_{00}$, $\delta D = -4.1^{0}/_{00}$) was more depleted than marine samples from within the cave. The open sea sample was also more depleted than the reported values for the Caribbean Sea along this coast ($\delta^{18}O = 1.3^{0}/_{00}$, $\delta D = 7.9^{0}/_{00}$) (Socki et al. 2002). Within zones E3, E4, and E6, there was a trend towards lighter values in the brackish layer, medium values in H2, and heavier values in the marine layer (Table 2.2). In addition, brackish samples from E1,

E2, and E4 were lighter than the freshwater sample from E1 ($\delta^{18}O = -1.5^{0}/_{00}$, $\delta D = -12^{0}/_{00}$) and much lighter than the seawater endmember.

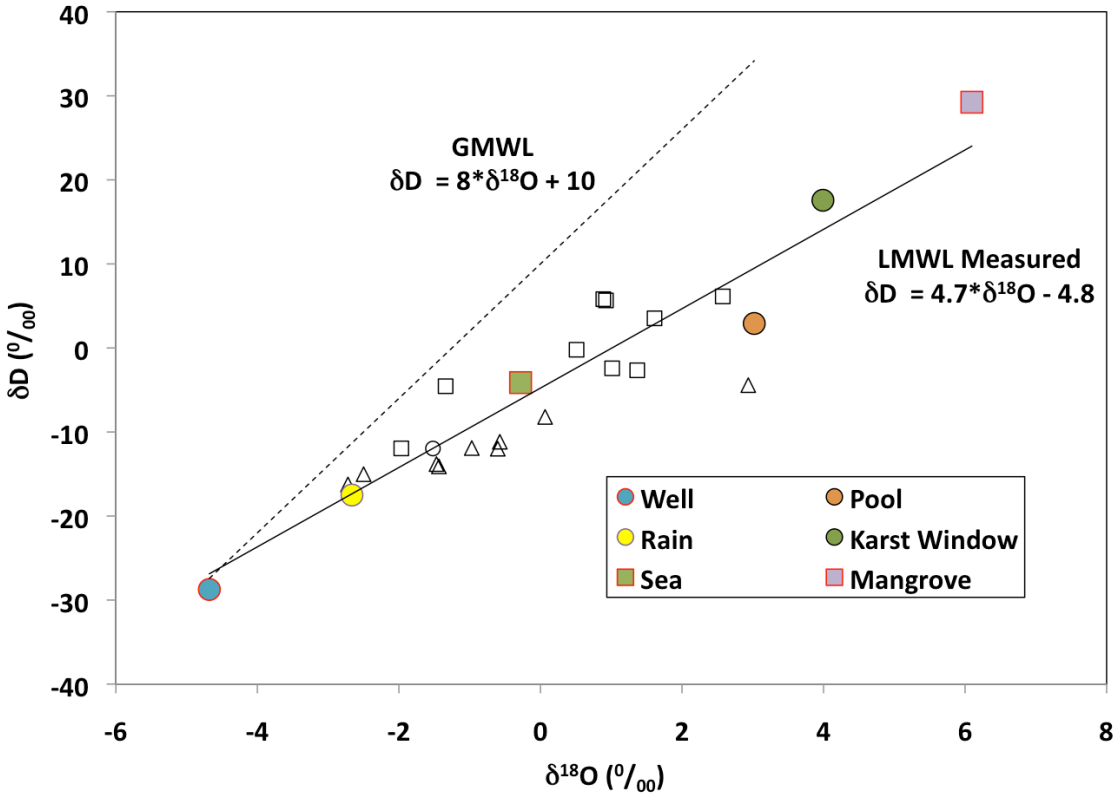

Fig. 2.8. δD and $\delta^{18}O$ of fresh (circles), brackish (triangles), and marine water (squares), collected from Sistema Crustacea and endmembers in March 2011. Endmembers include: well (blue circle), rain (yellow circle), open sea (green square), Crustacea pool (orange circle), and mangrove (purple square). The solid line represents the measured LMWL estimated by linear regression of the measured data. The dashed line represents the LMWL reported in Socki et al., 2002.

Discussion

Water Sources within Sistema Crustacea

As expected, the upper layer of Cenote Crustacea was relatively fresh (salinity = 1.34‰) compared to deeper layers. The composition of the pool ($\delta^{18}O$ = 3.0‰, δD = 2.9‰) was much more isotopically enriched than the rainwater endmember ($\delta^{18}O$ = -2.7‰, δD = -17.5‰) indicating that the water in the pool has undergone excessive evaporation (Fig. 2.9). The pool also exhibited elevated temperatures, most likely due to direct insolation. A source of the pool water may be derived from precipitation, ground water or more likely, a combination of both. However, since the final isotopic composition has been significantly enriched by evaporation, it is difficult to characterize the sources. Two other surface features, the mangrove endmember ($\delta^{18}O$ = 6.1‰, δD = 29.2‰) and the karst window endmember ($\delta^{18}O$ = 4.0‰, δD = 17.6‰) , also exhibited highly enriched values indicative of excessive evaporation. Each of these samples may also provide the isotopic composition of the interstitial soil water. Unfortunately each endmember sample collected near the surface is subject to increased variability from differing evaporation rates as well as varying precipitation sources. Therefore, it is more useful to compile all of the data points into a trend line such as the LMWL.

Table 2.2. $\delta^{18}O$ and δD values for samples from Sistema Crustacea and nearby end members, collected in March 2011. Isotopic values are in units of per mil ($^{0}/_{00}$).

Sample	$\delta^{18}O$	δD	Depth (m)
1-Pool	3.0	2.9	1.0
2-E1_fr	-1.5	-12.0	7.6
3-E1_H1	0.1	-8.2	9.5
4-E2a_br	-1.4	-14.1	11.6
5-E2b_br	-0.6	-11.2	14.6
6-E2c_br	-1.5	-13.8	14.5
7-E2d_br	-2.7	-16.2	14.6
8-E3_br	-1.0	-11.9	12.7
9-E3_H2	-1.3	-4.6	14.8
10-E3_ma	0.5	-0.2	16.8
11-E4_br	-2.5	-15.0	12.4
12-E4_H2	1.4	-2.7	14.8
13-E4_ma	0.9	5.8	15.6
14-E5_br	2.9	-4.4	12.2
15-E5_H2	-2.0	-12.0	14.3
16-E5_ma	1.6	3.5	16.1
17-E6_br	-0.6	-12.0	12.9
18-E6_H2	1.0	-2.4	14.9
19-E6_ma	0.9	5.7	16.1
20-W1_ma	2.6	6.1	15.1
21-W2_ma	0.9	4.8	18.7
22-W2Cr_ma	0.9	5.5	21.4
27-Karst	4.0	17.6	0.0
28-Rain	-2.7	-17.5	0.0
29-Well	-4.7	-28.7	0.3
31-Sea_ma	-0.3	-4.1	0.3
32-Mangrove	6.1	29.2	0.3

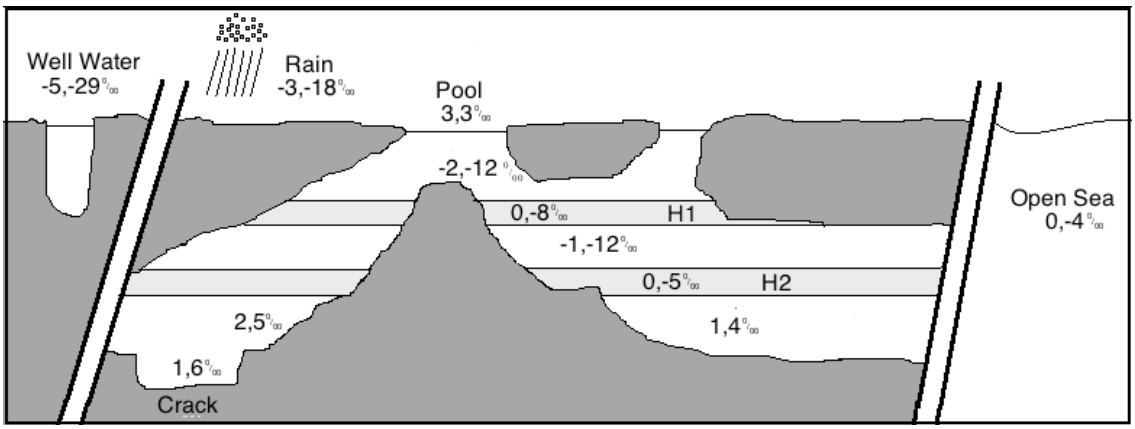

Fig. 2.9. Isotope values ($\delta^{18}O$, δD **‰)** from hydrologic layers of Sistema Crustacea as well as rain, well water, and open sea endmembers (outside the two slanted lines). Brackish, H2, and marine values are represented as the mean of all samples in that layer. All values were rounded to whole numbers.

The small value of the LMWL slope (4.7) suggests elevated levels of evaporation in this region of the Yucatan. The LMWLs from Hodell et al. (2012) and Socki et al. (2002) found little evidence of such intense evaporative enrichment. However, the LMWL from Lachniet and Patterson (2009) exhibits a similarly small slope indicating surface water in nearby Guatemala is also subject to evaporative enrichment. During our field sampling, the mean ambient humidity in Puerto Morelos was 77.4% (www.wunderground.com) and the measured LMWL should therefore plot near the 75% humidity line (Fig. 2.2). However, our LMWL still plots beneath the 75% line, indicating additional factors are responsible for the excessive evaporation, (discussed in the paragraph below). The location of the LMWL beneath the GMWL also suggests δO^{18} and δD enrichment from re-circulation of seawater. A similar trend was observed in hydrological investigations of SGD around Sicily (Schiavo et al. 2009).

The low deuterium excess (d = -4.8) of our measured LMWL indicates that the atmospheric vapor source of precipitation in the region is more isotopically depleted than the global average, the d-excess (d = 10) of the GMWL. The negative d-excess in the LMWL from Lachniet and Patterson (2009) also indicates an isotopically depleted vapor source. It is unlikely that transpiration leads to such negative values. Transpiration does not affect the d-excess since the moisture from the vegetation that is returned to the atmosphere is identical to the local precipitation (Marfia et al. 2004). Negative d values have been linked to raindrop evaporation (Peng et al. 2010), which may be responsible for the values observed here. In their hydrological investigation of the Yucatan Peninsula, Beddows et al. (2007) observed a general cooling in the freshwater layer near the Caribbean coast and proposed that the primary source of recharge in the aquifer is precipitation from convective cells, during which condensation takes place at much higher and cooler elevations. As the elevation of the atmospheric source increases, the precipitation temperature decreases, resulting in a water source that is much cooler than the surface. Precipitation derived from higher elevations is also more isotopically depleted, a phenomenon known as the "altitude effect" (Gat 1996). I can therefore conclude that the primary source of freshwater recharge along the coast is derived from higher elevation precipitation (convective storm cells) that is subject to raindrop evaporation.

The most depleted values were observed in the well water ($\delta^{18}O$ = -4.7‰, δD = -28.7‰) indicating either 1) the groundwater located farther inland is subject to less evaporation or 2) the meteoric source to the groundwater farther inland is more depleted

than the rains along the coast or a combination of both. With increasing distance inland the values of the rain become more depleted, a phenomenon commonly referred to as the "continental effect" (Ingraham 1998). Additional isotopic depletion may arise from the "amount effect" in which increased rainfall yields more depleted isotopic composition of the precipitation (Gat 1996). Considering the amount of rainfall during the norte in February, it is likely that this event contributed significantly to recharge and the inherent isotopic composition within the aquifer. The LMWL from Socki et al. (2002) is similar to the GMWL, which intersects our measured LMWL near the well water data point (Fig. 2.8), a sample collected only 2 km inland. This intersection indicates that the freshwater source farther inland is subject to less evaporationand is more isotopically consistent.

The presence of the temperature minimum at 7 m (2 m above H1) suggests an influx of cool freshwater, from either groundwater sources upstream or low temperature precipitation near the coast, as described above. The isotopic composition of this layer ($\delta^{18}O$ = -2‰, δD = -12‰) is much closer to the rainwater than the well water endmember. The resulting isotopic composition is therefore likely derived from cooler, isotopically depleted precipitation, i.e., the rainwater endmember ($\delta^{18}O$ = -2.7‰, δD = -17.5‰), mixing with a depleted freshwater source, like the cenote pool endmember ($\delta^{18}O$ = 3‰, δD = 2.9‰).

The brackish and marine layers exhibited values of medium (salinity = 13.5‰) and full strength salinities (salinity = 36‰) respectively; the salinity in the latter was equivalent to the nearby open sea endmember. Isotopic compositions also mix

conservatively and therefore the final composition of a sample should approach the intermediate between the endmembers, along the LMWL. Based on the average isotopic composition within the brackish layer ($\delta^{18}O$ = -1‰, -δD = 12‰) and the median values in the salinity profiles, I can disregard the freshwater layer ($\delta^{18}O$ = -1.5‰, δD = -12‰) above H1 as the mixing source in the brackish layer; the isotopic values are too similar and do not agree with the basic mixing model. The isotopic composition of the brackish layer therefore resides between two sets of endmembers, both of which represent viable sources. The first is the well water ($\delta^{18}O$ = -4.7‰, δD = -28.7‰) and deep marine layer ($\delta^{18}O$ = 1‰, δD = 4‰) endmembers. The second is the rainwater ($\delta^{18}O$ = -2.7‰, δD = -17.5‰) and open sea ($\delta^{18}O$ = -0.3‰, δD = -4.1‰) endmembers. It is likely that the inland well water is subject to some evaporation along the underground path, based on the LMWL. Such evidence suggests that the brackish layer is derived from precipitation recharge mixing with the open sea endmember. Such mixing would indicate counter current flow of the shallow Caribbean waters inland. Evidence for and against the counter current model within Sistema Crustacea is discussed in the section below.

Evidence for Decoupled Saline Circulation

Contrary to my expectations, the mean value of the marine layer ($\delta^{18}O$ = 1‰, δD = 4‰) was isotopically enriched, suggesting that the shallow seawater endmember ($\delta^{18}O$ = -0.3‰, δD = -4.1‰) is not the source. According to the isotopic composition, the marine layer is derived from deeper waters within the aquifer, which most likely originate from isotopically enriched (i.e., heavier) seawater infiltrating the limestone

platform at unknown depths. Values in the marine layer resembled the reported values for the Caribbean Sea ($\delta^{18}O = 1.4‰$) (Teal et al. 2000); unfortunately δD values could not be located in the literature, further supporting the need for additional isotopic investigations in this region. The different $\delta^{18}O$ values for the open sea suggest that the isotopic values of the marine layer are highly variable. Our specific values may represent a snapshot of the seawater composition when the water infiltrated the aquifer. The values may also represent a seasonal average of the open sea. Different rates of precipitation and rainfall may create temporal variability in the isotopic composition of surface waters along the coast (Gat 1996), including the Caribbean Sea. Regardless, anomalies within the temperature and DO profiles indicate the influx of recent, oxygenated seawater within the upper 2 m of the marine layer, just beneath H2. Additionally, the water samples used for isotope analysis within the marine layer were collected 2 m below H2, the same depth at which the temperature and DO began to decrease. If two separate sources of marine water within the marine layer exist, as indicated by the differences in DO and temperature, our water sampling methods to collect isotope data did not accurately sample all sources within this layer. Based on the sampling bias of the marine layer, the following section provides additional evidence for decoupling of the saline circulation.

The increased DO and temperature within the upper 2 m of the marine layer present an anomaly within each of the profiles. The temperature and DO indicate an influx of warm, oxygenated marine waters just below H2. It is apparent from the elevated DO concentrations however, that exothermic microbial respiration is not the

source of the elevated temperatures. Additionally, the decreased DO and temperature of the waters below 17 m suggests that the deeper marine waters in the system are older and replenished less frequently. For instance, waters within the crack in the Western Section exhibited the coldest temperatures in the system as well as the lowest DO. The isotopic composition however does not suggest a water source inherently different from the other marine layer samples. This water is most likely derived from an unknown depth within the aquifer. These waters do not appear, however to be subject to the geothermal heating proposed in the generic convection circulation model.

The conventional circulation model proposes that seawater enters the carbonate platform and rises via geothermal heating or entrainment (Fig. 2.1) (Cooper 1959). In such a case, all of the marine waters within the cave would exhibit similar, depleted DO levels due to the geothermal heating and any potential respiration within the deep aquifer. The conventional circulation models however, do not account for the DO and temperature anomalies in the upper 2m of the marine layer. Instead, the evidence suggests that counter current flow of saline water, driven by tidal forces, induces an influx of warm, oxygenated waters within Sistema Crustacea. Although the isotope data does not support such flow, the sampling design may not have accurately portrayed the processes at work.

The question herein is the final fate of the seawater flowing inland. One serious implication in understanding seawater flow within the Yucatan is the fate of wastewater injected into the aquifer. Deep well injection into the saline water below the mixing zone is currently the government-mandated method of liquid waste disposal (Beddows et al.

2007). Based on the conventional model where marine water flows in the same direction as the freshwater, wastewater injected into the marine layer would flow offshore affecting reef and submarine ecosystems. However, based on the counter current model supported by our data, the inland flow of the marine layer would transport wastewater further inland with the potential for contamination of the freshwater aquifers (Beddows et al. 2007). Further work is needed in this area to determine the flow direction and driving forces of saline water transport. It is important to approach this subject with knowledge of both the conventional and counter current models in order to better manage resources within groundwater ecosystems and GDEs. Overall, a greater understanding of the hydrologic layers and their respective water sources in the groundwater of the Yucatan is needed. It is apparent from our research that future investigations of all anchialine systems should assess physicochemical parameters in the field in order to fine-tune sample design. Early detection of anomalies, such as the DO and temperature maximums observed in our study, can be used to more efficiently characterize the various water sources in the water column.

Spatial Variability of Salinity

The presence of such an intensely stratified system indicates there is little mixing within the water column. Overall, the evidence suggests that the brackish layer is derived from another location or another time. In the Yucatan, the brackish layer becomes thinner with increasing distance inland (pers. comm. T. Iliffe). This layer may derive from mixing processes between the fresh and marine layers further upstream. The

brackish layer may also derive from intense mixing events such as tropical storms or periods of immense rainfall. The temporal variations observed in the salinity profiles indicate that several processes may affect the formation of the brackish layer. Further work is needed to determine the source of this layer in various regions of the Yucatan.

Ecological Implications of Physicochemical Parameters

Recent investigations indicate that anchialine caves are spatially and temporally variable environments (Beddows et al. 2007; Pohlman et al. 1997; Seymour et al. 2007). Sinkholes and large entrances to cave systems provide a significant flow path for organic matter and water recharge (Pohlman et al. 1997; Simon et al. 2007). While Chapter III directly assesses the spatial variability of the organic matter in the system, the current chapter considers the spatial variability of physicochemical parameters directly influenced by biogeochemical processes within the water column, with particular emphasis on microbially mediated reactions.

Pohlman (2011) describes two conceptual models of microbial processes in anchialine caves: 1) a eutrophic system with sufficient organic matter influx to induce hypoxia and 2) an oligotrophic system with limited organic matter influx and therefore normoxic conditions throughout the water column. The water column in Cenote Crustacea exhibits conditions similar to the eutrophic model, with extreme hypoxia in the brackish layer and moderate hypoxia in the marine layer. Cenote Thermosbaenacea however, resembles the oligotrophic model with moderate hypoxia in the shallow portion of the brackish layer and normoxic conditions throughout the deeper parts of the

brackish layer and the entire marine layer. Cup 9 also resembles the oligotrophic model with normoxic conditions throughout the brackish and marine layers. In turn, the physicochemical profiles are noticeably different with increasing distance from the Cenote Crustacea entrance. I therefore propose the term "entrance effect" to describe the variability of conditions with increasing distance from the primary cenote entrance. While the concept of variable conditions with increasing cave penetration has been outlined in submarine caves (Gili et al. 1986; Gottstein et al. 2007), little work has been done to outline the variability of oxic states specifically within anchialine caves.

As expected, the DO, pH, and temperature in Cenote Crustacea were elevated in the photic zone of the surface waters. The Cenote Crustacea surface pool is much larger (ca. 300 m^2) than the Thermosbaenacea pool (ca. 10 m^2), which is completely covered over by foliage. The increased insolation of the Cenote Crustacea pool yields greater temperatures and greater oxygen production. The basic pH (8.1) within the open cenote is presumably derived from the photosynthetic consumption of inorganic carbon and production of bicarbonates. Also, meteoric water that interacts with the surrounding limestone becomes saturated in carbonates and bicarbonates before flowing into the open pool, further raising the alkalinity and pH (Schmitter-Soto et al. 2002). In addition to increased photosynthesis, direct sunlight penetrating to the cenote floor is capable of intense photodegradation of organic matter in the open water. Elevated temperatures also increase the rate of microbial biodegradation of vegetative detritus. Each of these factors can contribute to the formation and degradation of DOM within the water column.

Larger cenotes should therefore exhibit inherently greater influx of OM into the nearby cave passage (more on this in Chapt. 3).

DO and pH gradually decreased with penetration into the cave and increasing distance from the photic zone, indicating a transition from photosynthesis to respiration and further outlining the entrance effect. In Cenote Crustacea, a DO/pH minimum occurred in H1 suggesting that intense respiration is taking place, presumably within microbial communities. Without additional profiles of sulfur, methane, and nitrogen species, it is difficult to determine which particular microbial processes are responsible for the consumption of O_2. However, the investigation of the CDOM source in Chapter III provides information on the presence of microbial processes in the water column. For now, conclusions can be inferred from the aforementioned anchialine research in which microbial populations were linked to field observations and anomalies within the DO/pH profiles (Opsahl and Chanton 2006; Pohlman et al. 1997; Seymour et al. 2007).

White clouds, similar to those observed in Sistema Crustacea, have been reported from other anchialine cave around the globe (Gonzalez et al. 2011; Seymour et al. 2007). In Western Australia's Bundera Sinkhole, elevated bacterial populations were detected at the same depth as a H_2S maximum and DO minimum. H_2S production has been linked to the microbially mediated oxidation of organic matter coupled with sulfate reduction (Seymour et al. 2007). Based on the characteristic H_2S odor emanating from the floor of Cenote Crustacea and the visual presence of a white cloud within the haloclines, it is likely that there is a significant concentration of H_2S within H1. The presence of H_2S

indicates that its production and its consumption are taking place through sulfate reduction and aerobic sulfide oxidation, respectively.

In Cenote Crustacea, organic matter collects at the shallow halocline and becomes oxidized by aerobic heterotrophs. Once the oxygen is consumed, alternate electron acceptors are utilized. Presumably, sulfate from the marine and brackish waters becomes reduced, resulting in H_2S production. The extreme hypoxia in H1 and the brackish layer both provide conditions favorable to sulfate reduction. Any H_2S that flows into nearby more oxygenated layers, such as the moderately hypoxic marine layer, becomes aerobically oxidized by the microbial community.

Investigations of Cenote Mayan Blue have revealed a similar DO/pH minimum within the halocline accompanied by a spike in NO_3 (Pohlman et al. 1997). This DO minimum was attributed to microbially mediated oxidation of OM, coupled with nitrification. The source of the organic matter was POM trapped in the pycnocline associated with the halocline. While there is potential for nitrification and other microbial processes (e.g., methanogenesis, methanotrophy, denitrification) in Sistema Crustacea, the white clouds and strong H2S odor indicate that sulfate reduction and sulfide oxidation are the dominant processes responsible for the DO/pH minimum.

Within H2 of both Cenote Thermosbaenacea and Cup 9, a sharp DO/pH minimum suggests the presence of localized microbial respiration. If sulfate reduction is responsible for this local minimum, then both the brackish layer above and the marine layer below H2 provide normoxic zones for H_2S oxidation to occur. The Western Section exhibited a sharp increase in DO and pH at 11 m marking the lower boundary of

an oxycline not present in Cenote Crustacea. It is likely that the upstream position of the Western Section prevents the flow of OM beyond the vegetative debris fallout region of the Cenote Crustacea entrance. Therefore, the intense respiration that takes place near the cenote entrance does not reach as far into the Western Section. Profiles should indicate decreased levels of DOM in this section of the cave suggesting minimal energy sources for microbial respiration to take place.

The data here indicates that a single cave system can range from oxic to hypoxic to anoxic states. Based on the energy transfer models provided in Pohlman's (2011) overview of biogeochemistry in caves, different trophic states within a cave can produce inherently different microbial processes and diverse oxic states. The abundance of multiple oxic boundaries helps create transition zones allowing microbes to couple redox reactions. In turn, the increased diversity of microhabitats should lead to greater microbial and invertebrate biodiversity within a single cave system.

Temporal Variability of Physicochemical Parameters

It is important to note the large differences across seasons and years for several reasons. Like deep-sea environments, anchialine caves were originally believed to exhibit stable conditions throughout the year (Iliffe 1986). The data provided in this investigation indicates that salinity and pH can fluctuate with time. In addition, the depth of H1 can migrate vertically over the seasons, resulting in both ecological and geological implications. Based on the relatively constant depth of H2 over the years, the vertical migration of H1 can increase or decrease the habitat size for stygobitic species such as

atyid shrimp. During certain brackish water low or high stands, H1 can migrate below the cave floor or above the cave ceiling, greatly limiting the open water habitat available to stygobitic species. Geologically, the migration of H1 can lead to increased dissolution of the limestone at various levels. The decrease or increase in pH over time can also lead to faster or slower dissolution rates (Engel et al. 2004).

In July 2006, divers noted the lack of remipedes in the system. Remipedes from anchialine caves around the world have only been observed in the fully marine layer (Neiber et al. 2011). Such a restricted habitat range indicates that during significant disturbances the remipedes can only retreat into voids within the marine layer, most likely in deeper locations inaccessible to divers. Additionally, remipede larvae have been found in only one anchialine cave in the Bahamas (Tom Iliffe pers. comm.), but never in Sistema Crustacea or any other cave in the Yucatan Peninsula. It is possible that the same voids providing refuge for the remipedes during disturbance events also provide an important nursery habitat. Interestingly, the year in which all of the remipedes disappeared, 2006, was also the year with the lowest pH, DO, and salinity in the marine layer. In fact, it was the only year where the pH was lowest in the marine layer compared to the layers above. Based on the anomalous distribution of remipedes across the globe, future research characterizing the physicochemical ranges of remipedes would be profitable. Further knowledge of the physicochemical limits and geographic distribution of remipedes may provide additional insight into their routes of dispersion and colonization.

Future investigations should include monitoring daily and weekly fluxes within the ecologically significant sections of the cave. Additional research is needed to understand the effects of disturbance events on anchialine caves and how specific species react to such events. Although cave systems are typically highly stable environments, large disturbances from flooding events and hurricanes could significantly alter energy flow and physicochemical conditions within the water column. Additionally, a local rise in sea level caused by hurricanes or similar events may provide insight into the conditions and ecological implications that may occur with a 1 – 5 m rise in sea level due to global climate change.

Conclusions

Anomalies in the DO and pH profiles indicate the presence of microbial communities within Sistema Crustacea. The occurrence of H_2S and white clouds within H1 suggest the presence of sulfate reducing bacteria. Results from the quality and quantity of DOM affected by these microbial communities are presented in Chapter III. Additionally, results from the investigation of invertebrate diversity in relation to physicochemical variability are presented in Chapter IV. While the intense local minimums in the DO and pH profiles suggest microbial respiration is taking place, it is difficult to constrain which specific microbial processes are responsible. Therefore, it is important that future researchers also measure methane and the dissolved species of sulfur and nitrogen throughout the water column. Additionally, it is necessary to understand water sources in order to interpret which physicochemical parameters are a

result of microbial processes and which parameters represent conditions within the water source. In a system where oxygen production is limited to the open pool of the cenote, it is important to follow oxygen transport and consumption in order to locate microbial hot spots and potential food sources to higher trophic levels.

One of the most important findings in the spatial variability of the profiles is that a profile created from a single transect within this anchialine cave does not accurately depict the physicochemical conditions throughout the entire system. Often researchers utilize a single profile to characterize an anchialine cave habitat. Based on the profiles in this dataset however, the different sections of a cave can exhibit significantly different environments and each section can host a variety of microhabitats. Different habitats within the coastal zone may influence biogeochemical processes depending on the oxic state of different layers in the subterranean estuary and therefore directly affect the nature of the nutrients and DOM entering the coastal region via SGD. Furthermore, the variability of the DO and pH profiles between Cenote Crustacea and the farthest reaches of the system indicate different trophic states with increasing distance, a process we termed "the entrance effect." While this effect has been outlined in several previous investigations (Gonzalez et al. 2011; Humphreys 1999; Seymour et al. 2007), I propose the adoption of the term in future anchialine studies.

Overall, hydrological investigations in Sistema Crustacea indicate that intense biogeochemical reactions are capable of affecting the conditions within the various layers and boundaries. Increased research attention is needed to comprehend the processes that dictate the physicochemical conditions within these globally distributed

subterranean estuaries and the resulting SGD. Further understanding of such processes will help manage these underground ecosystems and the nearshore GDEs that they support.

CHAPTER III

SPATIAL VARIABILITY OF DISSOLVED ORGANIC MATTER

Introduction

Dissolved organic matter (DOM) has received extensive research attention based on its importance to biogeochemical and ecological processes. DOM plays an important role in microbial ecology, plankton ecology, carbon cycling, trace metal transport, polycyclic hydrocarbon (PAH) toxicity, and the optical properties of natural waters (Amon and Benner 1996; Shank et al. 2004; Stedmon et al. 2003). In addition DOM represents one of the largest reservoirs of carbon on earth and is the primary source of carbon and energy for heterotrophic bacteria (Hansell et al. 2009). Derived from production and diagenetic processes including leaf litter leaching, algal exudation, biological grazing, viral lysis, and *in situ* microbial production, DOM composition varies with the distance of the source and the exposure to degradation (Coble 2007). Chromophoric or colored dissolved organic matter (CDOM) represents the fraction of the DOM pool that absorbs ultraviolet (UV) and visible light (Birdwell and Engel 2010). The optical properties of CDOM have been used in conjunction with satellite imagery to refine budgets of carbon and freshwater the coastal oceans (Coble 2007). Still, the factors controlling the concentration and composition of CDOM within coastal environments are poorly understood (Del Vecchio and Blough 2004). It is therefore important to understand the potential sources and processes that affect CDOM within the coastal oceans.

In order to understand CDOM dynamics within a surface estuary, it is important to follow different components of CDOM throughout the ecosystem (Stedmon et al. 2003). The objective of this study is to apply this same approach within a subterranean estuary in order to understand the sources and biogeochemical processes responsible for CDOM variability within an anchialine cave in the Yucatan Peninsula of Mexico. As previously mentioned, there is little interstitial filtration or biodegradation within the limestone landscape of the Yucatan and rapid touristic development has led to increasing nutrient loading, both anthropogenic and natural. Still the coastal waters of the Yucatan do not exhibit hypoxic characteristics like those found in coastal ecosystems with similar environmental nutrient input (Morales-Ojeda et al. 2010). It is becoming increasingly important to understand the processes affecting organic matter variability within the subterranean estuary in order to fully comprehend the role of submarine groundwater discharge (SGD) along any coastline, particularly the Caribbean coast of the Yucatan.

Dissolved organic carbon (DOC) is the most commonly used parameter to quantitatively measure DOM in natural waters. Recently, fluorescence spectroscopy has become increasingly employed to investigate DOM sources within estuarine environments (Huguet et al. 2009; Moran et al. 2000; Parlanti et al. 2000). Based on the principle that chemical composition and concentration directly influence a substance's optical properties, fluorescence spectroscopy can be used to constrain the sources of CDOM (Birdwell and Engel 2010). The two major constituents of CDOM include humic-like signals derived from photosynthetic sources (both terrestrial and marine) and

protein-like signals derived from autochthonous, microbial sources (Baker and Lamont-Black 2001).

Source and concentration of CDOM is directly linked to light penetration in natural waters, therefore playing an important role in DOM photodegradation. The global production of biologically labile DOC from photodegradation is approximately 206 x 10^{12} g C yr^{-1}, a quantity comparable to the global, annual flux of riverine DOC (Miller et al. 2002). In the Amazon River basin, photodegradation of DOC is up to seven times greater than microbial degradation in surface waters, and therefore represents a significant sink of DOC (Amon and Benner 1996). CDOM also plays an important role in light attenuation near coral reefs. Acting as a natural sunscreen, CDOM absorbs ultraviolet radiation (UVR) wavelengths between 280 – 490 nm, protecting nearshore reefs from harmful solar radiation and photooxidative stress, while still allowing sufficient light for healthy levels of photosynthesis by zooxanthellae (Ayoub et al. 2008). The lack of knowledge pertaining to DOM dynamics in anchialine caves in the Yucatan is surprising considering their DOM processing potential, their distribution adjacent to the world's second longest reef system, and the importance of light attenuation by CDOM near reefs. As the primary drainage for inland runoff, large volumes of water pass through these cave ecosystems with little to no photodegradation. Little is known about the quantity and quality of OM flowing through these ecosystems (Pohlman 2011). Anchialine caves therefore provide a unique opportunity to investigate CDOM processing in a biologically active, although lightless, subterranean estuary

Fluorescence spectroscopy can be used to constrain sources of CDOM through

the measurement of the excitation wavelength (λ Ex) and the emission wavelength (λ Em). Concentration and chemical composition of a substance dictate the intensity and wavelength at which emission/excitation maxima take place (Coble 2007). Plotting λ Ex vs. λ Em from individual water samples creates a "fluorescence landscape" known as an excitation-emission matrix (EEM), which can be used to constrain the source of the CDOM. Traditional peak picking techniques can be used to determine the type of fluorophores present in an EEM, but recently researchers have taken to using multivariate statistics such as parallel factor analysis (PARAFAC). The PARAFAC modeling process deconstructs each EEM to determine the relative contribution of different fluorophore groups (labeled as components) based on EEMs from the entire sample set. PARAFAC can be used to characterize numerous CDOM sources (i.e., terrestrial humic, marine humic, and microbial) within a single sample, as well as their relative, quantitative contribution (Birdwell and Engel 2010; Walker et al. 2009).

The objective of this chapter is to characterize the spatial variability of CDOM and DOC throughout Sistema Crustacea. Characterization will include constraining the quality of the CDOM source (i.e., humic vs. protein), the total fluorescence intensity, and relative proportion of the total fluorescence made up by each component. Quantitative assessments also include direct measurements of the amount of DOC (quantitative) in various zones of the system. Another objective is to determine the relationship between DOC and CDOM in order to find the best proxy for constraining DOC concentrations using fluorescence data. Characterization of the spatial variability of DOM in subterranean estuaries can help to better understand the sinks and sources of

organic matter along this SGD dominated coastline. Based on the role of CDOM in refining coastal carbon and freshwater budgets, it is important to first understand the processes affecting DOM variability prior to discharge.

Methods

The samples collected in March 2011 for the hydrological parameters portion of this investigation (Chapter II) were also used for DOC and CDOM analysis in this chapter. See Chapter II for a full description of the methods used to collect the 2011 samples. Preliminary samples were collected during the week of June 24th, 2010. Sampling design however, was different during the two years. The 2010 samples were taken in triplicate from each location with fewer sample stations (Table 3.1), whereas a single sample was taken from a greater number of stations in 2011. Each year's sampling method possessed inherent advantages. The 2010 sampling provided replicate samples within a limited number of sampling stations, while the 2011 method allowed for increased number of sampling stations in more zones of the cave.

Endmember samples from 2010 were collected from the cenote pool and the open sea (Table 3.1). Cave samples were taken from zone E1 in the freshwater layer (E1_fr) and shallow halocline (E1_H1). Samples were also taken from zone E2 in the brackish layer (E2_br) as well as zone E3 within the deep halocline (E3_H2) and the marine layer (E3_ma). Samples were collected from zone W2 of the Western Section within the marine layer (W2_ma) and the crack in the floor (W2Cr_ma).

Table 3.1. Water sampling matrix for Sistema Crustacea, June 2010.

Sample	Location	Zone	Depth (m)	Cave penetration (m)
1	1-Pool _2010	Pool	1	0
2	2-Pool _2010	Pool	1	0
3	3-Pool _2010	Pool	1	0
4	4-E1_fr_2010	E1	8.7	8.7
5	5-E1_fr_2010	E1	8.7	8.7
6	6-E1_fr_2010	E2	8.7	8.7
7	7-E1_H1_2010	E1	10.7	10.7
8	8-E1_H1_2010	E1	10.7	10.7
9	9-E1_H1_2010	E1	10.7	10.7
10	10-E2_br_2010	E2	12.8	12.8
11	11-E2_br_2010	E2	12.8	12.8
12	12-E2_br_2010	E2	12.8	12.8
16	16-E3_H2_2010	E3	15.9	76
17	17-E3_H2_2010	E3	15.9	76
18	18-E3_H2_2010	E3	15.9	76
19	19-E3_ma_2010	E4	17.1	78
20	20-E3_ma_2010	E4	17.1	78
21	21-E3_ma_2010	E4	17.1	78
22	22-W2_ma_2010	W2	19.8	130
23	23-W2_ma_2010	W2	19.8	130
24	24-W2_ma_2010	W2	19.8	130
25	25-W2Cr_ma_2010	W2	22.9	132
26	26-W2Cr_ma_2010	W2	22.9	132
27	27-W2Cr_ma_2010	W2	22.9	132
31	31-Sea_ma_2010	n/a	1	n/a
32	32-Sea_ma_2010	n/a	1	n/a
33	33-Sea_ma_2010	n/a	1	n/a

After collection, the samples were placed on ice and transported to the field lab for filtration. Before filtration, 25 mL of each sample was poured into a funneled glass vial and stored at 5 °C for O/H isotope analysis. The remaining samples were filtered into a sterile 125 mL Nalgene FLPE bottle through a 0.7 μm pre-combusted GF/F Whatman ® filter. Filtered samples were stored at 5 °C until CDOM analysis. After CDOM analysis, the samples were frozen until DOC analysis was completed. All

samples were analyzed for CDOM and DOC within three months of field collection. Unfortunately, samples 6 and 12 were not used for DOM analysis after they were deemed contaminated. Particulates were observed in the filtered water upon return to Texas A&M at Galveston.

Optical measurements were based on techniques described in Walker et al. (2009). Water samples were warmed to room temperature (22 °C) on the day of analysis. Absorbance spectra were measured from 200 – 800 nm at 0.5 nm increments, using a Shimadzu UV-1800 with a 5 cm cuvette. Each sample was blank corrected using Milli-Q water as a reference. Fluorescence measurements were made with a Photon Technologies International Fluorometer (Quanta Master-4 SE) using a 1 cm cuvette with excitation and emission slit widths set to 5 nm. EEM fluorescence spectra for each sample were obtained by collecting a series of emission wavelength scans ranging from 230 to 600 nm (2 nm increments) at specific excitations wavelengths ranging from 220 to 450 nm (5 nm increments). Instrument specific bias was corrected by applying manufacturer correction files to each individual sample EEM. Excitation wavelengths below 240 nm and emission wavelengths below 300 nm were removed from reach EEM because these regions contained low fluorescence information with increased noise (Stedmon et al. 2003).

The PARAFAC analysis was performed using the "DOMFluorToolbox" in MATLAB as specified by Stedmon and Bro (2008). Originally, 52 samples were collected over the course of June 2010 (n = 27) and March 2011 (n = 25). After removing samples 6 and 12 from the 2010 dataset, the remaining samples (n = 50) were

used to create a 2-year model. The initial PARAFAC model was run with default settings and nonnegativity restraints. After running simple two and three component models, outliers were identified as single samples that exhibited substantial loading on the PARAFAC model (Stedmon and Bro 2008). Two outliers were removed from the original 2010 sample set including: 10-E2_br_2010 and 19-E3_ma. Four outliers were removed from the 2011 dataset including: 1-Pool_2011, 2-E1_fr_2011, 27_Karst_2011, and 32-Mangrove_2011. After outliers were removed, the model was run with a series of one to six components. A six-component model was validated using split-half analysis under the methods prescribed by Stedmon and Bro (2008). Residual analysis was used to assess how much of the data could not be explained by the six-component model; very few residuals were observed. Therefore, I am confident that the six-component model based on the 2-year dataset sufficiently represents the groups of fluorophores present in Sistema Crustacea. The fluorophore groups characterized by the PARAFAC model are not the only fluorophores present in the system. They are however, the only groups present in the majority of the samples with enough statistical influence to explain the variability throughout the sample set (Stedmon and Bro 2008).

Fluorophore groups were qualified as either humics or proteins. Peak A (UV-C excited) and C (UV-A excited) are commonly associated with terrestrial, humic signals (Fig. 3.1). Humics with a blue shifted position (smaller λ Em) are less aromatic and represent more labile CDOM sources (Tedetti et al. 2011). Red shifted peaks indicate increased aromaticity and high molecular weight (HMW) DOM (Moran and Zepp 1997). Peak M has a low emission range and is primarily associated with marine humics created

from marine phytoplankton production. Protein-like signals have been linked to measured concentrations of amino acids tyrosine and tryptophan (peaks B and T). These peaks indicate microbially derived DOM, exhibit a lower λ Em than humics (Fig. 3.1), and have been found in high levels in urban wastewater (Birdwell and Engel 2010).

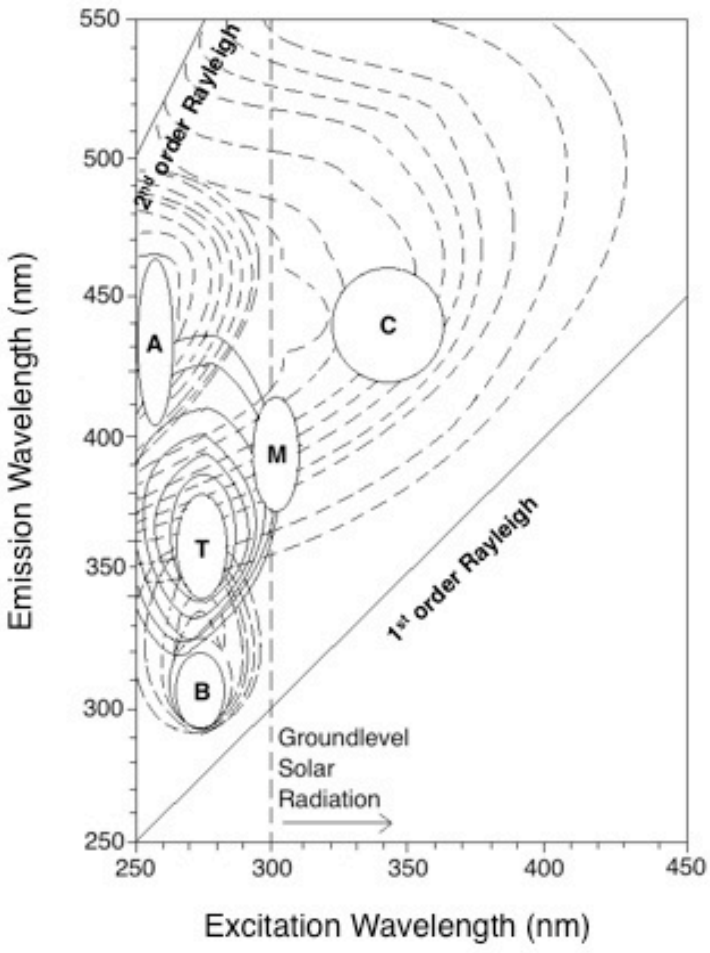

Fig. 3.1. Excitation-emission matrix of naturally occurring fluorophore peaks: A (UV-C humic), C (UV-A humic), M (marine humic), T (tryptophan), and B (tyrosine). 1st and 2nd order Rayleigh scatter are also shown. Adapted from (Birdwell and Engel 2009).

EEM data was also used to calculate fluorescent intensity ratios, known also as indices, to analyze additional qualitative parameters of CDOM in natural waters. The Fluorescence Index (FI; Fig. 3.1) is the ratio of emission intensity at λEm 450 nm to that at λEm 500 nm, with excitation at λEx 370 nm. FI > 1.9 indicates microbially (autochthonous) derived DOM, while FI < 1.4 indicates terrestrial (allochthonous) DOM (Birdwell and Engel 2010). The Biological/autochthonous Index (BIX) can be used to determine the relative contribution of autochthonous DOM. BIX is the ratio of shorter to longer emission wavelengths (λEm 380 nm: λEm 430 nm) at λEx 310 nm. The intensity of the marine peak M and the terrestrial peak C directly influence the BIX. BIX values between 0.8 and 1.0 indicate newly produced DOM from biological or microbial sources while values below 0.6 suggest little to no autochthonous input (Birdwell and Engel 2010). The Humification Index (HIX) can be used to determine the degree of humification, an indicator of OM age in an ecosystem. Substances with increased humification and inherently increased aromaticity are associated with resistance to diagenesis. These recalcitrant compounds are expected to persist longer than substances with a low degree of humification (Birdwell and Engel 2010). The HIX is calculated as the ratio of the sum of emission scans from λEx 435 – 480 nm (long wavelengths associated with high humification) to the sum from λEx 300 – 345 nm (shorter wavelengths associated with low humification) at λEx = 254 nm (Fig. 3.1). Values of HIX < 5 indicate relatively new DOM derived from plants and increase with the degree of humification (Birdwell and Engel 2010). HIX is strongly correlated to aromaticity and has been observed to decrease with increasing salinity (Huguet et al. 2009).

DOC and TN concentrations were measured using a Shimadzu TOC-VCPN organic carbon analyzer. DOC levels were measured as non–purgeable organic carbon (NPOC), the total organic carbon (TOC) remaining after purging an acidified sample with gas, as specified by the Shimadzu manual. Throughout the paper, this will be referred to as DOC, while TN refers to the total dissolved organic and inorganic nitrogen. A calibration curve encompassing the range of each sample's DOC and TN concentrations was generated daily. Samples were regularly compared to a deep-sea consensus reference material (CRM) provided by the DOC-CRM Program at the University of Miami, Rosenstiel School of Marine and Atmospheric Science. The absorption coefficients at 350 nm were calculated according to Kowalczuk et al. (2010) (Eq. 3.1.), where A (350) is the absorbance at 350 nm^{-1} and L is the cuvette path length in meters.

$$a_{CDOM}(350) = 2.303 * A(350) / L \quad (3.1)$$

Results

Characterization of CDOM using the PARAFAC model

Six components, labeled C1-C6, were derived from a 2-year PARAFAC model for the 2010 and 2011 samples (Fig. 3.2 and 3.3). Table 3.1 outlines the excitation and emission maxima of components derived from the 2-year model along with previously identified components and their respective sources. Previous research has identified C1, C2, and C3 as terrestrially derived sources (Coble 2007). Within an underwater cave system these sources are considered allochthonous. C4 contains components primarily

derived from terrestrial material (Peak A) with additional evidence (i.e., a secondary peak) indicating a phytoplankton source that has been altered by microbes (Peak M) (Coble 2007). The fluorescence spectrum of C5 indicates a primary phytoplankton source with some evidence of terrestrially derived material. Much like C1-3, both C4 and C5 are considered allochthonous sources in this cave system. The only autochthonous source of DOM found throughout our study was C6. The low emission and excitation maxima in C6 closely match the protein like peak associated with tryptophan (peak T) indicating a microbial, autochthonous source (Birdwell and Engel 2010; Coble 2007).

Table 3.2. Excitation and emission maxima of the six components identified using PARAFAC to model the 2-year dataset from Sistema Crustacea. Maxima are compared to previously identified components from Coble (2007). A description of each component is provided.

Component	Excitation maximum (nm)	Emission maximum (nm)	Coble (2007)	Source	Description
C1	265 (360)	456	A (C)	allochthonous terrestrial	UVC humic (UVA fulvic)
C2	275 (355)	436	A* (C)	allochthonous terrestrial	UVC humic (UVA fulvic)
C3	275 (380)	504	UVA Humic-like	allochthonous terrestrial	UVC humic (UVA fulvic)
C4	<240 (310)	396	A* (M)	allochthonous terrestrial (allochthonous microbial)	UVC humic (phytoplankton source altered by microbes)
C5	320 (<240)	388	M* (A*)	allochthonous microbial, (allochthonous terrestrial)	phytoplankton source altered by microbes (UVC humic)
C6	280 (<240)	336	T*	microbial, autochthonous	tryptophan like

*not exact match

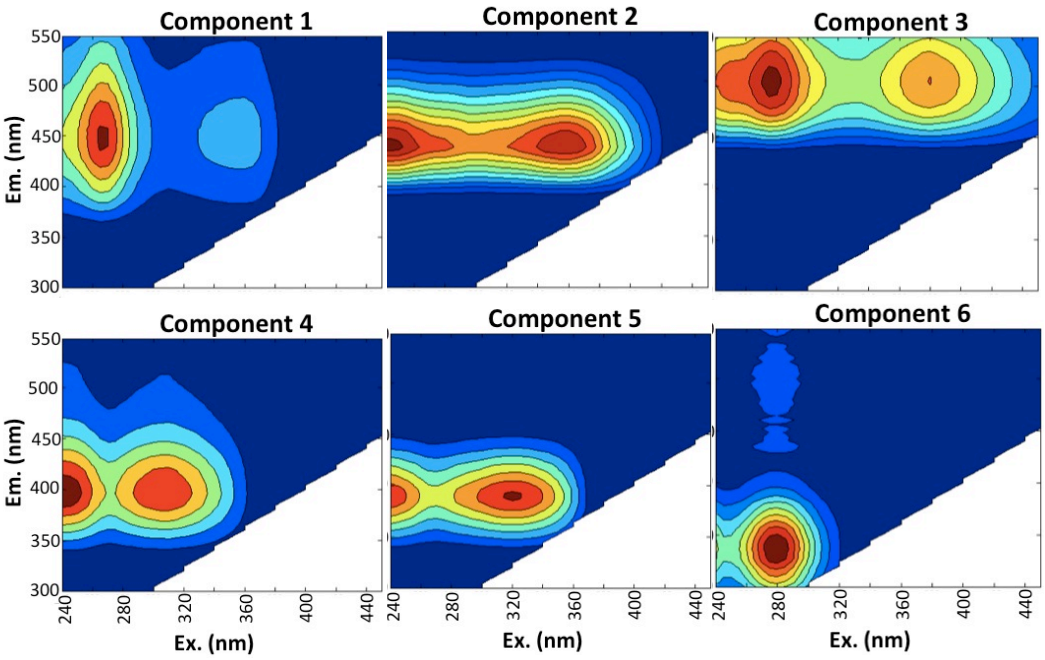

Fig. 3.2. EEMs for components 1-6 identified in the PARAFAC model for Sistema Crustacea including 2010 and 2011 samples.

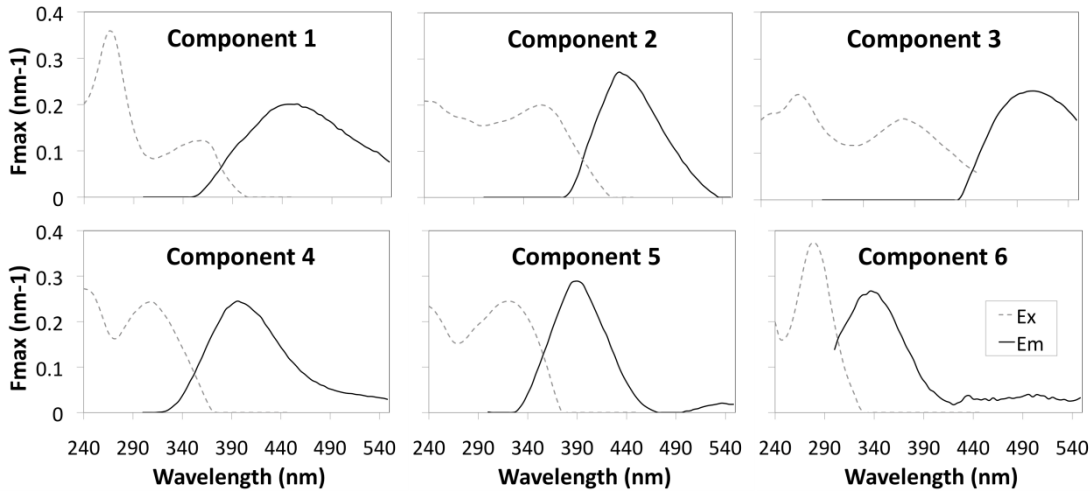

Fig. 3.3. Excitation (dashed) and emission (solid) lines represent the fluorescence spectra of the 6 components identified in the PARAFAC model for Sistema Crustacea dataset including 2010 and 2011 samples.

Relationship between DOC and CDOM

The intensity of C1 (I_{C1}) and C3 (I_{C3}) had the strongest linear relationship to DOC (Table 3.3). In fact, there was a strong linear relationship between DOC and the intensity of each component except C6 ($R^2 = 0.554$). The total fluorescence intensity (I_{TOT}) also exhibited a strong relationship with DOC and although greater I_{TOT} values do not always indicate greater DOC concentrations (Stedmon et al. 2003), they are a good proxy for DOC ($R^2 = 0.956$) within our dataset. A strong linear relationship was also observed between the absorption coefficient $a_{CDOM}(350)$ and DOC ($R^2 = 0.834$) (Table 3.3). While this does not exhibit the strongest relationship within our data, Kowalczuk et al. (2010) found consistently accurate results using $a_{CDOM}(350)$ to estimate known and unknown DOC concentrations in a coastal environment. Therefore, $a_{CDOM}(350)$ and the linear regression equation (Eq. 3.2) can be used to roughly estimate DOC in samples where DOC was not directly measured, including the 2010 samples and sample 11-E4_br_2011.

$$DOC = 19.3 * a_{CDOM}(350) + 55 \quad (3.2)$$

Table 3.3. Coefficient of determination (R^2) between DOC concentration, absorption coefficient $a_{CDOM}(350)$, total fluorescence intensity I_{TOT}, and intensity of each PARAFAC component (I_{C1-C6}) from 2011 samples. R2 values that are statistically significant are marked with an *.

Correlation parameters	Coefficient of determination R^2	Sample size n
$a_{CDOM}(350)$ vs DOC	0.834 *	21
I_{TOT} vs. DOC	0.956 *	21
I_{C1} vs. DOC	0.957 *	21
I_{C2} vs. DOC	0.955 *	21
I_{C3} vs. DOC	0.957 *	21
I_{C4} vs. DOC	0.724 *	21
I_{C5} vs. DOC	0.950 *	21
I_{C6} vs. DOC	0.554 *	21

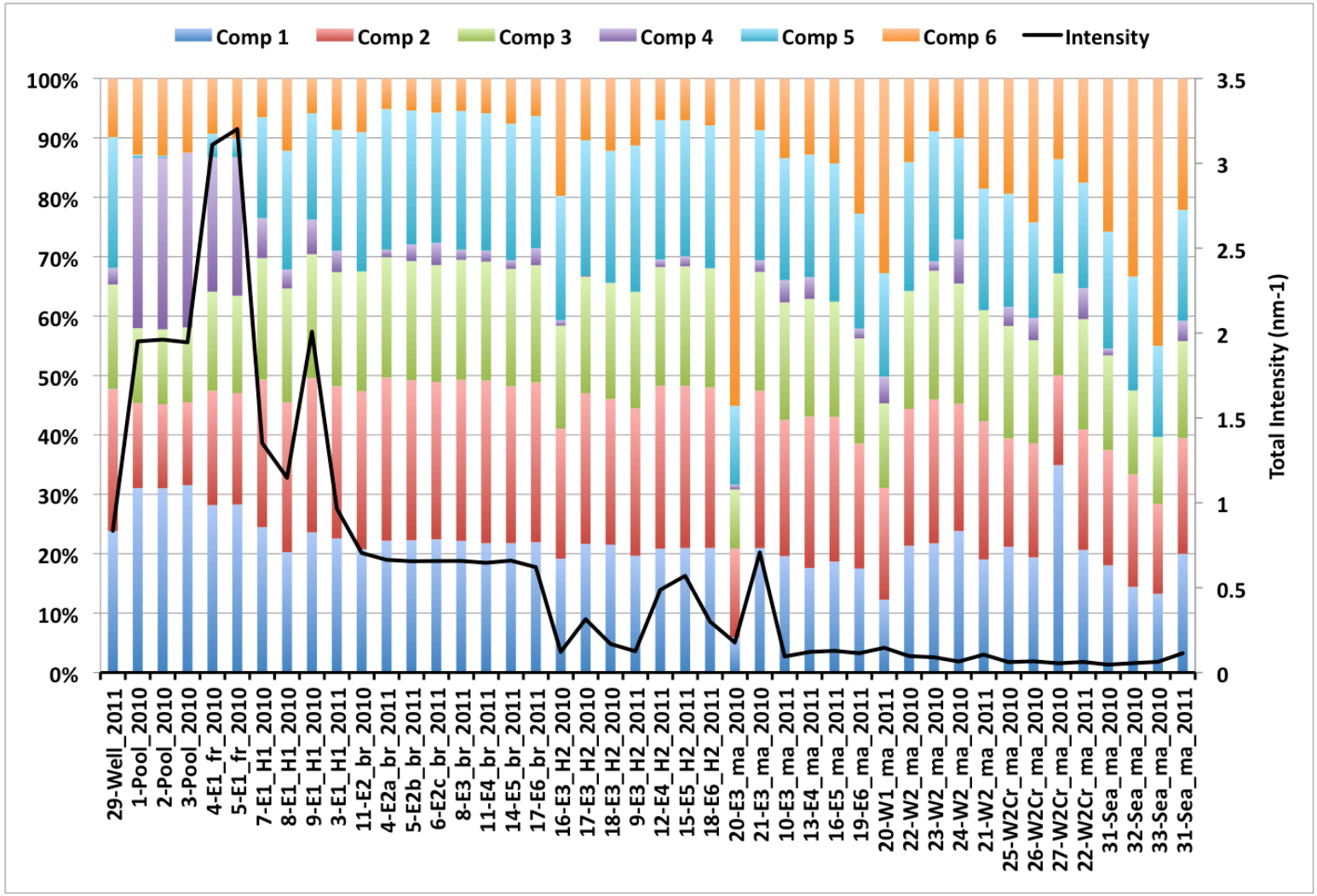

Fig. 3.4. Total fluorescence intensity (nm -1) and percent composition of PARAFAC components in Sistema Crustacea, 2010 and 2011. Samples are arranged in order of increasing salinity with endmembers located at each end.

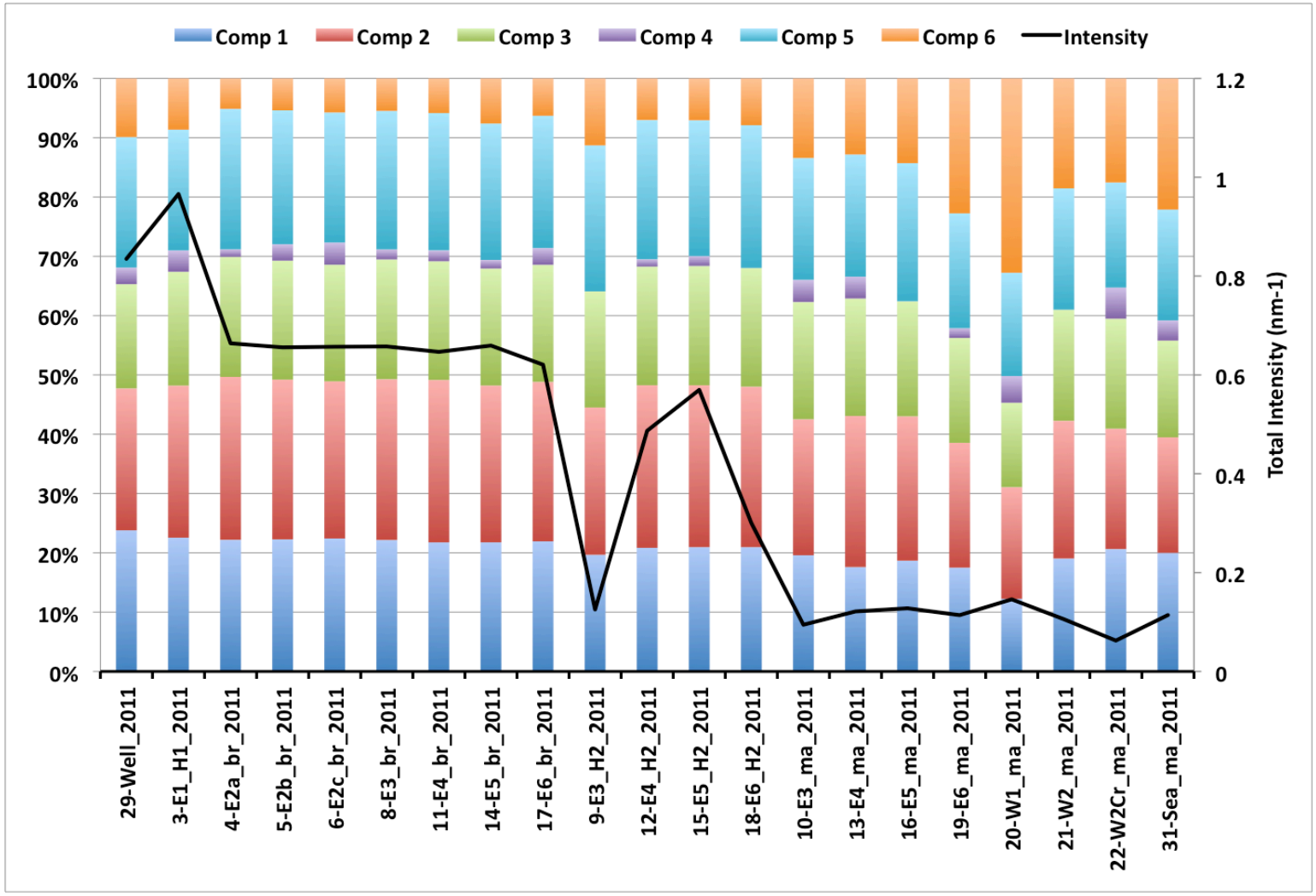

Fig. 3.5. Total intensity (nm -1) and percent composition of PARAFAC components in Sistema Crustacea, 2011. Samples are arranged in order of increasing salinity with endmembers located at each end.

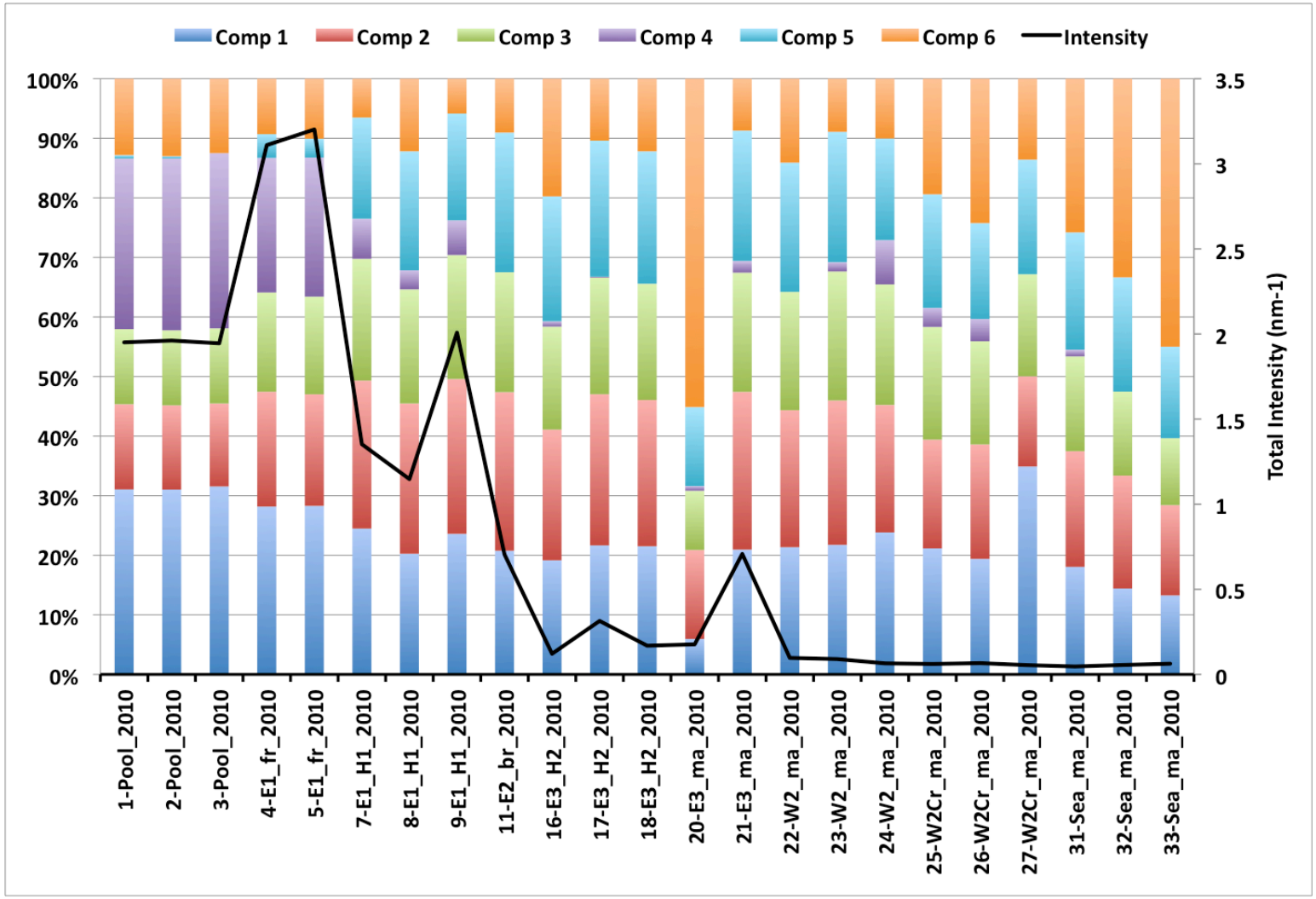

Fig. 3.6. Total intensity (nm -1) and percent composition of PARAFAC components in Sistema Crustacea, 2010. Samples are arranged in order of increasing salinity with endmembers located at each end.

Spatial Variability of CDOM and DOC

Figure 3.4 displays the spatial variability of the I_{TOT} and the percent composition made up by each component for both years. While the sampling design was different for each year, the results were similar. Figures 3.5 and 3.6 divide the same data into two separate years, 2011 and 2010 respectively. Figure 3.7 displays the I_{TOT}, individual component intensity ($I_{1\text{-}6}$), and the DOC of each sample for the two years combined. Figures 3.8 and 3.9 also divide the data into two separate years (2011 and 2010). Throughout both years, DOC concentrations were greatest in the freshwater, median in the brackish layer, and the smallest in the marine layer.

Based on the close relationship between I_{TOT} and DOC, the same trend is expected to persist throughout the water column for both of these parameters. For instance, the greatest I_{TOT} values were observed in the aphotic zone of the entrance in samples 4-E1_fr_2010 (I_{TOT} = 3.2 nm^{-1}) and 5-E1_fr_2010 (I_{TOT} = 3.1 nm^{-1}) (Fig. 3.4). These two samples also exhibited the greatest DOC concentrations (298 and 317 μM)(Fig. 3.5). From here forward, I will only refer to DOC variability, as the I_{TOT} values followed a similar trend.

After the aphotic zone of the entrance, the next highest DOC concentrations were observed in the cenote pool in 2010 ((248 ± 55 μM) (Tables 3.4 and 3.5). The pool and entrance samples from 2010 also exhibited the largest portion of C4 (27 ± 3%) indicating DOM derived from terrestrial and microbial sources (Fig. 3.4). With increasing depth and penetration into the cave, DOC sharply decreased in both years (Fig. 3.7). In the 2-year dataset, there was a general trend of moderate DOC values

within H1 (137 ± 28 μM) with lower values in the brackish layer (101 ± 12 μM) and H2 (67 ± 16 μM). Meanwhile, the lowest DOC values were found in the marine layer of the Eastern (53 ± 17 uM) and Western Sections (50 ± 15 μM). The open sea exhibited slightly greater DOC concentrations (72 ± 20 μM) than the marine layer within the cave. In general, the marine samples were composed of the largest portion of C6 (32 ± 10%) than any other layer (Fig. 3.4) suggesting the greatest influence of autochthonous, microbial activity was in the marine layer.

Conservative Mixing Analysis of DOC and TN

DOC and TN were plotted against salinity in order to create conservative mixing plots (Fig. 3.10A and B). These plots were only created using measured data from 2011; none of the 2010 DOC values derived from linear regression were used. DOC concentrations within the brackish layer plotted below the conservative mixing line indicating there was non-conservative removal of DOC within this layer (Fig. 3.10A). There was also non-conservative removal of TN within the brackish layer (Fig. 3.10B). However, increased TN (53.5 uM) within the freshwater sample (2-E1_fr_2011) indicates either the addition of nitrogen in the aphotic zone of the freshwater layer or more likely the removal of nitrogen in the pool.

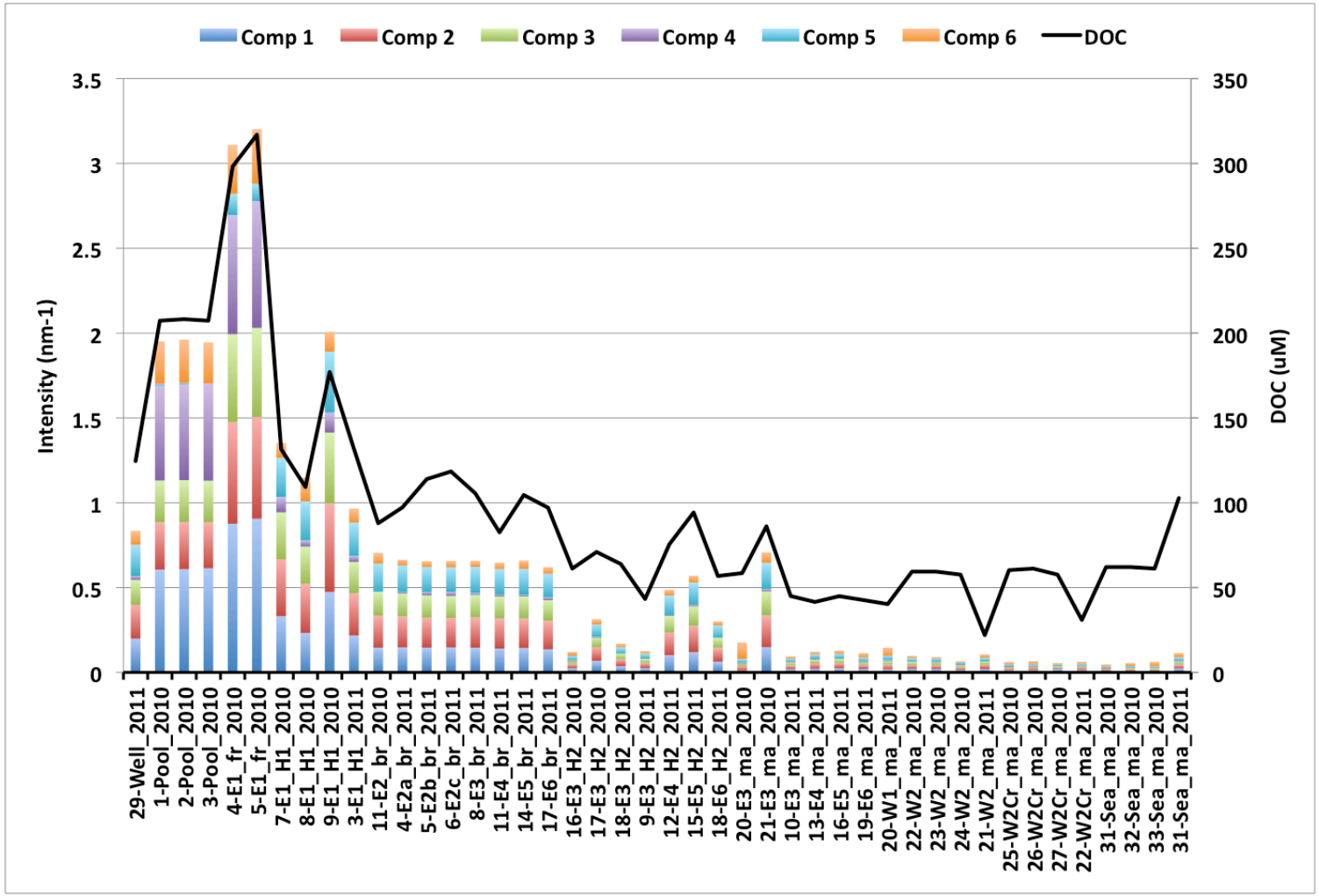

Fig. 3.7. CDOM and DOC levels in Sistema Crustacea from 2010 and 2011 sampling. DOC levels from 2010 and sample 11-E4_br_2011 were calculated using a linear regression (Eq. 3.1). Samples are arranged in order of increasing salinity with endmembers located at each end.

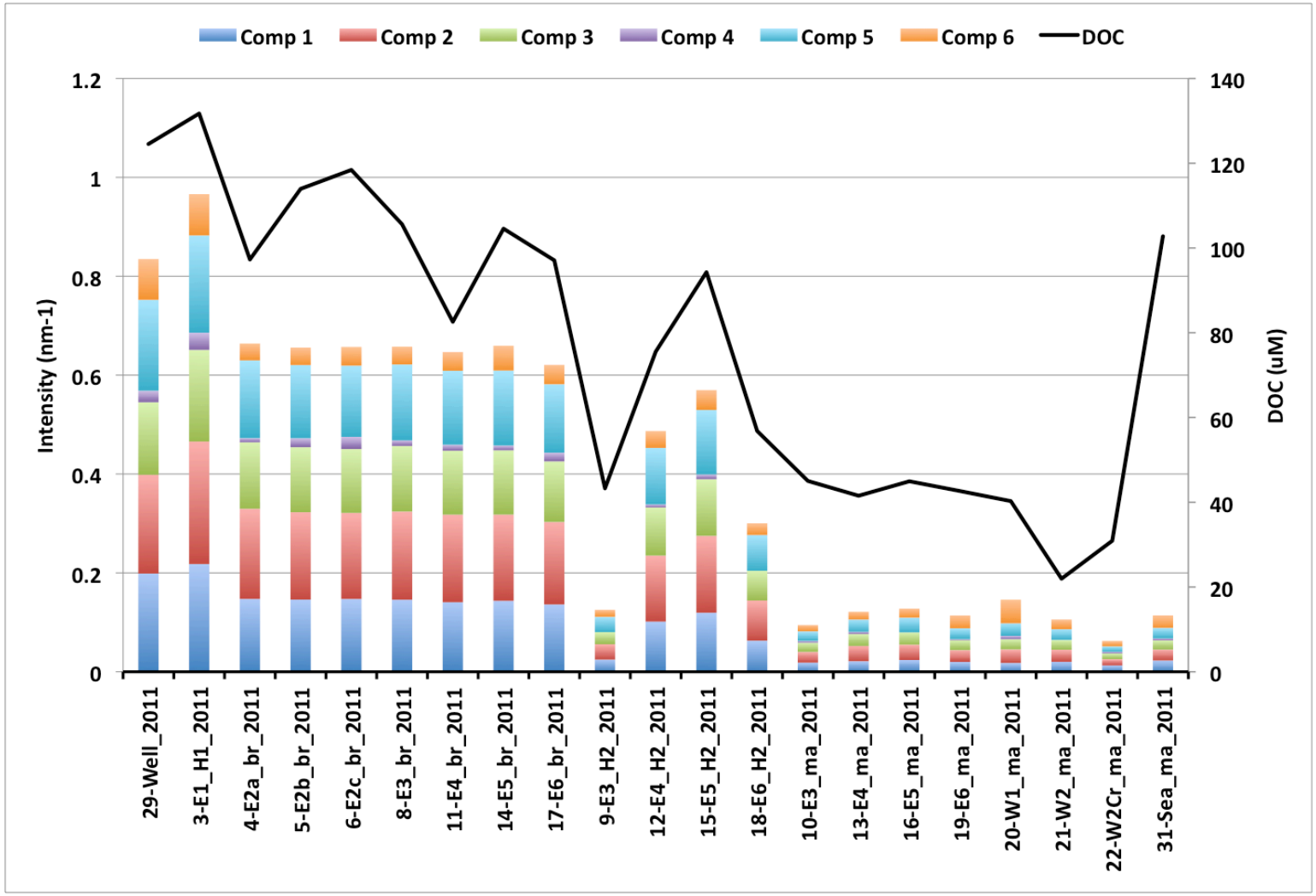

Fig. 3.8. Total intensity (nm -1) of PARAFAC components and DOC in Sistema Crustacea, 2011. Samples are arranged in order of increasing salinity with endmembers located at each end.

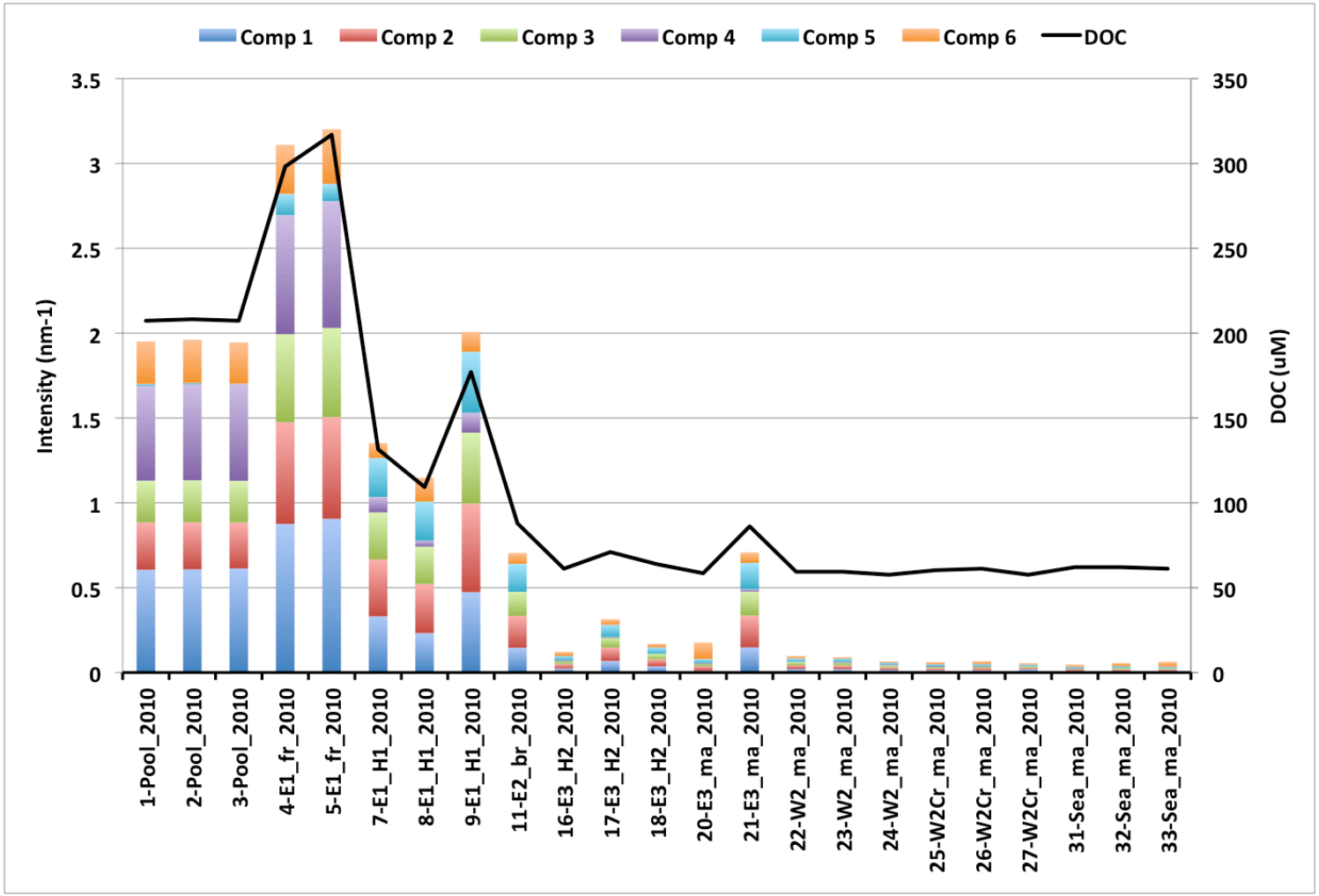

Fig. 3.9. Total intensity (nm^{-1}) of PARAFAC components and DOC in Sistema Crustacea, 2010. DOC for each sample was calculated using a linear regression (Eq. 3.1).

Table. 3.4. DOC, TN, BIX, HIX, and FI of 2011 samples. Dashes represent bad data or no data.

Location	Depth (m)	Cave penetration (m)	Salinity (ppt)	DOC (µM)	TN (µM)	BIX	HIX	FI
1-Pool_2011	1.0	0	1.3	231.6	32.5	0.77	8.30	1.27
2-E1_fr_2011	7.6	4	1.7	233.5	53.5	0.69	12.90	1.27
3-E1_H1_2011	9.5	6	11.1	131.7	9.4	0.72	12.54	1.32
4-E2a_br_2011	11.6	8	13.6	97.3	9.1	0.72	16.75	1.34
5-E2b_br_2011	14.6	18	13.9	114.0	10.9	0.71	17.12	1.32
6-E2c_br_2011	14.5	28	13.9	118.4	-	0.72	16.51	1.33
7-E2d_br_2011	14.6	38	13.7	-	-	-	-	-
8-E3_br_2011	12.7	76	13.6	105.6	10.3	0.73	16.99	1.30
9-E3_H2_2011	14.8	78	33.7	43.3	5.9	0.78	7.23	1.38
10-E3_ma_2011	16.8	80	35.8	45.0	3.4	0.70	5.65	1.30
11-E4_br_2011	12.4	118	14.0	79.9		0.73	16.40	1.29
12-E4_H2_2011	14.8	120	33.6	75.5	9.9	0.72	13.24	1.28
13-E4_ma_2011	15.6	122	35.4	41.5	4.8	0.77	6.30	1.33
14-E5_br_2011	12.2	130	13.9	104.6	9.1	0.73	11.72	1.32
15-E5_H2_2011	14.3	132	32.3	94.3	11.3	0.70	13.70	1.30
16-E5_ma_2011	16.1	134	35.7	45.0	6.9	0.76	5.73	1.28
17-E6_br_2011	12.9	160	13.6	97.1	10.1	0.72	14.64	1.33
18-E6_H2_2011	14.9	162	32.6	56.8	10.2	0.72	12.03	1.38
19-E6_ma_2011	16.1	164	35.9	42.6	4.3	0.74	3.93	1.46
20-W1_ma_2011	15.1	78	34.7	40.3	12.1	0.88	2.72	1.42
21-W2_ma_2011	18.7	130	35.2	22.0	9.9	0.73	3.95	1.38
22-W2Cr_ma_2011	21.4	132	35.7	30.9	6.5	0.87	4.93	1.50
27-Karst_2011	0.0	n/a	1.0	229.1	69.1	0.72	6.65	1.24
28-Rain_2011	0.0	n/a	1.0	-	-	-	-	-
29-Well_2011	0.3	n/a	1.0	124.5	39.7	0.77	9.35	1.36
31-Sea_ma_2011	0.3	n/a	36.0	102.8	7.1	0.83	3.57	1.19
32-Mangrove_2011	0.3	n/a	30.0	254.7	71.4	0.88	5.26	1.22

Table. 3.5. DOC, BIX, HIX, and FI of 2010 samples. Salinity was derived from same samples at same depth in 2011. DOC was calculated using linear regression (Eq. 3.2).

Location	Depth (m)	Cave penetration (m)	Salinity (ppt)	DOC (uM)	BIX	HIX	FI
1-Pool_2010	1.0	0	1.3	207.3	0.74	7.74	1.26
2-Pool_2010	1.0	0	1.3	208.2	0.73	7.70	1.24
3-Pool_2010	1.0	0	1.3	207.3	0.74	7.73	1.26
4-E1_fr_2010	8.7	8.7	1.7	298.2	0.66	10.81	1.22
5-E1_fr_2010	8.7	8.7	1.7	316.9	0.67	10.07	1.23
7-E1_H1_2010	10.7	10.7	11.1	131.6	0.68	16.09	1.26
8-E1_H1_2010	10.7	10.7	11.1	109.3	0.72	8.18	1.28
9-E1_H1_2010	10.7	10.7	11.1	177.0	0.66	16.25	1.29
11-E2_br_2010	12.8	12.8	13.8	87.9	0.75	11.61	1.33
16-E3_H2_2010	15.9	76	33.7	61.2	0.74	4.84	1.26
17-E3_H2_2010	15.9	76	33.7	71.0	0.76	9.47	1.30
18-E3_H2_2010	15.9	76	33.7	63.9	0.72	7.03	1.31
20-E3_ma_2010	17.1	78	35.8	58.5	0.75	7.34	1.37
21-E3_ma_2010	17.1	78	35.8	86.1	0.74	6.24	1.30
22-W2_ma_2010	19.8	130	35.2	59.4	0.75	4.19	1.24
23-W2_ma_2010	19.8	130	35.2	59.4	0.71	5.30	1.29
24-W2_ma_2010	19.8	130	35.2	57.6	0.74	4.21	1.32
25-W2Cr_ma_2010	22.9	132	35.7	60.3	0.85	2.11	1.29
26-W2Cr_ma_2010	22.9	132	35.7	61.2	0.86	2.96	1.26
27-W2Cr_ma_2010	22.9	132	35.7	57.6	0.86	3.70	1.37
31-Sea_ma_2010	1.0	n/a	36.0	62.1	0.95	1.96	1.28
32-Sea_ma_2010	1.0	n/a	36.0	62.1	1.00	1.55	1.50
33-Sea_ma_2010	1.0	n/a	36.0	61.2	0.97	1.36	1.39

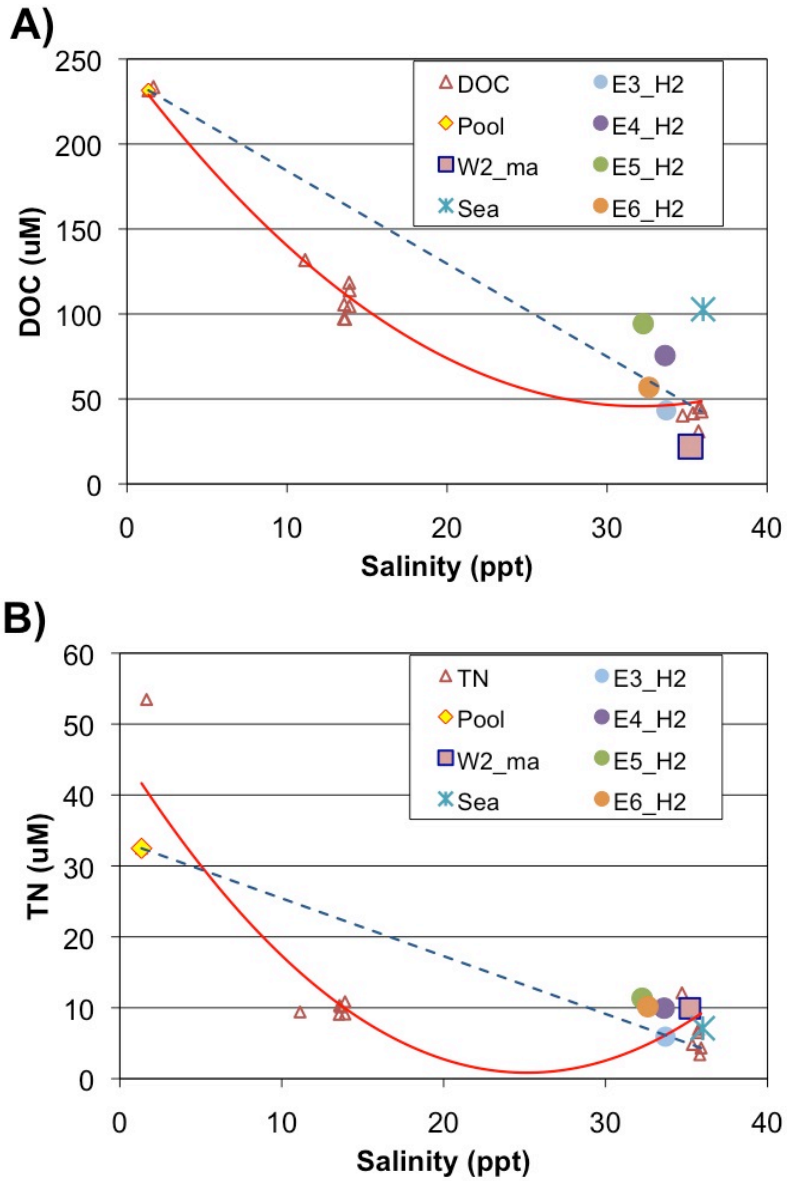

Fig. 3.10. Conservative mixing plot for DOC (A) and TN (B) in Sistema Crustacea, 2011. Dashed line represents conservative mixing between endmembers (pool and marine layer), the open sea was the only other endmember included. The solid line represents a moving average of concentrations within the system.

Spatial Variability and Conservative Mixing Analysis of Fluorescence Indices

There was little variability within the FI and BIX indices (Fig. 3.11). FI values

< 1.4 indicate DOM of terrestrial origin, whereas values above 1.9 represent microbially derived material (Birdwell and Engel 2010). The FI in 2011 remained between 1.2 and 1.5 (Fig. 3.11), indicating these samples were primarily composed of terrestrially derived DOM. According to Huguet et al. (2009), BIX values between 0.8 and 1.0 indicate freshly produced DOM that has been diagenetically altered by biological or microbial activity, while values less than 0.6 contain little autochthonous input. The pool exhibited a greater BIX value than the freshwater samples from the aphotic zone in both years (Tables 3.4 and 3.5), indicating DOM within the photic zone is subject to increased diagenetic alteration. During 2011, the system maximum for BIX (0.88) and the system minimum for HIX (2.7) were found in the marine layer of the Western Section (sample 20-W1_ma_2011), suggesting this location contains a fresh source of DOM with little humification. DOM from this part of the cave also exhibited the greatest percent composition of C6 (32.8%) in 2011, indicating that the DOM in this location is derived primarily from microbial activity. Overall the DOC concentrations were very low in this region of the cave (40.3 μM).

HIX values < 5 indicate recently derived DOM and values increase with the degree of humification (Birdwell and Engel 2010). The greatest HIX values were found in the brackish layer in 2011 (Fig. 3.11) indicating that the DOM in these layers is highly humified. Meanwhile, the lowest HIX values in the system were observed in the marine layer and the open sea indicating little humification. These samples also exhibited the lowest overall DOC concentrations.

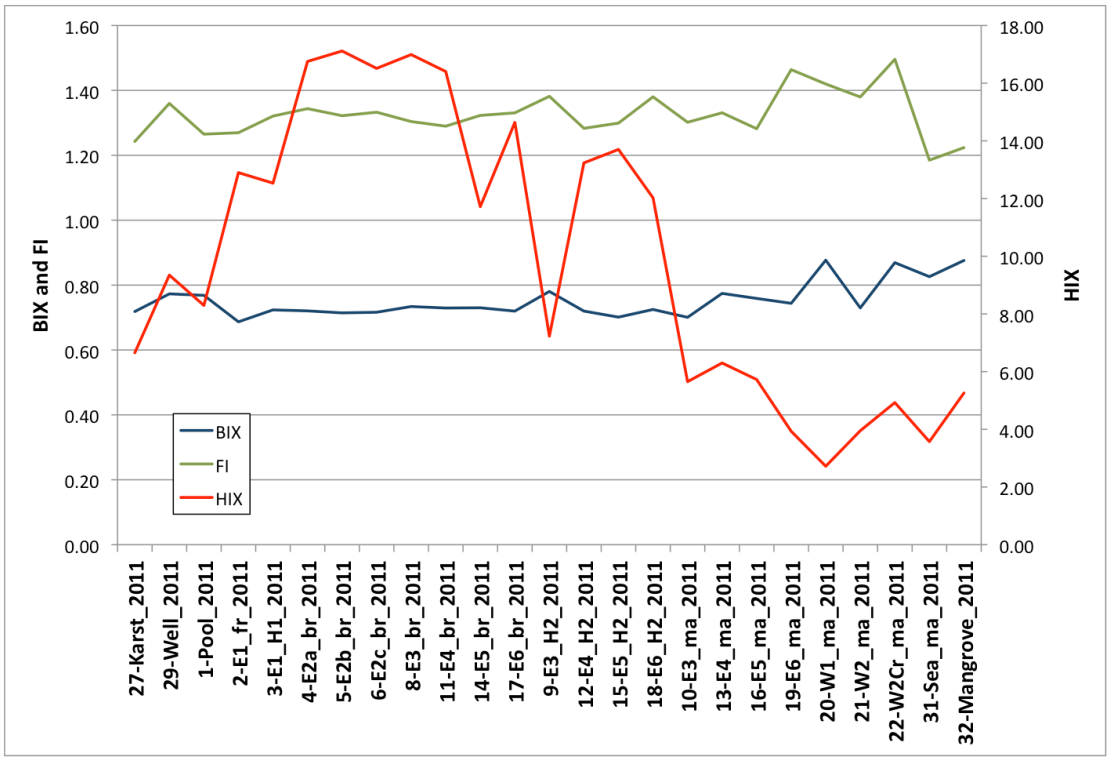

Fig. 3.11. BIX, FI, and HIX for Sistema Crustacea, 2011. Samples are arranged in order of increasing salinity with endmembers located at each end.

Discussion

PARAFAC Modeling Process

Using the 6-component model allowed us to detect minute changes in the structure of the CDOM and therefore infer small changes in the quality of the CDOM. However, indices such as the BIX, HIX, and FI can also be used to infer structural changes within CDOM sources. It is therefore important to model the system based on the core questions of the investigation. In our case, this was to determine spatial variability throughout numerous sections of the cave. Different sampling strategies can be used to answer different questions about the biogeochemical processes within this

anchialine cave. The 2010 sample design restricted the sample set to only a few locations within the cave; however, the dataset from these samples is more robust. During the 2011 sampling design, a single sample was taken from each station with an increased number of stations. Based on the variability of the physicochemical profiles in various sections of the cave, it is important to understand CDOM variability throughout the various oxic states within the cave. Overall, the 2011 methods using increased sampling stations provided the greatest understanding of DOM spatial variability. Replication can therefore be obtained by sampling several stations within the same layer. Future studies should consider these findings and the overall questions of their investigations when creating a sampling design in similar ecosystems.

Characterization of CDOM Components

The fluorescence spectrum of C4 has a lower emission maximum (388 nm) than C5 (396 nm). This lower emission maximum is known as a blue shift and is a good indicator that this group of fluorophores is more oxidized. Photodegradation (also known as photooxidation) has been shown to induce a blue shift in emission maxima (Coble 2007). Based on inherent optical properties, CDOM sources with decreased aromaticity emit at a shorter wavelength. Photodegradation of DOM has been shown to yield low molecular weight (LMW) DOM thereby inducing a blue shift in the fluorescence spectrum. Evidence suggests that the resulting product is more biologically labile than the parent DOM (Moran and Zepp 1997). Therefore, CDOM that is composed of more blue shifted components will likely exhibit increased bioavailability over the red shifted

components. The rank of component emission maxima from highest (red shifted, more reduced, higher aromaticity, and therefore a higher molecular weight) to lowest emission maxima (blue shifted, more oxidized, lower aromaticity, and therefore lower molecular weight) is: C3> C1> C2> C4> C5> C6. Both Table 3.2 and Fig. 3.3 display the decreasing emission maxima of the components.

The fluorescence spectrum from each of the hydrologic layers was comprised of primarily C1-C4, indicating that a terrestrial source dominates the CDOM signal within freshwater layers and the Cenote Crustacea pool. However, there is a clear shift from greater C4 proportions in the pool towards greater proportions of C5 and C6 in the deeper layers. C5 has been linked to phytoplankton sources that have been diagenetically altered by microbial activity; C6 is described as a direct product of microbial activity (Coble 2007). A measurable decrease in DOC concentrations also coincided with this shift in DOM sources. Such a shift in DOC quantities and CDOM source with increasing depth is expected with dilution of marine waters. Evidence for non-conservative removal however, indicates that microbial processes within the water column may be responsible (discussed below).

Spatial Variability of DOC and CDOM

The DOC concentrations and I_{TOT} were greatest in the freshwater samples (Fig. 3.7). I expected to observe the highest DOC and I_{TOT} in the photic zone of the pool, but these maxima were instead observed in the aphotic zone (samples 4-E1_fr_2010 and 5-E1_fr_2010). Dilution of the terrestrially derived DOM signal is expected with

increasing marine water influx. Such evidence is observed as the I_{TOT} and DOC concentration decreases with depth and penetration into the cave. However, there is additional non-conservative removal of DOC within Sistema Crustacea, particularly in the brackish layer (Fig. 3.11A and B). In addition, evidence from Chapter II suggests that microbial respiration is taking place within the aphotic zone of the freshwater layer and brackish layer.

Researchers have found that terrestrially derived DOC and DON are more biologically labile in estuarine conditions than in a limnic environment due to the shift in the physicochemical parameters (Stepanauskas et al. 1999; Wikner et al. 1999). I believe that the increased levels of DOC and CDOM within the Cenote Crustacea pool provide a DOM source for intense microbial respiration in the photic zone of the pool. A significant portion of this DOM migrates into the aphotic zone of the cave entrance where maximum DOC and I_{TOT} were observed. This influx of DOM from the pool into the cave potentially supports microbial respiration within the aphotic zone of the cave entrance. I expect this respiration is the primary driver of hypoxia within the water column, much like the eutrophic model described by Pohlman (2011). Further research is needed to determine which microbial processes are responsible for the DO and pH minimums described in Chapter II.

Fluorescence spectroscopy has been used in other estuarine systems to detect eutrophication in natural waters from wastewater runoff (Coble 2007). Polluted waters often exhibit high intensity protein peaks in the B and T region of sample EEMs, which is indicative of increased microbial activity (Coble 2007). Based on the high

susceptibility to nutrient loading, the lack of wastewater treatment in the Yucatan, and physicochemical evidence for microbial respiration (Chapter II), I expected to find increased proportion of protein peaks within Sistema Crustacea. While the C6 peak indicates the presence of tryptophan, a protein peak commonly associated with microbial activity (Coble 2007), there were not any samples in which the component dominated the overall fluorescence signal. Due to the limited sample size of both years, it is likely that our sampling method did not locate microbial hotspots within the cave. Microbial communities in caves have been observed in the form of mats on the sediment floor and cave walls (Gonzalez et al. 2011; Sarbu et al. 1996). White clouds, much like those in H1 of Cenote Crustacea, have also been observed in an anchialine sinkhole in Western Australia and found to contain strains of sulfur oxidizing bacteria (Seymour et al. 2007). Additionally any significant chemosynthetic production of DOC would occur in anoxic regions such as the haloclines. Sampling within these thin layers (in many places less than 0.2 m thick) is difficult and may not have sufficiently captured microbially derived DOM. Further research is needed to determine if and where the microbial hotspots are located within Sistema Crustacea.

Spatial Variability of TN

Humic DOM (H-DOM) has been disregarded as an important source of nitrogen in microbial-based food webs because the humic-bound nitrogen has a low biological availability in marine and freshwater systems. Increased C:N ratios of humic substances represent insufficient nitrogen relative to the amount of carbon needed for growth in

heterotrophic bacteria (Biers et al. 2007). Such high ratios also impose constraints on the formation of NH_4, derived from humic DOM degradation, to be used by chemoautotrophic bacteria. Studies have found however, that assimilable nitrogen levels increased when humic substances were subject to photodegradation from sunlight (Bushaw et al. 1996). Based on this evidence, the greatest TN levels are expected within the cenote pool, an area subject to direct photodegradation and increased DOC flux from terrestrially derived DOM. The greatest TN levels however were found in the aphotic zone of the freshwater layer (53.5 uM) in 2011. The pool exhibited much lower TN levels (32.5 uM). It is unclear what processes would lead to decreased TN in the open pool of the cenote. One potential avenue for TN removal in the photic zone is the uptake of dissolved nitrogen by photosynthetic and microbial processes. After uptake, the particulate nitrogen may settle out of the water column as phytoplankton and bacteria or is filtered out of the water sample during post collection processing. Either process would lead to the decreased levels observed in our study. The other potential method for nitrogen removal is denitrification. This is unlikely to take place in the normoxic pool however, because this process is only known to proceed under hypoxic conditions (Pohlman 2011).

TN concentrations quickly decreased with penetration and depth. The lowest TN levels were observed in the brackish and marine layers. Mixing diagrams for TN indicate that non-conservative removal of nitrogen is taking place within the brackish layer of the cave. The removal of N via microbial denitrification has been observed in another Yucatan cave, Cenote Mayan Blue (Pohlman et al. 1997), and may also serve as the

primary source of N removal in the deeper layers of Sistema Crustacea. Further research is needed however to quantify the role of microbial communities on N budgets within this system. Regardless of the method of N removal, evidence suggests that Sistema Crustacea serves as a sink for TN.

Conclusions

Touristic and residential development along the Caribbean Coast of the Yucatan is expected to increase nutrient loading from point and non-point source pollution including deep well injection of wastewater (Aranda-Cirerol et al. 2006; Beddows 1999). In order to manage and conserve GDEs along this developing coastline, it is important to understand the role of subterranean estuaries in coastal C and N cycling. Based on the evidence for non-conservative removal of DOC and TN in the brackish layer of Sistema Crustacea, subterranean estuaries and their subcategory of anchialine caves can serve as a significant sink of C and N in the coastal ocean. Additionally, evidence for microbial respiration (discussed in Chapter II) indicates that microbial communities play an important role in shaping the physicochemical properties within this portion of the coastal aquifer. This evidence also suggests that microbial communities are responsible for some of the C and N removal within Sistema Crustacea. Further research is needed to quantify the degree to which microbes alter C and N flow to the coastal ocean. In a region where anthropogenic nutrient loading is responsible for the degradation of the world's second longest reef system, it is important to understand biogeochemical processes within anchialine caves and the coastal ecosystems they support.

CHAPTER IV

SPATIAL VARIABILITY OF THE INVERTEBRATE POPULATION

Introduction

From the early 1500s to the mid 1900s, groundwater ecology research focused primarily on taxonomy and the description of new species (Hancock et al. 2005). As expected, the first objective of investigating a new ecosystem is to describe the indigenous fauna. Stygobitic species are often endemic to a single cave system, and thus the discovery or exploration of new caves is likely to result in the discovery of new species. Throughout the world, numerous unexplored caves and undiscovered species still exist, indicating the continued need for taxonomic-based research in cave systems. As the field grows however, there is an increasing need to understand the ecological aspects of groundwater communities. In past 20 years, there has been such a shift towards more ecologically based groundwater investigations, including those conducted in anchialine caves (Hancock et al. 2005; Opsahl and Chanton 2006; Pohlman et al. 1997; Seymour et al. 2007). Considering the increasingly significant influence of SGD in coastal oceans (as mentioned in Chapter II), there is also a growing need to understand the ecology and function of stygobitic communities within the context of subterranean estuaries.

In order to understand the relationship between DOM and the stygobitic community in an anchialine cave, it is important to understand the trophic structure within the system. Pohlman et al. (1997) remains one of the few studies in the field of

anchialine cave research to determine trophic structure using stable isotope analysis. That study conducted in Cenote Mayan Blue, an anchialine cave in Quintana Roo, identified 2 – 2.5 trophic levels of invertebrates that feed on a range of sources including nitrifying bacteria, soil particulate organic matter (SPOM), pool particulate organic matter (PPOM), and lower trophic level invertebrates (Pohlman et al. 1997). Within Mayan Blue, the atyid shrimp, *Typhlatya mitchelli,* exhibited a range of depleted $\delta^{13}C$ values indicating a diet that included depleted $\delta^{13}C$ sources, such as nitrifying bacteria, as well as organic matter from the pool (PPOM) and soil (SPOM). The thermosbaenacean *Tulumella unidens* exhibited a similar range of $\delta^{13}C$ and $\delta^{15}N$ indicating that these two species represent the same, lower trophic level and perform similar functions within the ecosystem. The remipede *Xibalbanus tulumensis* within Mayan Blue exhibited specific $\delta^{13}C$ and $\delta^{15}N$ values that indicated this species feeds on organisms from lower trophic levels such as *Typhlatya mitchelli, Tulumella unidens*, isopods, and ostracods (Pohlman et al. 1997).

In addition to trophic structure, small-scale habitat variability plays an important role in nutrient limited environments and is often overlooked in anchialine cave studies. As reported in Chapters II and III, high DOC (maximum of 233.5 μM) and low DO (minimum of 0.36 mg/L) concentrations were observed near the Cenote Crustacea entrance. DOC was found to decrease and DO increased with increasing penetration and depth into the cave. Anomalies within the DO profiles indicate the presence of microhabitats even within each relatively homogeneous layer (Chapter II). Although some stygobitic species may tolerate a range of temperature, pH, salinity, DO, and/or

DOC concentration, these same species may prefer a specific zone with optimal physicochemical conditions.

In many cases, physicochemical conditions within anchialine caves resemble the deep-sea environment. Both ecosystems have been described as having hypoxic waters and low nutrient influx (Pohlman et al. 1997; Schmitter-Soto et al. 2002; Seymour et al. 2007). In addition, several stygobitic invertebrates have close relatives inhabiting the deep sea (Humphreys et al. 2009; Iliffe et al. 1984). Recent studies, including ours, indicate that hypoxia does not persist throughout the entire cave and certain regions are not nutrient limited (Humphreys 1999; Pohlman et al. 1997; Seymour et al. 2007). Unlike the deep-sea however, anchialine caves exhibit elevated temperatures that pose a particular problem for dealing with the hypoxic, low nutrient environment. Stygobitic organisms have adapted to such extreme environments by maintaining a decreased metabolism (Bishop and Iliffe 2012; Bishop et al. 2004). The refuge provided by a small change in physicochemical parameters, such as temperature or DO, could therefore make a large difference in the metabolic rate of small, stygobitic invertebrates.

Sistema Crustacea is a cave system aptly named for the high abundance of crustaceans, particularly shrimp, and remipedes. To date nine species of crustaceans have been identified within the system: atyid shrimp *Typhlatya pearsei*, cirolanid isopod *Metacirolana mayana*, remipedes *Xibalbanus tulumensis* and *Xibalbanus fuchscockburni*, thermosbaenacean *Tulumella unidens*, halocyprid ostracod *Danielopolina mexicana,* and weckeliid amphipods *Tuluweckelia cernua* and

Mayaweckelia cenoticola (Botosaneanu and Iliffe 2002; Hoenemann et al. 2013; Hunter et al. 2008; Neiber et al. 2011).

Observations during preliminary dives in Sistema Crustacea indicate that there are an unusually high number of *Typhlatya pearsei* and *X. tulumensis* within the Eastern Section of the cave. There is also a clear division in remipede species' distribution with *X. fuchscockburni* found only in the Western Section and *X. tulumensis* only inhabiting the Eastern Section (Neiber et al. 2012). Additionally, the evidence presented in Chapters II and III suggest significant microbial respiration is taking place within the different layers of the water column. Based on all of these findings, the purpose of this chapter is to characterize the invertebrate community throughout each section of the cave.

My data is also meant to supplement the work of M.J. Pakes (UC Berkley), who is currently using stable isotope analysis to determine the trophic structure within Sistema Crustacea. The objective of my portion of this study is to census the stygobitic community in order to determine the ecological differences between hydrologic layers and cave zones. This characterization will allow future researchers to better understand habitat range of stygobitic species as well as habitat preference within this cave. Increased understanding of habitat range will allow researchers in new caves to better understand where new or related species may be distributed. Increased understanding of habitat preference will direct researchers where to focus research efforts. For example, *Typhlatya pearsei* have been observed in a large range of physicochemical conditions throughout anchialine caves in the Yucatan (Hunter et al. 2008). However, within

Cenote Crustacea this habitat preference of this species is not well understood. Through this study I aim to characterize the habitat preference of *Typhlatya pearsei* and other invertebrate species within Sistema Crustacea.

Methods

Visual Census of Invertebrate Population

Visual transects were conducted to characterize the spatial variability of the invertebrate community. Paired SCUBA divers conducted censuses on the left and right side of the main guideline in both the Eastern and Western Sections of the cave. Each transect was 3 m in length with diver enumerating stygobitic invertebrates (remipedes, shrimp, amphipods, isopods, ostracods, and thermosbaenaceans) within 3 m of the left (or right) side of the line extending 1.5 m above and 1.5 m below the line (total volume = 3 m x 3 m x 3 m or 27 m^3). Diver pairs selected a random number of kicks (1 – 5) between each transect in order to promote random distribution of transects within each zone. In locations where the transect border extends beyond the cave passage, divers only counted those organisms visible in the water column, excluding those *Typhlatya* on the cave wall, floor, or ceiling. When disturbed by the bubbles of open circuit divers, resting *Typhlatya* began to swarm into the water column making it very difficult to estimate the total number in the water column or on the cave wall. Therefore the individuals located on the cave wall, floor, or ceiling were purposefully excluded from this census. To reduce diver impact (i.e., bubbles dislodging invertebrates from the ceiling), divers only counted organisms in front of their path in undisturbed water. In

order to minimize the ecological impact of the scientific investigation in this system, no invertebrates were collected during this field study. Instead, identification to family level was conducted underwater and based on species identification from previous researchers. Macro invertebrates, such as the remipedes and shrimp, were large enough to visually identify underwater. Micro invertebrates such as the amphipods, isopods, ostracods, and thermosbaenaceans, were identified based on their unique swimming patterns.

In the Western Section, each diver conducted four transects in the marine layer of W2. In the Eastern Section, each diver conducted four transects in the brackish layer of E2 as well as two transects above Halocline 2 and two transects below Halocline 2 in zones E3, E4, and E5. Transects from the left and right side of the line were treated as independent transects. Non-parametric Mann-Whitney U test was run to determine if there was a significant difference between the left and right sides of transects, and transects were deemed to be statistically similar ($P > 0.05$).

Ecological diversity measures were used to characterize the visual transect data including species richness (S) where S is the total number of species, total number of individuals (N), Shannon diversity (H') and evenness (J') indices (Magurran 1988). The Shannon diversity index was calculated using Eq. 4.1 where p_i is the fraction of the entire population composed of species *i*.

$$H' = - \Sigma p_i \ln p_i \quad (4.1)$$

Evenness was calculated using Eq. 4.2 where S is the total number of species.

$$J' = H'/\ln S \quad (4.2)$$

Statistical Analysis

In order to compare species density among zones, the datasets were first tested for normality and homogeneity of variance. None of the datasets met these assumptions and therefore each set was log transformed. After log transforming the data sets, only *Typhlatya* density met the assumptions. Significant difference of *Typhlatya* density among the zones was further investigated using the non-parametric post hoc analysis, Scheffe's method, due to the unequal sample size between zones. The *Xibalbanus* density dataset did not meet the assumption of normality and was therefore statistically evaluated among zones using the non-parametric test Kruskall-Wallis. Other species were not observed in great enough numbers to statistically evaluate.

Results

Overall, 570 individuals were counted in Sistema Crustacea with 462 from the brackish layer and 108 from the marine layer (Table 4.1). A total of six crustacean taxa were observed throughout the system; *Typhlatya* was the only crustacean found in every zone. Previous researchers have identified *T. pearsei* from within the system (Hunter et al. 2008). However, there is some debate as to the presence of *Typhlatya mitchelli* in the system (pers. comm. M.J. Pakes). I will therefore refer to cave shrimp as *Typhlatya* spp. throughout the paper since other species were only identified to genus in this study. Censuses in the brackish and marine layer of both the Eastern and Western Sections were dominated by the presence of *Typhlatya*. Such evidence suggests that the habitat range of *Typhlatya* is not restricted by conditions within the brackish or marine layers.

Based on the results of the nested ANOVA (Table 4.1), there was a significantly lower ($P < 0.05$) average density of *Typhlatya* (individuals/ 27 m^3) in the marine layer (3.7 ± 4.4) compared to the brackish layer (23.1 ± 14.0). There was also a significant difference in the *Typhlatya* density between zones based on the post hoc analysis using Scheffe's test (Table 4.1). In particular, E3_ma (labeled as "c" in Table 4.1) and W2_ma (labeled as "h" in Table 4.1) exhibited significantly lower density than the brackish zones (a, b, d, and f). Meanwhile, the greatest density of *Typhlatya* was observed in zone E5_br (Table 4.1). Based on these differences, *Typhlatya* within Cenote Crustacea prefer specific zones within the brackish layer.

According to our March 2011 observations, zone E5_br exhibited normoxic conditions (4.42 mg/L) and brackish salinity (14 ‰). In addition to increased *Typhlatya*, the brackish layer also exhibited greater range in DOC concentrations (79.9 to 118.4 μM) than the marine layer (42.6 to 45.0 μM) (Fig. 4.1). Based on the limited sample size within this one cave system, I am unable to determine whether DOC concentration directly influences *Typhlatya* distribution.

The brackish zones exhibited the greatest number of *Typhlatya* and but also the lowest species richness (S = 1). Meanwhile, the marine zones hosted the greatest species richness, all of which were greater than 1 (Table 4.2). Overall, zone W2_ma exhibited the greatest species richness (S = 1.9 ± 1.2), evenness (J' = 0.5 ±0.5), and diversity (H' = 0.5 ± 0.5). The physicochemical parameters within this zone included high salinity (35 ‰), normoxic waters (4.75 mg/L), and low DOC (22.0 μM).

Table 4.1. Average density of invertebrate species (± standard deviation) per transect (27 m^3) in Sistema Crustacea from March 2011. Parametric results are given for *Typhlatya*. Non-parametric results are included for *Xibalbanus*. Zones are represented as letters a-h, paired letters represent significant differences between zones.

Zone	*Typhlatya*	*Xibalbanus*	Weckeliid	*Metacirolana*	*Tulumella*	*Danielopolina*
E2_br(a)	20.3±9.2	0	0	0	0	0
E3_br(b)	16.2±10.6	0	0	0	0	0
E3_ma(c)	1.2±1.0	1.2±1.5	0	0	0	0
E4_br(d)	27.2±20.3	0	0	0	0	0
E4_ma(e)	6.5±6.7	0	0.5±0.6	0	0	0
E5_br(f)	31.2±18.1	0	0	0	0	0
E5_ma(g)	8.2±5.1	0.2±0.5	0	0	0	0
W2_ma(h)	1.8±1.4	0.2±0.6	0.2±0.4	0.1±0.3	0.8±1.3	0.5±1.0
Nested ANOVA	*	n/a	n/a	n/a	n/a	n/a
Scheffe's	ac,ah,bc,bh, cd,cf,dh,fh	n/a	n/a	n/a	n/a	n/a
Kruskal-Wallis	n/a	ns	†	†	†	†

* significant at P < 0.05, ns: not significant
† not analyzed due to low abundance

Table 4.2. Species richness (S), evenness (J'), and Shannon diversity (H') indices for marine and brackish layer of each zone in Sistema Crustacea. Results are based on visual censuses from March 2011. *N* represents the number of transects. Total number of individuals is also included.

Zone	*N*	S	J'	H'	Number of individuals
Brackish	**20**				**462**
E2_br(a)	8	1	0	0	163
E3_br(b)	4	1	0	0	65
E4_br(d)	4	1	0	0	109
E5_br(f)	4	1	0	0	125
Marine	**22**				**108**
E3_ma(c)	4	1.2±1.0	0.4±0.5	0.3±0.4	10
E4_ma(e)	4	1.5±0.6	0.2±0.3	0.1±0.2	28
E5_ma(g)	4	1.2±0.5	0.1±0.3	0.1±0.2	34
W2_ma(h)	10	1.9±1.2	0.5±0.5	0.5±0.5	36

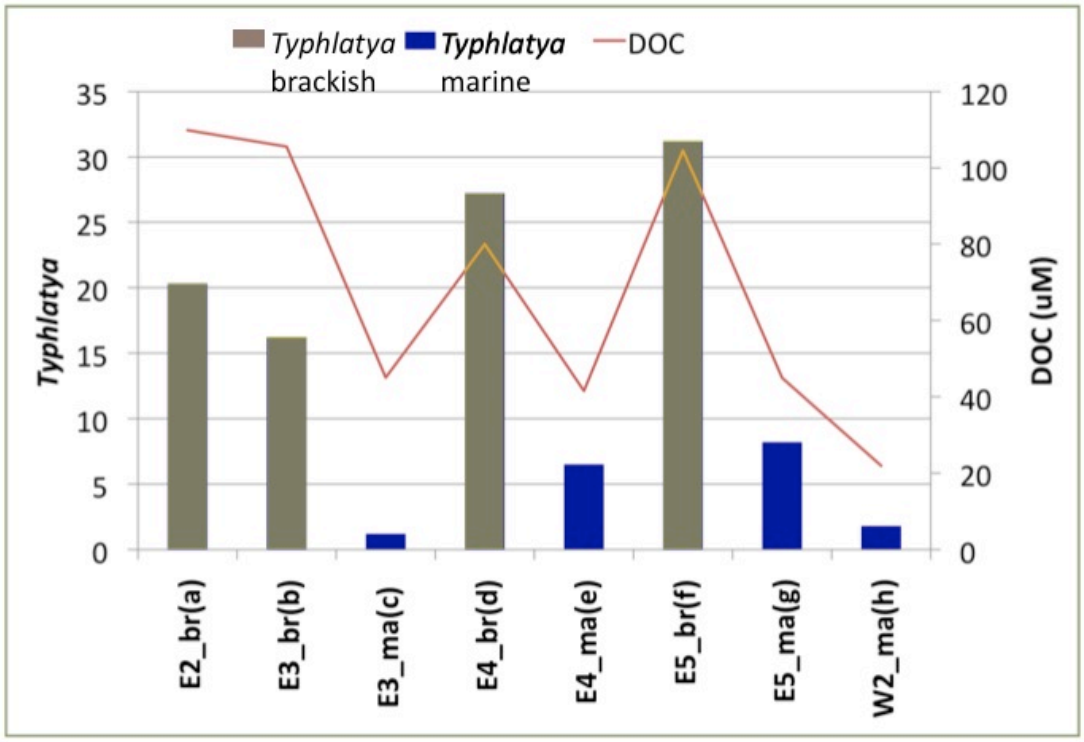

Fig. 4.1. Mean density of *Typhlatya* (individuals/ 27 m^3) and DOC concentrations (μM) from each zone of Sistema Crustacea.

There was no significant difference ($P > 0.05$) in the number of *Xibalbanus* sp. among the 8 zones, presumably due to the low number of individuals observed (Table 4.1). *Xibalbanus* were only observed in the marine layer of this anchialine cave, as is the case with all other remipede species worldwide. Normoxic conditions persisted in the upper limits of the marine layer (4.2 mg/L) where the remipedes were observed. The densities of other species were not observed in great enough numbers to statistically evaluate.

Discussion

Sistema Crustacea is a rare case in which remipedes inhabit normoxic waters. Other examples in which this occurs include an anchialine cave on San Salvador Island, Bahamas, where surface water DO ranges from 3 – 5 mg/L (Yager and Carpenter 1999), and the lava cave of Lanzarote, in the Canary Islands, where DO ranges from 3.7 – 5.7 mg/L (Wilkens et al. 2009). Sistema Crustacea is the type and sole locality for *X. fuchscockburni* and thus the only known cave in the Yucatan to contain two species of *Xibalbanus* (Hoenemann et al. 2013; Neiber et al. 2012). This system is one of seven known remipede habitats in the Yucatan and one of only 44 around the world. While few studies have attempted to discern the species density of *Xibalbanus* and *Typhlatya* in underwater caves around the world, the anomalously high densities of both of these species in Sistema Crustacea suggests it is a unique anchialine habitat.

It is important for researchers to continue to investigate the class Remipedia for several reasons. For one, remipedes represent a unique crustacean lineage with global distribution; despite such distribution, no species have been found in the open oceans. In addition, remipedes are believed to derive from an ancient origin remaining relatively unchanged for millions of years, a sort of living fossil (Yager and Humphreys 1996). Still, despite an increased understanding of this recently discovered class, there is a dearth of knowledge pertaining to their ecology. I therefore encourage the conservation of Sistema Crustacea in order to allow future research on remipede distribution and colonization patterns, while also preventing habitat loss along this rapidly developing coastline.

As anchialine cave studies shift from a taxonomic to more ecological focus, there is an increasing need for an established method of visual censuses. While the swimming transects used in this study were a useful method for enumerating *Typhlatya* in the water column, our census methods purposefully excluded individuals attached to the cave wall and therefore underestimated the total number of *Typhlatya* present in each zone. Previous divers' observations suggest that the number of *Xibalbanus* can exceed 30 individuals within a 27 m^3 long transect, typically within zones E3 through E5. It is therefore important to adapt a visual census method that accurately depicts a system's stygobitic community across species.

It is unclear what drives the increased number of *Xibalbanus* in Sistema Crustacea. I hypothesize that the increased density of the *Typhlatya* within the brackish layer of zone E5 is the primary driver for the increased density of *X. tulumensis*. Unfortunately, there was not sufficient evidence to support this hypothesis and it is possible the *Typhlatya* provide a "conveyor belt" of energy, transferring DOC from near the cenote entrance to the normoxic, energy deficient reaches of the Eastern Section. Further research is needed to determine the role *Typhlatya* play in the transfer of energy within Sistema Crustacea.

Similarly, it is unclear what is responsible for the distribution of two different species of *Xibalbanus* in the separate sections of the cave. Because these sections are less than 200 m apart and divers can easily swim between them while remaining within the cave environment, some population mixing would be expected. However, neither species has been found in the section inhabited by its congener. With increasing distance

from Cenote Crustacea, the physicochemical parameters in the marine layer of the two sections are not inherently different. Both exhibit normoxic conditions with decreased DOC as well as similar temperatures, salinities, and pH (Chapters II and III). The primary difference is that the Eastern Section contains a more direct connection to the open sea, as found in Chapter II. Therefore, I can only infer that the anoxic zone associated with the Cenote Crustacea entrance provides a genetic barrier that prevents the mixing of the two *Xibalbanus* species. As mentioned above, Neiber et al. (2012) found sufficient genetic and morphological differences between remipedes in the Eastern and Western Sections to define two separate species. However, their study found minimal genetic difference between the populations of *X. tulumensis* from Cenote Crustacea and Cenote Mayan Blue, nearly 80 km to the south. Further research is needed to understand what processes led to the existence of two distinct species populations within Sistema Crustacea in a region where *X. tulumensis* is so widely distributed.

With increased cave research and exploration, additional stygobitic species and extensions of habitat ranges are still to be discovered. In such a field, it is important to constrain and document the habitat range of each species. Utilizing this information, both researchers and explorers will be able to determine the potential for specific stygobitic taxa within each zone of the cave. As mentioned in Chapter II, it is equally important to understand physicochemical parameters throughout the entire cave in order to characterize what trophic or oxic state exists within different zones. Understanding the range of habitats of stygobitic species and the range of habitats in a single system should increase the efficiency of taxonomic surveys within anchialine caves.

It is important to accurately determine species abundance and diversity in sensitive ecosystems such as coastal aquifers. Within these systems ecosystem diversity can serve as a key indicator of water quality over time. Stygobitic species can therefore act as useful bioindicators of both pollution and nutrient loading from anthropogenic sources. While our investigation could not link ecosystem health to water quality, it still serves as a starting point for the long-term analysis of the ecosystem within Sistema Crustacea. In the following years, investigators need to continue population assessments within this cave in order to determine the temporal variability of the stygobitic community and the health of the coastal aquifer.

CHAPTER V

CONCLUSIONS

Findings from this investigation indicate that the greatest concentration of DOC occurred in the freshwater pool with decreasing values in the deeper layers. Evidence of non-conservative removal suggests that Sistema Crustacea acts as a sink for terrestrially derived DOC destined to reach the coast. The physicochemical profiles also suggest microbial respiration is partly responsible for this carbon removal. Such evidence supports our hypothesis that biogeochemical processes within this particular anchialine cave can alter the carbon budget and future research is needed to determine the extent to which Sistema Crustacea influences carbon cycling in nearby coastal ecosystems.

Throughout the Yucatan the rise of coastal development and increasing anthropogenic influence pose a particular threat to the coastal ocean, a trend also observed around the world. Increasing evidence suggests that nutrient transport via SGD to the coastal oceans is equal to or greater than surface rivers. Still, further investigations are needed to understand the regional influence of SGD and this need is often reflected in inaccurate carbon budgets in coastal areas (Burnett et al. 2006). Additionally, there is a lack of understanding about the biogeochemical processes affecting carbon cycling within the coastal aquifers directly associated with SGD (Moore 1999). The findings of this investigation indicate that biogeochemical processes within this specific subterranean estuary are capable of qualitatively and quantitatively altering carbon budgets throughout the water column, potentially affecting coastal carbon budgets. I

expect that further investigation of similar systems throughout the Yucatan and the rest of the world will find similar results. It is therefore important to determine the role of subterranean estuaries and anchiaine caves in coastal carbon cycles around the world.

In the wake of increasing coastal development, it is becoming increasingly necessary to preserve the physical and biological integrity of these subterranean ecosystems by reducing the impact of anthropogenic influences. Inclusion of wastewater management and best management practices on the local and regional level is essential to the health of not only these subterranean estuaries but also the coral reefs and near-shore ecosystems that depend upon them.

REFERENCES

Alvarez-Gongora, C., and J. A. Herrera-Silveira. 2006. Variations of phytoplankton community structure related to water quality trends in a tropical karstic coastal zone. Mar. Pollut. Bull. **52:** 48-60.

Amon, R. M. W., and R. Benner. 1996. Photochemical and microbial consumption of dissolved organic carbon and dissolved oxygen in the Amazon River system. Geochim. Cosmochim. Acta **60:** 1783-1792.

Aranda-Cirerol, N., J. A. Herrera-Silveira, and F. A. Comin. 2006. Nutrient water quality in a tropical coastal zone with groundwater discharge, northwest Yucatan, Mexico. Estuar. Coast Shelf S. **68:** 445-454.

Baker, A., and J. Lamont-Black. 2001. Fluorescence of dissolved organic matter as a natural tracer of ground water. Ground Water **39:** 745-750.

Beddows, P. A. 1999. Conduit hydrogeology of a tropical coastal carbonate aquifer: Caribbean coast of the Yucatan Peninsula. M.S. Thesis. McMaster University: Hamilton, Canada.

Beddows, P. A., P. L. Smart, F. F. Whitaker, and S. L. Smith. 2007. Decoupled fresh-saline groundwater circulation of a coastal carbonate aquifer: spatial patterns of temperature and specific electrical conductivity. J. Hydrol. **346:** 18-32.

Biers, E. J., R. G. Zepp, and M. A. Moran. 2007. The role of nitrogen in chromophoric and fluorescent dissolved organic matter formation. Mar. Chem. **103:** 46-60.

Birdwell, J. E., and A. S. Engel. 2009. Variability in terrestrial and microbial contributions to dissolved organic matter fluorescence in the Edwards Aquifer, central Texas. J. Cave Karst Stud. **71:** 144-156.

Birdwell, J. E., and A. S. Engel. 2010. Characterization of dissolved organic matter in cave and spring waters using UV-Vis absorbance and fluorescence spectroscopy. Org. Geochem. **41:** 270-280.

Bishop, R.E., and T.M. Iliffe. 2012. Ecological physiology of the anchialine shrimp *Barbouria cubensis*: a comparison of epigean and hypogean populations. Mar. Biodiversity, **42:** 303-310.

Bishop, R. E., B. Kakuk, and J. J. Torres. 2004. Life in the hypoxic and anoxic zones: metabolism and proximate composition of Caribbean troglobitic crustaceans with

observations on the water chemistry of two anchialine caves. J. Crustacean Biol. **24:** 379-392.

Botosaneanu, L., and T. M. Iliffe. 2002. Stygobitic isopod crustaceans, already described or new, from Bermuda, the Bahamas, and Mexico. Bull. L'Inst. Roy. Sci. Nat. Belg. **72:** 101-112.

Burnett, W. C., P. K. Aggarwal, A. Aureli, H. Bokuniewicz, J. E. Cable, M. A. Charette, E. Kontar, S. Krupa, K. M. Kulkarni, A. Loveless, W. S. Moore, J. A. Oberdorfer, J. Oliveira, N. Ozyurt, P. Povinec, A. M. G. Privitera, R. Rajar, R. T. Ramassur, J. Scholten, T. Stieglitz, M. Taniguchi, and J. V. Turner. 2006. Quantifying submarine groundwater discharge in the coastal zone via multiple methods. Sci. Total Environ. **367:** 498-543.

Bushaw, K. L., R. G. Zepp, M. A. Tarr, D. SchulzJander, R. A. Bourbonniere, R. E. Hodson, W. L. Miller, D. A. Bronk, and M. A. Moran. 1996. Photochemical release of biologically available nitrogen from aquatic dissolved organic matter. Nature **381:** 404-407.

Coble, P. G. 2007. Marine optical biogeochemistry: the chemistry of ocean color. Chem. Rev. **107:** 402-418.

Cooper, H. H. 1959. A hypothesis concerning the dynamic balance of fresh water and salt water in a coastal aquifer. J. Geophys. Res. **64:** 461-467.

Coronado, C., J. Candela, R. Iglesias-Prieto, J. Sheinbaum, M. Lopez, and F. J. Ocampo-Torres. 2007. On the circulation in the Puerto Morelos fringing reef lagoon. Coral Reefs **26:** 149-163.

Crook, E. D., D. Potts, M. Rebolledo-Vieyra, L. Hernandez, and A. Paytan. 2012. Calcifying coral abundance near low-pH springs: implications for future ocean acidification. Coral Reefs **31:** 239-245.

Del Vecchio, R., and N. V. Blough. 2004. Spatial and seasonal distribution of chromophoric dissolved organic matter and dissolved organic carbon in the Middle Atlantic Bight. Mar. Chem. **89:** 169-187.

Engel, A. S., L. A. Stern, and P. C. Bennett. 2004. Microbial contributions to cave formation: new insights into sulfuric acid speleogenesis. Geology **32:** 369-372.

Fry, B. 2006. Stable Isotope Ecology. Springer Verlag, New York.

Gat, J. R. 1971. Comments on stable isotope method in regional groundwater investigations. Water Resour. Res. **7:** 980-996.

Gat, J. R. 1996. Oxygen and hydrogen isotopes in the hydrologic cycle. Annu. Rev. Earth Planet. Sci. **24:** 225-262.

Gili, J. M., T. Riera, and M. Zabala. 1986. Physical and biological gradients in a submarine cave on the western Mediterranean Coast (Northeast Spain). Mar. Biol. **90:** 291-297.

Gonzalez, B. C., T. M. Iliffe, J. L. Macalady, I. Schaperdoth, and B. Kakuk. 2011. Microbial hotspots in anchialine blue holes: initial discoveries from the Bahamas. Hydrobiologia **677:** 149-156.

Gottstein, S., M. Ivkovic, I. Ternjej, B. Jalzic, and M. Kerovec. 2007. Environmental features and crustacean community of anchihaline hypogean waters on the Kornati islands, Croatia. Mar. Ecol.-Evol. Persp. **28:** 24-30.

Hancock, P. J., A. J. Boulton, and W. F. Humphreys. 2005. Aquifers and hyporheic zones: towards an ecological understanding of groundwater. Hydrogeol. J. **13:** 98-111.

Hodell, D. A., A. V. Turchyn, C. J. Wiseman, J. Escobar, J. H. Curtis, M. Brenner, A. Gilli, A. D. Mueller, F. Anselmetti, D. Ariztegui, and E. T. Brown. 2012. Late Glacial temperature and precipitation changes in the lowland Neotropics by tandem measurement of delta O-18 in biogenic carbonate and gypsum hydration water. Geochim. Cosmochim. Acta **77:** 352-368.

Hoenemann, M., M.T. Neiber, W.F. Humphreys, T.M. Iliffe, D. Li, F.R. Schram and S. Koenemann. 2013. Phylogenetic analysis and systematic revision of Remipedia (Nectiopoda) from Bayesian analysis of molecular data. J. Crust. Biol. **33:** 603-619.

Huguet, A., L. Vacher, S. Relexans, S. Saubusse, J. M. Froidefond, and E. Parlanti. 2009. Properties of fluorescent dissolved organic matter in the Gironde Estuary. Org. Geochem. **40:** 706-719.

Humphreys, W. F. 1999. Physico-chemical profile and energy fixation in Bundera Sinkhole, an anchialine remiped habitat in north-western Australia. J. Roy. Soc. West. Aust. **82:** 89-98.

Humphreys, W. F., and D. L. Danielopol. 2005. Danielopolina (Ostracoda, Thaumatocyprididae) on Christmas Island, Indian Ocean, a sea mount island. Crustaceana **78:** 1339-1352.

Humphreys, W. F., L. S. Kornicker, and D. L. Danielopol. 2009. On the origin of *Danielopolina baltanasi* sp n. (Ostracoda, Thaumatocypridoidea) from three

anchialine caves on Christmas Island, a seamount in the Indian Ocean. Crustaceana **82:** 1177-1203.

Hunter, R. L., M. S. Webb, T. M. Iliffe, and J. R. A. Bremer. 2008. Phylogeny and historical biogeography of the cave-adapted shrimp genus *Typhlatya* (Atyidae) in the Caribbean Sea and western Atlantic. J. Biogeogr. **35:** 65-75.

Iliffe, T. M. 1986. The zonation model for the evolution of aquatic faunas in anchialine caves. Stygologia **2:** 2-9.

Iliffe, T. M., H. Wilkens, J. Parzefall, and D. Williams. 1984. Marine lava cave fauna - composition, biogeography, and origins. Science **225:** 309-311.

Ingraham, N. L. 1998. Isotopic variations in precipitation., p. 91-103. *In* C. Kendall and J. J. McDonnell [eds.], Isotope Tracers in Catchment Hydrology. Elsevier Science B.V., New York.

Kowalczuk, P., W. J. Cooper, M. J. Durako, A. E. Kahn, M. Gonsior, and H. Young. 2010. Characterization of dissolved organic matter fluorescence in the South Atlantic Bight with use of PARAFAC model: relationships between fluorescence and its components, absorption coefficients and organic carbon concentrations. Mar. Chem. **118:** 22-36.

Lachniet, M. S., and W. P. Patterson. 2009. Oxygen isotope values of precipitation and surface waters in northern Central America (Belize and Guatemala) are dominated by temperature and amount effects. Earth Planet. Sci. Lett. **284:** 435-446.

Magurran, A. E. 1988. Ecological Diversity and Its Measurement. Princeton University Press: Princeton, NJ.

Marfia, A. M., R. V. Krishnamurthy, E. A. Atekwana, and W. F. Panton. 2004. Isotopic and geochemical evolution of ground and surface waters in a karst dominated geological setting: a case study from Belize, Central America. Appl. Geochem. **19:** 937-946.

McClain, M. E., E. W. Boyer, C. L. Dent, S. E. Gergel, N. B. Grimm, P. M. Groffman, S. C. Hart, J. W. Harvey, C. A. Johnston, E. Mayorga, W. H. McDowell, and G. Pinay. 2003. Biogeochemical hot spots and hot moments at the interface of terrestrial and aquatic ecosystems. Ecosystems **6:** 301-312.

Metcalfe, C. D., P. A. Beddows, G. G. Bouchot, T. L. Metcalfe, H. X. Li, and H. Van Lavieren. 2011. Contaminants in the coastal karst aquifer system along the Caribbean coast of the Yucatan Peninsula, Mexico. Environ. Pollut. **159:** 991-997.

Moore, W. S. 1999. The subterranean estuary: a reaction zone of ground water and sea water. Mar. Chem. **65:** 111-125.

Morales-Ojeda, S. M., J. A. Herrera-Silveira, and J. Montero. 2010. Terrestrial and oceanic influence on spatial hydrochemistry and trophic status in subtropical marine near-shore waters. Water Research **44:** 5949-5964.

Moran, M. A., W. M. Sheldon, and R. G. Zepp. 2000. Carbon loss and optical property changes during long-term photochemical and biological degradation of estuarine dissolved organic matter. Limnol. Oceanogr. **45:** 1254-1264.

Moran, M. A., and R. G. Zepp. 1997. Role of photoreactions in the formation of biologically labile compounds from dissolved organic matter. Limnol. Oceanogr. **42:** 1307-1316.

Mutchler, T., K. H. Dunton, A. Townsend-Small, S. Fredriksen, and M. K. Rasser. 2007. Isotopic and elemental indicators of nutrient sources and status of coastal habitats in the Caribbean Sea, Yucatan Peninsula, Mexico. Estuar. Coast Shelf S. **74:** 449-457.

Mylroie, J. E., and J. R. Mylroie. 2011. Void development on carbonate coasts: creation of anchialine habitats. Hydrobiologia **677:** 15-32.

Neiber, M. T., F. C. Hansen, T. M. Iliffe, B. C. Gonzalez, and S. Koenemann. 2012. Molecular taxonomy of *Speleonectes fuchscockburni*, a new pseudocryptic species of Remipedia (Crustacea) from an anchialine cave system on the Yucatan Peninsula, Quintana Roo, Mexico. Zootaxa **3190:** 31-46.

Neiber, M. T., T. R. Hartke, T. Stemme, A. Bergmann, J. Rust, T. M. Iliffe, and S. Koenemann. 2011. Global biodiversity and phylogenetic evaluation of Remipedia (Crustacea). PLoS ONE **6:** e19627.

Opsahl, S. P., and J. P. Chanton. 2006. Isotopic evidence for methane-based chemosynthesis in the Upper Floridan aquifer food web. Oecologia **150:** 89-96.

Parlanti, E., K. Worz, L. Geoffroy, and M. Lamotte. 2000. Dissolved organic matter fluorescence spectroscopy as a tool to estimate biological activity in a coastal zone submitted to anthropogenic inputs. Org. Geochem. **31:** 1765-1781.

Peng, T. R., C. H. Wang, C. C. Huang, L. Y. Fei, C. T. A. Chen, and J. L. Hwong. 2010. Stable isotopic characteristic of Taiwan's precipitation: a case study of western Pacific monsoon region. Earth Planet. Sci. Lett. **289:** 357-366.

Pohlman, J. W. 2011. The biogeochemistry of anchialine caves: progress and possibilities. Hydrobiologia **677:** 33-51.

Pohlman, J. W., T. M. Iliffe, and L. A. Cifuentes. 1997. A stable isotope study of organic cycling and the ecology of an anchialine cave ecosystem. Mar. Ecol.-Prog. Ser. **155:** 17-27.

Santos, I. R., W. C. Burnett, J. Chanton, B. Mwashote, I. Suryaputra, and T. Dittmar. 2008. Nutrient biogeochemistry in a Gulf of Mexico subterranean estuary and groundwater-derived fluxes to the coastal ocean. Limnol. Oceanogr. **53:** 705-718.

Sarbu, S. M., T. C. Kane, and B. K. Kinkle. 1996. A chemoautotrophically based cave ecosystem. Science **272:** 1953-1955.

Schiavo, M. A., S. Hauser, and P. P. Povinec. 2009. Stable isotopes of water as a tool to study groundwater-seawater interactions in coastal south-eastern Sicily. J. Hydrol. **364:** 40-49.

Schmitter-Soto, J. J., F. A. Comin, E. Escobar-Briones, J. Herrera-Silveira, J. Alcocer, E. Suarez-Morales, M. Elias-Gutierrez, V. Diaz-Arce, L. E. Marin, and B. Steinich. 2002. Hydrogeochemical and biological characteristics of cenotes in the Yucatan Peninsula (SE Mexico). Hydrobiologia **467:** 215-228.

Seymour, J. R., W. F. Humphreys, and J. G. Mitchell. 2007. Stratification of the microbial community inhabiting an anchialine sinkhole. Aquat. Microb. Ecol. **50:** 11-24.

Shank, G. C., S. A. Skrabal, R. F. Whitehead, and R. J. Kieber. 2004. Strong copper complexation in an organic-rich estuary: the importance of allochthonous dissolved organic matter. Mar. Chem. **88:** 21-39.

Simon, K. S., T. Pipan, and D. C. Culver. 2007. A conceptual model of the flow and distribution of organic carbon in caves. J. Cave Karst Stud. **69:** 279-284.

Sket, B. 1996. The ecology of anchihaline caves. Trends Ecol. Evol. **11:** 221-225.

Socki, R. A., E. C. Perry, and C. S. Romanek. 2002. Stable isotope systematics of two cenotes from the northern Yucatan Peninsula, Mexico. Limnol. Oceanogr. **47:** 1808-1818.

Stedmon, C. A., and R. Bro. 2008. Characterizing dissolved organic matter fluorescence with parallel factor analysis: a tutorial. Limnol. Oceanogr.-Meth. **6:** 572-579.

Stedmon, C. A., S. Markager, and R. Bro. 2003. Tracing dissolved organic matter in aquatic environments using a new approach to fluorescence spectroscopy. Mar. Chem. **82:** 239-254.

Stepanauskas, R., H. Edling, and L. J. Tranvik. 1999. Differential dissolved organic nitrogen availability and bacterial aminopeptidase activity in limnic and marine waters. Microb. Ecol. **38:** 264-272.

Teal, C. S., S. J. Mazzullo, and W. D. Bischoff. 2000. Dolomitization of Holocene shallow-marine deposits mediated by sulfate reduction and methanogenesis in normal-salinity seawater, northern Belize. J. Sediment. Res. **70:** 649-663.

Tedetti, M., P. Cuet, C. Guigue, and M. Goutx. 2011. Characterization of dissolved organic matter in a coral reef ecosystem subjected to anthropogenic pressures (La Reunion Island, Indian Ocean) using multi-dimensional fluorescence spectroscopy. Sci. Total Environ. **409:** 2198-2210.

Vacher, H. L. 1988. Dupuit-Ghyben-Herzberg analysis of strip-island lenses. Geol. Soc. Am. Bull. **100:** 580-591.

Walker, S. A., R. M. W. Amon, C. Stedmon, S. W. Duan, and P. Louchouarn. 2009. The use of PARAFAC modeling to trace terrestrial dissolved organic matter and fingerprint water masses in coastal Canadian Arctic surface waters. J. Geophys. Res. **114:** G00F06.

Wikner, J., R. Cuadros, and M. Jansson. 1999. Differences in consumption of allochthonous DOC under limnic and estuarine conditions in a watershed. Aquat. Microb. Ecol. **17:** 289-299.

Wilkens, H., T. M. Iliffe, P. Oromi, A. Martinez, T. N. Tysall, and S. Koenemann. 2009. The Corona lava tube, Lanzarote: geology, habitat diversity, and biogeography. Mar. Biodiv. **39:** 155-167.

Yager, J., and J. H. Carpenter. 1999. *Speleonectes epilimnius* new species (Remipedia, Speleonectidae) from surface water of an anchialine cave on San Salvador Island, Bahamas. Crustaceana **72:** 965–97.

Yager, J., and W. F. Humphreys. 1996. *Lasionectes exleyi*, sp nov, the first remipede crustacean recorded from Australia and the Indian Ocean, with a key to the world species. Invertebr. Taxon. **10:** 171-187.